

**MINISTERE DE L'ENSEIGNEMENT SUPERIEUR ET DE LA  
RECHERCHE SCIENTIFIQUE**

**UNIVERSITE MOHAMED KHIDER BISKRA**

**FACULTE DES SCIENCES EXACTES ET  
DES SCIENCES DE LA NATURE ET DE LA VIE**

**Département des Sciences de la matière**

**THESE**

Présentée par

**Mariam GHAMRI**

En vue de l'obtention du diplôme de :

**Doctorat en chimie**

**Option :**

Chimie Moléculaire

**Intitulée**

***Étude de la structure et des propriétés SAR/QSAR de  
quelques molécules à visée thérapeutique***

Soutenue le :13/01/2022

Devant la commission d'examen :

Mr. Salah BELAIDI	Prof.	Univ. Biskra	Président
Mme. Dalal HARKATI	Prof.	Univ. Biskra	Directrice de thèse
Mr. Ammar DIBI	Prof.	Univ. Batna 1	Examineur
Mr. Lazhar BOUHLALEG	MC/A	Univ. Batna 2	Examineur



**MINISTRY OF HIGHER EDUCATION AND SCIENTIFIC RESEARCH**

**MOHAMED KHIDER BISKRA UNIVERSITY**

**FACULTY OF EXACT SCIENCES AND SCIENCES OF NATURE AND  
LIFE**

**Matter Sciences Department**

**THESIS**

Presented by

**Mariem GHAMRI**

In order to obtain the diploma of:

**PhD in Chemistry**

Option:

**Molecular chemistry**

**Entitled**

***Study of the structure and SAR / QSAR  
properties of some therapeutic molecules***

Defended on : 13/01/2022

In front of the thesis committee members:

Mr. Salah BELAIDI	Prof.	Biskra Univ.	President
Mme. Dalal HARKATI	Prof.	Biskra Univ.	Supervisor
Mr. Ammar DIBI	Prof.	Batna 1 Univ.	Examiner
Mr. Lazhar BOUHLALEG	MC/A	Batna 2 Univ.	Examiner

*To my dear parents*

*To my husband*

*To my siblings*

*To all those who are dear to me*

## *Acknowledgements*

*First of all, I pray to Allah, the almighty for providing me this opportunity and granting me the capability to proceed successfully.*

*At the outset, I would like to thank my supervisor Prof. Karkati Dalal for providing me an opportunity to do my doctoral research under his supervision, continuous support, encouragement throughout my research, and for his useful comments and discussion to make my thesis complete.*

*I wish to extend my sincere thanks to Mr. Belaidi Salah, Professor at the University of Biskra, for accepting to chair the dissertation of my thesis.*

*I would also like to thank the committee members, Mr. Ammar Diobi, Professors at the University of Batna 1, and Mr. Lazhar Bouchlaleg at the University of Batna 2, for agreeing to examine and judge my work.*

*I would like to thank all the members of group of computational and pharmaceutical chemistry, LMCE Laboratory at Biskra University, with whom I had the opportunity to work. They provided me a useful feedback and insightful comments on my work.*

*I would like to express my special thanks to Prof. Kouchlaf Majdi and his team member Liguerrri Roberto and Gilberte Chambaud from Gustave Eiffel University for the help with a smile, the good hospitality and the good reception during my training in their Multiscale Modeling and Simulation Lab.*

*Last, but not least, I would like to dedicate this thesis to my beloved parents whom raised me with a love of science and supported me in all my pursuits, my husband and my siblings for their love and continuous support – both spiritually and materially.*



## Table of contents

### ACKNOWLEDGMENTS

### TABLE OF CONTENTS

### LIST OF FIGURES

### LIST OF TABLES

<b>General Introduction</b>	<b>2</b>
<b>Chapter I: Drug discovery: finding a lead</b>	
<b>I.Context: drug research</b>	<b>5</b>
I.1 Research and Development (R&D)	6
I.1.1 Target identification and validation	6
I.1.1.1 Choosing a disease	6
I.1.1.1.1 General about cancer	6
I.1.1.1.1.1 Definition of cancer	7
I.1.1.1.2 Types of cancer	8
I.1.1.1.3 Distribution of cancer	9
I.1.1.1.4 Anticancer drugs	10
I.1.1.1.4.1 The various types of anticancer drugs and their mechanisms of action	10
I.1.1.1.4.2 Toxicity of anticancer drugs	12
I.1.1.1.5 Signs and symptoms	12
I.1.1.1.6 Treatment	13
I.1.1.1.6.1 Surgery	13
I.1.1.1.6.2 Radiotherapy	13
I.1.1.1.6.3 Medical treatment	13
I.1.1.1.6.4 Radiation therapy	13
I.1.1.1.6.5 Hormone therapy	13
I.1.1.1.6.6 Biological response modifier therapy	14

## Table of contents

I.1.1.1.6.7 Immunotherapy	14
I.1.1.1.6.8 Bone marrow transplant	14
I.1.1.2 Choosing a drug target	14
I.1.1.2.1 Historical Overview	14
I.1.1.2.2 Drug targets	15
I.1.1.2.3 Discovering drug targets	16
I.1.1.3 Finding a lead compound	18
I.1.1.3.1 Generation of Hits and Leads	18
I.1.1.3.2 Screening on the targets	18
I.1.1.3.3 Phenotypical screening	19
I.1.1.4 Lead Optimization	19
I.1.1.4.1 Rationalize the selection	20
I.1.1.4.1.1 "Drug-like" compounds	20
I.1.1.4.1.2 "lead-like" compounds	21
I.1.2 Pre-clinical trials	22
I.1.3 Clinical tests	22
I.2. Limitations and failures	24
I.3. Medicinal Chemists Today	25
I.4 Conclusion	25
I.5 References	27
<b>Chapter II</b>	
<b>Part I: Computer in medicinal chemistry</b>	
II.1 Theoretical Background for Quantum Mechanical Calculations	35
II.1.1 Molecular mechanics	36
II.1.1.1 Introduction	36

## Table of contents

II.1.1.1.1 Elongation energy	38
II.1.1.1.2. Bending energy	39
II.1.1.1.3. Torsional energy	39
II.1.1.1.4. Van der Waals energy	40
II.1.1.1.5. Electrostatic energy	41
II.1.1.2 Force Fields	42
II.1.1.3 Limitations of Molecular Mechanics	43
II.1.2 Quantum Mechanics	44
II.1.2.1 Introduction	44
II.1.2.2 HF and DFT Methods	45
II.1.2.3 Semi-empirical methods	46
II.1.2.4 Limitations of Quantum Mechanics	47
II.2 Choice of method	49
II.3 Minima search method	50
II.3.1 Introduction	50
II.3.2 Minimization algorithms	50
II.3.2.1 The "steepest descent" method	51
II.3.2.2. The conjugate gradient method	52
II.3.2.3. The Newton-Raphson method	52
II.3.2.4. The simulated annealing method	53
II.4 Molecular Modeling	53
II.4.1 Elements of Computational Chemistry	53
II.4.1.1 Drawing chemical structures	53
II.4.1.2 Three-dimensional structures	55
II.4.1.3 Molecular Structure Databases	56

## **Table of contents**

II.4.1.4 Energy minimization	58
II.4.1.5 Molecular dimensions	59
II.4.2 Molecular properties	60
II.4.2.1 Geometric Parameters	61
II.4.2.1.1 Bond length	61
II.4.2.1.2 Valence angle	61
II.4.2.1.3 Dihedral Angle (Torsion angle)	62
II.4.3 Electronic Parameters	63
II.4.3.1 Atomic charges	63
II.4.3.2 Molecular electrostatic potentials	63
II.4.3.3 Molecular orbitals	65
II.4.3.4 Fukui functions	66
II.5. Studies of vibrational properties	67
II.5.1 Introduction	67
II.5.2 Theoretical aspects of infrared vibration spectroscopy	67
II.5.3 Principle of infrared spectroscopy	68
II.5.3.1 Electromagnetic radiation	68
II.5.3.2 Infrared	70
II.5.3.3 Infrared absorption	70
II.5.4 Theoretical aspects	72
II.5.4.1 Internal vibration modes	72
II.5.4.2 Classification of vibration modes	73
II.5.4.3 Factors that influence vibration frequencies	74
II.5.5 Application	75
II.6 Conclusion	75

## Table of contents

<b>Part II: Computer-Assisted Drug Design</b>	
II.1 Predictive Quantitative Structure–Activity Relationship Modeling	<b>78</b>
II.2. Principle of QSPR / QSAR methods	<b>79</b>
II.3 Key Quantitative Structure–Activity Relationship Concepts	<b>80</b>
II.3.1 Molecular Descriptors	<b>82</b>
II.3.3 Quantitative Structure–Activity Relationship Modeling Approaches	<b>83</b>
II.3.3.1 General Classification	<b>83</b>
II.3.3.2. General methodology of a QSPR / QSAR study	<b>84</b>
II.3.3.3 Transforming the Bioactivities	<b>85</b>
II.3.3.4 Determination of the Best Set of Descriptors Approaches	<b>85</b>
II.4 Building Predictive Quantitative Structure–Activity Relationship Models: The Approaches to Model Validation	<b>86</b>
II.4.1 Data analysis methods	<b>86</b>
II.4.1.1 Neural networks	<b>86</b>
II.4.1.2 Multiple linear regression	<b>88</b>
II.4.1.2.1 Randomization test	<b>90</b>
II.4.2 Interpretation and validation of a QSPR / QSAR model	<b>91</b>
II.4.2.1 The Importance of Validation	<b>91</b>
II.4.2.1.1 Internal Validation	<b>92</b>
II.4.2.1.1.1 Least Squares Fit	<b>92</b>
II.4.2.1.1.2 Fit of the Model	<b>93</b>
II.4.2.1.2 External validation	<b>94</b>
II.5 Application of QSAR	<b>95</b>
II.6 References	<b>96</b>

## Table of contents

<b>Chapter III: Results and Discussion</b>	
III.1 Introduction	<b>104</b>
III.2 Structure, spectroscopy and electronic properties of carbazole and its derivatives	<b>108</b>
III.2.1 Carbazole structure and properties	<b>109</b>
III.3 Carbazole derivatives structures	<b>120</b>
III.4 CDCAs derivatives physicochemical properties, descriptors and drug-likeness scoring	<b>123</b>
III.5 QSAR modelling studies	<b>129</b>
III.5.1 <i>Internal validation</i>	<b>129</b>
III.5.2 <i>External validation</i>	<b>130</b>
III.5.3 <i>Y-randomization</i>	<b>130</b>
III.6 Multiple linear regression (MLR)	<b>131</b>
III.7 Artificial Neural Networks (ANN)	<b>133</b>
<b>General Conclusion</b>	<b>137</b>
<b>APPENDIX</b>	<b>140</b>
<b>REFERENCES</b>	<b>160</b>
<b>ABSTRACT</b>	

## List of Figures

<b>Figure.I.1.</b> The (simplified) process of drug discovery is divided into four major steps.....	<b>5</b>
<b>Figure.I.2.</b> Understanding cancer start.....	<b>7</b>
<b>Figure.I.3.</b> How cancer spreads? .....	<b>8</b>
<b>Figure.I.4.</b> National Ranking of Cancer as a Cause of Death at Ages <70 Years in 2019. The numbers of countries represented in each ranking group are included in the legend.....	<b>10</b>
<b>Figure.I.5.</b> 2D & 3D structure for Etoposide (VP-16).....	<b>15</b>
<b>Figure.I.6.</b> Design of CDCAs as novel Topo II-targeting anticancer agents.....	<b>17</b>
<b>Figure.I.7.</b> Success rate of phase I clinical trials in obtaining marketing authorization for the ten largest pharmaceutical companies between 1991 and 2000. The success rate varies according to the pathologies targeted.....	<b>24</b>
<b>Figure.II.8.</b> An illustration of the various terms that contribute to a typical force field.....	<b>37</b>
<b>Figure.II.9.</b> Elongation between two atoms.....	<b>38</b>
<b>Figure.II.10.</b> Deformation of valence angles.....	<b>39</b>
<b>Figure.II.11.</b> Dihedral angle formed by atoms 1-2-3-4.....	<b>40</b>
<b>Figure.II.12.</b> Van der Waals energy curve.....	<b>41</b>
<b>Figure.II.13.</b> Electrostatic interactions between two atoms.....	<b>42</b>
<b>Figure .II.14.</b> Drawing chemical structures.....	<b>54</b>
<b>Figure .II.15.</b> Conversion of a 2D drawing to a 3D model.....	<b>56</b>
<b>Figure.II.16.</b> The Cambridge Crystallographic Data Centre (CCDC).....	<b>57</b>
<b>Figure.II.17.</b> The Protein Data Bank (PDB).....	<b>58</b>
<b>Figure.II.18.</b> Diagram of energy minimization.....	<b>59</b>
<b>Figure.II.19.</b> Different methods of visualizing molecules.....	<b>60</b>
<b>Figure II.20.</b> Molecular dimensions for adrenaline (3D Hyperchem).....	<b>60</b>

## List of Figures

<b>Figure.II.21.</b> Tetrahedral shape of CCl <sub>4</sub> .....	<b>62</b>
<b>Figure.II.22.</b> Newman projection.....	<b>62</b>
<b>Figure.II.23.</b> Ring variation on cromakalim.....	<b>64</b>
<b>Figure.II.24.</b> Bicyclic models in cromakalim study.....	<b>64</b>
<b>Figure.II.25.</b> Molecular electrostatic potentials (MEPs) of bicyclic models (III) and (IV)...	<b>65</b>
<b>Figure.II.26.</b> HOMO and LUMO molecular orbitals for ethene.....	<b>66</b>
<b>Figure.II.27.</b> The various spectral domains of electromagnetic radiation.....	<b>69</b>
<b>Figure.II.28.</b> Movement of atoms during the phenomenon of vibration.....	<b>71</b>
<b>Figure.II.29.</b> Movements associated with normal modes of vibration of a molecule containing 3 atoms.....	<b>74</b>
<b>Figure.II.30.</b> Molecular descriptors and fingerprints are examples of strategies that allow researchers to extract important information about compounds that can be used in additional computer-aided drug design techniques, such as virtual screening, quantitative-structure-activity relationship (QSAR).....	<b>81</b>
<b>Figure.II.31.</b> Representation of a formal neuron.....	<b>86</b>
<b>Figure.II.32.</b> Architecture of neural networks.....	<b>86</b>
<b>Figure.II.33.</b> Schematic overview of the QSAR process.....	<b>95</b>
<b>Figure.III.34.</b> Chemical structure of carbazole with atom numbering.....	<b>104</b>
<b>Figure.III.35.</b> The Synthetic or natural carbazole derivatives induces cancer cells death triggering the intrinsic apoptotic pathway by inhibition of Topoisomerase II.....	<b>108</b>
<b>Figure.III.36.</b> Dual descriptor ( $\Delta f$ ) Vs Atoms .....	<b>120</b>
<b>Figure.III.37.</b> Face and profile views of Compounds 1 and 3.....	<b>121</b>
<b>Figure.III.38.</b> Generic leverage plot of observed [11] (Observed pIC <sub>50</sub> ) versus predicted (Predicted pIC <sub>50</sub> ) activity according to the MLR model. The oblique line is the diagonal.....	<b>132</b>
<b>Figure.III.39.</b> The architecture (6-4-1) of the adopted ANN model.....	<b>134</b>

<b>Table.I.1.</b> Overview of anticancer drugs.....	<b>11</b>
<b>Table.II.2.</b> Molecular degrees of freedom.....	<b>73</b>
<b>Table.III.3.</b> Chemical structure and experimental activity ( $pIC_{50}$ [125]) of the CDCAs under study. $pIC_{50}$ is $\log_{10}(1/IC_{50})$ . * denotes the compounds selected for external validation (test set).....	<b>105</b>
<b>Table.III.4.</b> Equilibrium Geometrical Parameters (Bond lengths in Å and angles in degrees) of carbazole in its electronic ground state. The numbering of the atoms is given in Figure 34.....	<b>109</b>
<b>Table.III.5.</b> Comparison of the experimental and calculated anharmonic frequencies ( $\nu$ , in $cm^{-1}$ ) of carbazole. Computed at the B3LYP/6-311G(d,p) level of theory and we give also the computing of IR intensity (I in $km/mol$ ). Abbreviations used: $\nu$ , stretching; $\nu_s$ , sym. stretching; $\nu_{as}$ , asym. stretching; b, in-plane-bending; g, out-of-plane bending; Ben: Benzene; Pyr: pyrrole.....	<b>112</b>
<b>Table.III.6.</b> Outermost molecular orbitals of carbazole and of its derivatives of interest in the present study. $\Delta E$ (in eV) corresponds to the energy HOMO – LUMO gap.....	<b>113</b>
<b>Table.III.7.</b> Values of the Fukui functions of carbazole. See text for the definition of the different terms.....	<b>119</b>
<b>Table.III.8.</b> Physicochemical properties of CDCAs derivatives. For each compound, we give the energies of the HOMO ( $E_{HOMO}$ in a.u.) and of the LUMO ( $E_{LUMO}$ in a.u.), the polarizability (Pol in Å <sup>3</sup> ), the volume (V in Å <sup>3</sup> ), the surface area grid (SAG in Å <sup>3</sup> ) and the hydration energy (HE in kcal/mol). * denotes the selected compounds for external validation (test set).....	<b>124</b>
<b>Table.III.9.</b> Drug-likeness parameters and lipophilicity indices for the CDCAs under study. See text for the definition of these parameters and their description.....	<b>128</b>
<b>Table.III.10.</b> Numerical parameters used to confirm the QSAR model validity. See text for more details.....	<b>131</b>
<b>Table.III.11.</b> Random MLR model parameters.....	<b>132</b>

# **General Introduction**

Molecular modeling is a broad term encompassing different molecular graphing and computational chemistry techniques to display, simulate, analyze, calculate and store the properties of molecules; to determine the geometry of a molecule and to evaluate the associated physicochemical properties.

The comparison of the biological activity of certain molecules and their structures has made it possible in many cases to establish correlations between the structural parameters and the properties of a molecule.

The majority of heterocycles play a very important therapeutic role. Due to their biological interest, the chemistry of heterocycles is growing.

The majority of the heterocycles more to the complexes of therapeutic interest currently used clinically were obtained by chemical modification from natural molecules or by a total synthesis.

The research and synthesis of new chemical and biochemical compounds are today often associated with a molecular modeling study. Thanks to the computer development of recent years and the rise of intensive parallel computing in particular, molecular modeling has become a real game.

Molecular modeling can be defined as an application of computing to create, manipulate, calculate and predict molecular structures and associated properties.

There are many theoretical chemistry methods aimed at determining the physical or chemical properties of isolated molecules, be they thermodynamic properties such as binding enthalpies, relative energies of different conformers, or simulations of infrared, Raman or electronic.

Two main classes of simulation methods can be distinguished: on the one hand quantum chemistry methods that allow the precise determination of the electronic properties of molecules, on the other hand molecular mechanics methods that are based on empirical parameters that allow in particular to determine the structural parameters and secondly these methods make it possible to calculate the physicochemical parameters used in the QSAR study.

Quantitative Structure Activity Relationship (QSAR), as their names suggest, sets up a mathematical relationship using data analysis methods, linking microscopic molecular properties called descriptors, to an effect experimental (biological activity, toxicity, affinity for a receptor), for a series of similar chemical compounds. The starting point for such methods is the definition of empirical or theoretical molecular

## General Introduction

descriptors. The latter take into account information on the structure and the physicochemical characteristics of the molecules.

The choice of experimental reference databases is decisive in a QSAR study. It must consist of reliable experimental data obtained by following a unique experimental protocol. Indeed, the robustness of the model strongly depends on the base on which it is based.

Finally, the link between the descriptors and the database is determined through analysis tools such as multilinear regressions (MLRs), partial least squares (PLS) regressions, neural networks, and component analysis.

The main objective of this study is to predict molecules of pharmaceutical interest, ie to sort molecules before going to the experimental stage, or to interpret or predict the biological activation of molecules already synthesized. So, look for the preferred conformations by quantum and semi-empirical calculations of heterocyclic compounds of pharmaceutical interest (eg: carbazole and chalcone....) whose majority of derivatives are bioactive.

The effect of the substituents on their basic skeletons and the main structural motifs will be examined, and qualitative and quantitative studies of the structure-activity relationships, using the QSAR model, will be carried out in order to arrive at models for some series of these heterocycles of pharmaceutical interest.

# **Chapter I**

## **Drug discovery: finding a lead**

## I. Context: drug research

Drug discovery is a multidisciplinary cycle that takes quite a while (10-20 years) and costs a ton of cash. In the writing, there is an assortment of assessments for his complete expense, which goes from \$300 million to more than \$1.75 billion dollars [1]. DiMasi's investigation [2, 3], which is quite possibly frequently referred to, puts the expense at around 802 million dollars, while a later report puts it at under \$12 million [4]. Nonetheless, most of the studies concur on the huge measure of assets needed to finish a task, just as the continuous expansion in general interaction costs, which were assessed to be 138 million dollars during the 1970s and 300 million dollars during the 1980s [5]. To exacerbate the situation, the achievement pace of drug industry projects stays low [6], and the quantity of new drugs acquainted with the market has stayed stable, if not declining, since the year 2000 [5].

Subsequently, drug scientists are continually endeavoring to improve every one of the means prompting the commercialization of a medication. Drug organizations, for instance, are among the most universally contributed, with 10 to 20% of their income put resources into innovative work (R&D)[7].

The whole drug research interaction can be separated into four significant stages, as demonstrated in Figure 1. We'll portray them momentarily in the parts that follow, with an attention on the stages for which the techniques introduced in this theory were created.

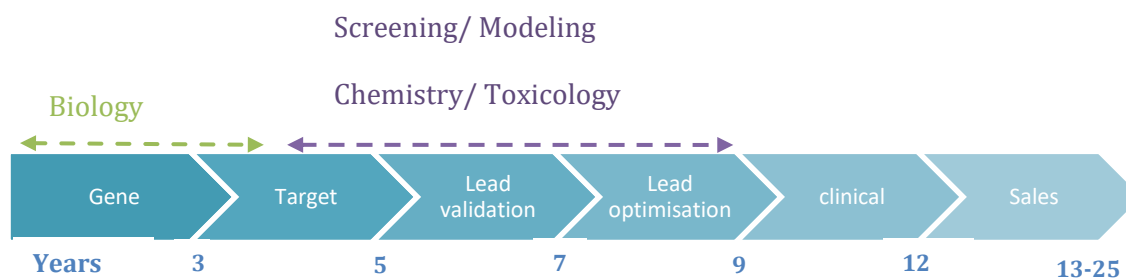


**Figure 1.**The (simplified) process of drug discovery is divided into four major steps.

## **I.1. Research and Development (R&D)**

One of the most goals of the R&D part is to deliver one or additional active and innovative drug candidates with quantity amount of toxicity potential, giving them the most effective probability of passing the next stages.

### **I.1.1. Target identification and validation**

The initial step is to recognize at least one biological entities whose movement can be regulated to give an advantageous impact with regard to a particular illness. Because all following research will be predicated on the notion that these targets are effectively related to the disease and that the medication's action would have a favorable effect on humans, this phase is crucial. It's a lot more delicate because the target's relevance to the targeted disease must be evaluated against the potential negative consequences of modifying the target's activity. The search for new targets has intensified since the human genome was sequenced and bioinformatics methods for comparing sequences and protein structures were developed. Many authors have also questioned the classic "one disease, one target, one drug" approach, claiming that biological network regulation can compensate for a molecule's influence on its target [8, 9], even if the molecule has a high chance of interacting with other proteins. Poly-pharmacology [10] and chemogenomic are two new sciences that have arisen in recent decades.

#### **I.1.1.1. Choosing a disease**

##### **I.1.1.1.1. General about cancer**

Cancer is one of the most important health problems of the current era and also a leading cause of death among populations. Cancer can simply be defined as unregulated cell division leading to a tumor formation in any part of the body. In its natural course, tumor mass continues to grow invading the surrounding tissues and finally tumor cells get access to the lymphatic and vascular systems spreading to distant organs which results in metastasis. In order to be successful in the treatment of cancer, early diagnosis, before the tumor spreads to the surrounding tissues or distant organs, is mandatory. It is now known that most cancer types result from accumulation

of multiple errors in DNA that may affect primarily the regulatory pathways in the cell. Although the currently used treatment modalities are mainly directed to the macroscopic destruction of the tumor mass, the presence of systemic dissemination could not be denied and systemic treatments are widely used in order to control the microscopic disease. Despite these advances in treatment, the development of new strategies towards the correction of molecular impairments in the cell is indispensable.

#### I.1.1.1.1. Definition of cancer

Cancer is defined by the uncontrollable growth and spread of aberrant cells, as well as apoptosis resistance. External agents or hereditary genetic factors are responsible for its occurrence. When a cell's repair system allows the accumulation of microscopic changes to escape, the cell becomes malignant.

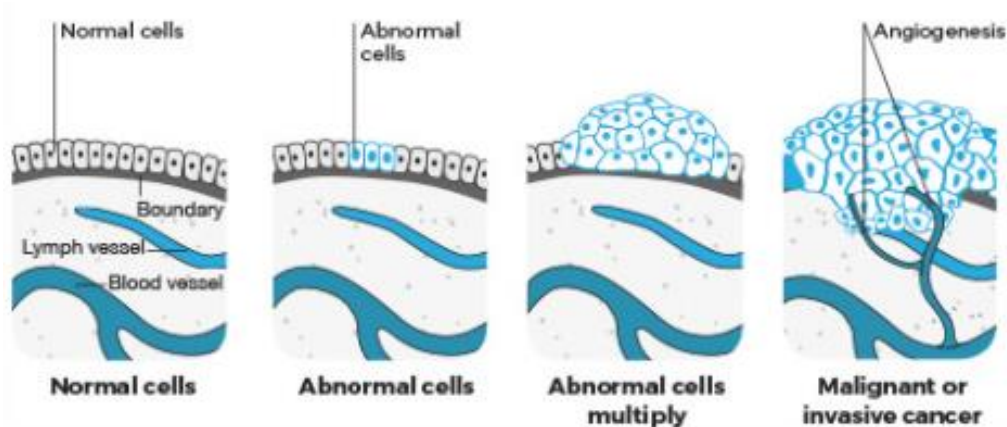


Figure .2. Understanding cancer start.

This cell divides fast and uncontrolled, resulting in an organ tumor. Through blood vessels and lymphatics, malignant cells can escape and spread to other tissues, causing metastases [11].

Sometimes cells don't grow, divide and die in the usual way. This may cause blood or lymph fluid in the body to become abnormal, or form a lump called a tumour. A tumour can be benign or malignant.

**Benign tumour:** Cells are confined to one area and are not able to spread to other parts of the body. This is not cancer.

**Malignant tumour:** This is made up of cancerous cells which have the ability to spread by travelling through the bloodstream or lymphatic system (lymph fluid).

Carcinogenesis is separated into three stages: initiation, promotion, and tumor progression [12].

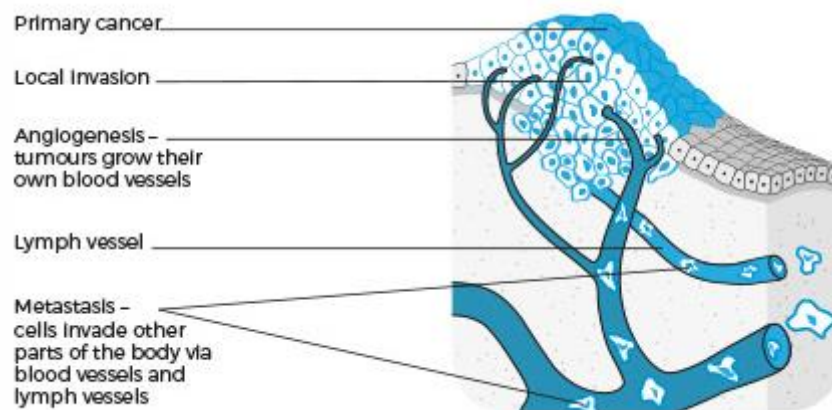


**Figure .3.**How cancer spreads?

### I.1.1.1.2 Types of cancer

Doctors divide cancer into types based on where it begins. Four main types of cancer are:

- **Carcinomas:** A carcinoma begins in the skin or the tissue that covers the surface of internal organs and glands. Carcinomas usually form solid tumors. They are the most common type of cancer. Examples of carcinomas include prostate cancer, breast cancer, lung cancer, and colorectal cancer.
- **Sarcomas:** A sarcoma begins in the tissues that support and connect the body. A sarcoma can develop in fat, muscles, nerves, tendons, joints, blood vessels, lymph vessels, cartilage, or bone.

- **Leukemias:** Leukemia is a cancer of the blood. Leukemia begins when healthy blood cells change and grow uncontrollably. The 4 main types of leukemia are acute lymphocytic leukemia, chronic lymphocytic leukemia, acute myeloid leukemia, and chronic myeloid leukemia.
- **Lymphomas:** Lymphoma is a cancer that begins in the lymphatic system. The lymphatic system is a network of vessels and glands that help fight infection. There are 2 main types of lymphomas: Hodgkin lymphoma and non-Hodgkin lymphoma.

### **I.1.1.1.3Distribution of cancer**

Cancer ranks as a leading cause of death and an important barrier to increasing life expectancy in every country of the world. According to estimates from the World Health Organization (WHO) in 2019, cancer is the first or second leading cause of death before the age of 70 years in 112 of 183 countries and ranks third or fourth in a further 23 countries (Fig. 4). Cancer's rising prominence as a leading cause of death partly reflects marked declines in mortality rates of stroke and coronary heart disease, relative to cancer, in many countries.

Overall, the burden of cancer incidence and mortality is rapidly growing worldwide; this reflects both aging and growth of the population as well as changes in the prevalence and distribution of the main risk factors for cancer, several of which are associated with socioeconomic development. [13]

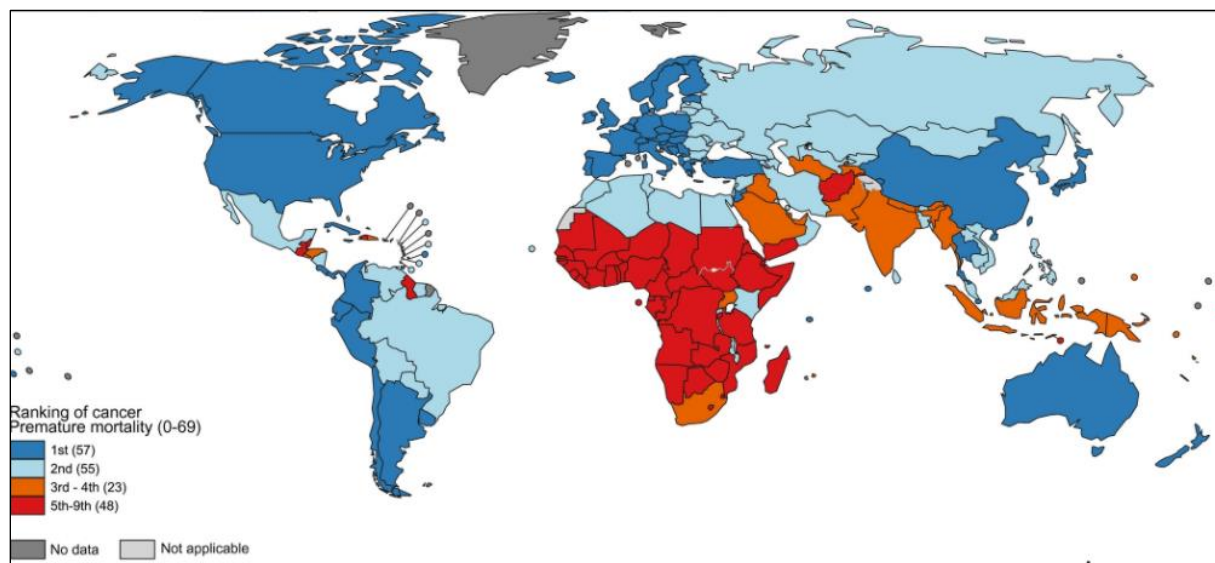


**Figure.4.** National Ranking of Cancer as a Cause of Death at Ages <70 Years in 2019. The numbers of countries represented in each ranking group are included in the legend.

#### I.1.1.1.4 Anticancer drugs

Anticancer agents are drugs that are used in chemo-therapies to treat cancer. It is used alone or in combination. They want to stop cells from proliferating uncontrollably because they have genetic and functional defects that set them apart from healthy cells. This chemotherapy isn't meant to kill the tumor locally; rather, it's meant to prevent tumor escape through the production of distant metastases [14].

##### I.1.1.1.4.1 The various types of anticancer drugs and their mechanisms of action

These compounds have been divided into three groups based on their pharmacological mechanisms:

- **Cytotoxic anticancer drugs:** The compounds employed in cytotoxic chemotherapy vary in their modes of action and chemical family membership. Alkylating agents, topoisomerase I and II inhibitors, microtubule poisons (intercalating agents), antimetabolites, and splitting agents are the six primary families.

## Drug discovery : finding a lead

- Targeted therapies: these are medications that operate on tumor cells at a specific level of their function or development. Extracellular medications (such as avastin, erbitux, etc.) are aimed against a membrane receptor located on the tumor cell, whereas intracellular medications (such as: multikinases, glivec ...) disrupt the proliferative signal transmission cell through enzymatic inhibition.
- Other anticancer drugs: these are anticancer drugs with different modes of action of two classes mentioned above.

**Table 1:** Overview of anticancer drugs.

DRUGS	DRUGS DESCRIPTION
AVASTIN®	is a monoclonal anti-vascular endothelial growth factor antibody used in combination with antineoplastic agents for the treatment of many types of cancer.
ERBITUX®	is an endothelial growth factor receptor binding fragment used to treat colorectal cancer as well as squamous cell carcinoma of the head and neck.
GLIVEC®	is a tyrosine kinase inhibitor used to treat a number of leukemias, myelodysplastic/myeloproliferative disease, systemic mastocytosis, hypereosinophilic syndrome, dermatofibrosarcoma protuberans, and gastrointestinal stromal tumors.
CABOMETYX®	is a tyrosine kinase inhibitor used to treat advanced renal cell carcinoma, hepatocellular carcinoma, and medullary thyroid cancer. (multikinases inhibitors).
PLATINOL®	is a platinum based chemotherapy agent used to treat various sarcomas, carcinomas, lymphomas, and germ cell tumors. (Alkylating agents).
ETOPOSIDE®	is a podophyllotoxin derivative used to treat testicular and small cell lung tumors. (topoisomerase I and II inhibitors)
AMSIDINE®	is a cytotoxic agent used to induce remission in acute adult

---

leukemia that is not adequately responsive to other agents.(intercalating agents)

---

#### **I.1.1.1.4.2 Toxicity of anticancer drugs**

The many drugs used in chemotherapy procedures are not only harmful to tumor cells, but they can also be toxic to healthy cells, particularly those that proliferate quickly. Cardiotoxicity, neurotoxicity, nephrotoxicity, hepatotoxicity, alopecia, dehydration, exhaustion, infertility, undernutrition, skin issues, allergies, and many more are examples of toxic effects [15].

#### **I.1.1.1.5 Signs and symptoms**

No matter your age or health, it's good to know the possible signs of cancer.

Common signs and symptoms of cancer in both men and women include:

- Pain. Bone cancer often hurts from the beginning. Some brain tumors cause headaches that last for days and don't get better with treatment. Pain can also be a late sign of cancer.
- Weight loss without trying. Almost half of people who have cancer lose weight. It's often one of the signs that they notice first.
- Fatigue. If you're tired all the time and rest doesn't help.
- Fever. If it's high or lasts more than 3 days. Some blood cancers, like lymphoma, cause a fever for days or even weeks.
- Changes in your skin.
- Sores that don't heal. Spots that bleed and won't go away are also signs of skin cancer.
- Cough or hoarseness that doesn't go away. A cough is one sign of lung cancer, and hoarseness may mean cancer of your voice box (larynx) or thyroid gland.
- Unusual bleeding. Cancer can make blood show up where it shouldn't be. Blood in your poop is a symptom of colon or rectal cancer. And tumors along your urinary tract can cause blood in your urine.

- Anemia. This is when your body doesn't have enough red blood cells, which are made in your bone marrow. Cancers like leukemia, lymphoma, and multiple myeloma can damage your marrow. Tumors that spread there from other places might crowd out regular red blood cells.

### **I.1.1.1.6 Treatment**

The treatment of a cancer patient requires a multidisciplinary approach. It employs a variety of techniques, the most well-known of which are surgery, radiation, and chemotherapy. Its goal is to get rid of the cancerous tumor and prevent it from spreading to other parts of the body [16].

#### **I.1.1.1.6.1 Surgery**

This method entails interfering directly at the tumor's level, i.e., removing the tumor, either partially or completely. When the tumor is localized, it is usually the first and most successful treatment.

#### **I.1.1.1.6.2 Radiotherapy**

It is a cancer treatment strategy based on the biological effect of ionizing radiation, particularly high-energy X-rays. It tries to modify cancer cells' reproduction capability by exposing them to high doses of radiation while maintaining as much healthy tissue and surrounding organs as feasible. It can be given alone or in conjunction with chemotherapy.

#### **I.1.1.1.6.3 Medical treatment**

Chemotherapy for cancer is designed to kill cells that are actively dividing. It is a treatment that involves ingesting a medication that slows the growth of tumor cells in an attempt to extend the patient's life expectancy and minimize pain from metastases.

#### **I.1.1.1.6.4 Radiation therapy**

This treatment kills cancer cells with high dosages of radiation. In some instances, radiation may be given at the same time as chemotherapy.

#### **I.1.1.1.6.5 Hormone therapy**

Sometimes hormones can block other cancer-causing hormones. For example, men with prostate cancer might be given hormones to keep testosterone (which contributes to prostate cancer) at bay.

#### **I.1.1.1.6.6 Biological response modifier therapy**

This treatment stimulates your immune system and helps it perform more effectively. It does this by changing your body's natural processes.

#### **I.1.1.1.6.7 Immunotherapy**

Sometimes called biological therapy, immunotherapy treats disease by using the power of your body's immune system. It can target cancer cells while leaving healthy cells intact.

#### **I.1.1.1.6.8 Bone marrow transplant**

Also called stem cell transplantation, this treatment replaces damaged stem cells with healthy ones. Prior to transplantation, you'll undergo chemotherapy to prepare your body for the process.

### **I.1.1.2 Choosing a drug target**

#### **I.1.1.2.1 Historical Overview**

Heterocycles are common structural units in marketed drugs and in medicinal chemistry targets in the drug discovery process. Over 80% of top small molecule drugs by US retail sales in 2010 contain at least one heterocyclic fragment in their structures. The one reason behind such high prevalence of oxygen, sulfur, and especially nitrogen-containing rings in drug molecules is obvious. The research process that leads to identification of an effective therapeutic treatment is largely based on mimicking nature by "fooling" it in a very subtle way. Because heterocycles are the core elements of a wide range of natural products such as nucleic acids, amino acids, carbohydrates, vitamins, and alkaloids, medicinal chemistry efforts often evolve around simulating such structural motifs. However, heterocycles play a much bigger

role in the modern repertoire of medicinal chemists. Some of the drug properties that can be modulated by a strategic inclusion of heterocyclic moiety into the molecule include:

1) Potency and selectivity through bioisosteric replacements, 2) Lipophilicity, 3) Polarity, and 4) Aqueous solubility [17].

- **Heterocyclic Compounds**

The IUPAC Gold Book describes heterocyclic compounds as:

- ✓ Cyclic compounds having as ring members atoms of at least two different elements, e.g. Carbazole, Carbazole Derivatives containing Chalcone Analogues (CDCAs) [18].
- ✓ Rings are considered as "heterocycles" only if they contain at least one atom selected from halogen, N, O, S, Se or Te as a ring member. Heterocyclic rings may be present as distinct entities or condensed, either with carbocycles or among themselves.

### I.1.1.2.2 Drug targets

The next step is to find an appropriate pharmacological target once a therapeutic area has been identified (e.g., receptor, enzyme, or nucleic acid). It's evident that knowing which biomacromolecules are involved in a given disease state is crucial. This enables the medicinal research team to determine if agonists or antagonists for a certain receptor or inhibitors for a certain enzyme should be developed. Many chemotherapeutic agents have been shown to be promising cancer weapons. Anticancer drugs as etoposide (Fig .5), doxorubicin, and amonafide, for example, strongly inhibit topoisomerase II (Topo II) [19]. Topo II is one of the most promising anticancer therapeutic targets because it can interfere with the enzyme-DNA complex, causing persistent DNA damage and cell death [20]. Over the past 40 years, topoisomerase inhibitors have been widely employed in the clinical treatment of cancer. At least one drug that targets these enzymes is used in around half of all chemotherapy regimens [21].

➤ **Etoposide (VP-16)**

Etoposide is an antitumor agent currently in clinical use for the treatment of small cell lung cancer, testicular cancer and lymphomas. Since the introduction of etoposide in 1971, its mechanism of action and potent antineoplastic activity has served as the impetus for intensive research activities in chemistry and biology. This drug acts by stabilizing a normally transient DNA-topoisomerase II complex, thus increasing the concentration of double-stranded DNA breaks. This phenomenon triggers mutagenic and cell death pathways. The function of topoisomerase II is understood in some detail, as is the mechanism of inhibition of etoposide at a molecular level. Etoposide has shortcomings of limited neoplastic activity against several solid tumors such as non-small cell lung cancer, cross-resistance to MDR tumor cell lines and low bioavailability. The design and synthesis of etoposide analogs is an activity of fundamental interest to the field of cancer chemotherapy.[22]

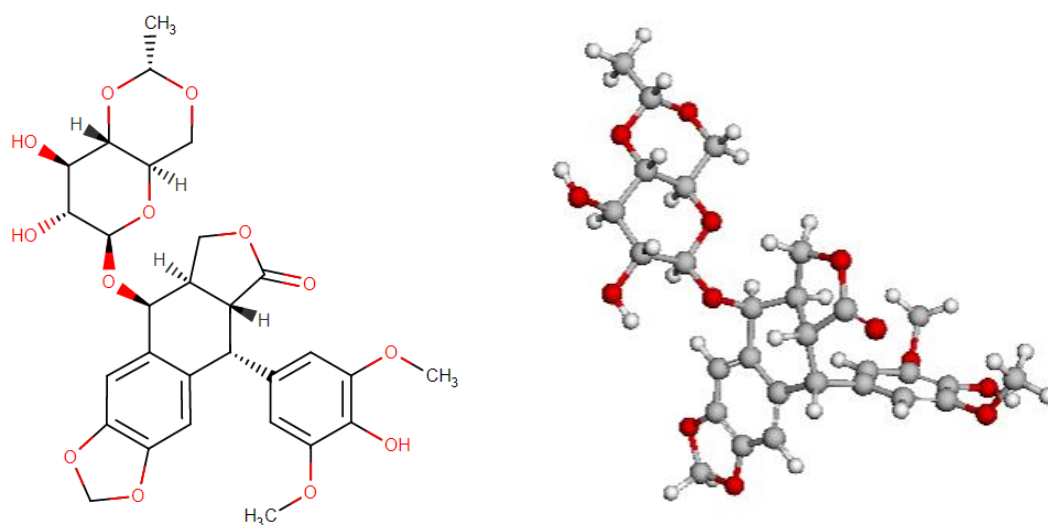


**Figure .5.** 2D & 3D structure for Etoposide (VP-16).

**I.1.1.2.3 Discovering drug targets**

If a drug or poison has a biological impact, that substance must have a molecular target in the body. Previously, finding drug targets necessitated first finding the drug.

## Drug discovery : finding a lead

Most Topo II inhibitors, like other anticancer drugs, have serious side effects, including cardiotoxicity, specific leukemia, and multidrug resistance [23-25]. As a result, finding new Topo II inhibitors in the form of CDCAs (carbazole derivatives including chalcone analogs) with high efficacy and low toxicity is a hot topic of research [26-31]. Many bioactive natural products and synthetic compounds with a wide range of biological activities, including antimalarial, antibacterial, and anticancer activity, contain the carbazole scaffold [32-34].

Furthermore, studies have revealed that carbazole derivatives may inhibit Topo II, which could explain their antitumor effects [35, 36]. Modifications/substitutions of the carbazole ring have become a hot focus in the development of novel Topo II-targeting anticancer agents in recent years. For example (Figure 6), Compound 1 operates as a possible non-intercalative Topo II catalytic inhibitor (Figure 6) [37]. Compound 2 showed substantial cytotoxicity against the HL-60 cell line as a Topo II catalytic inhibitor [38].

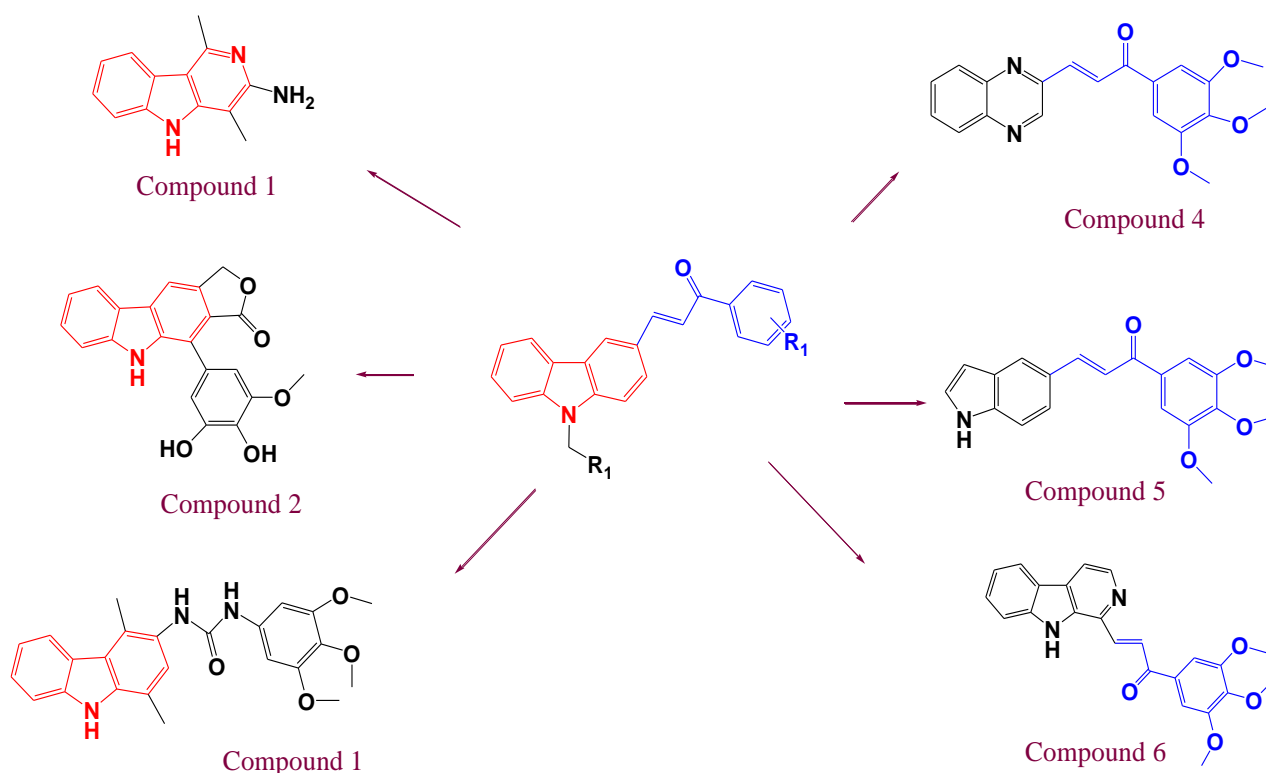


**Figure 6.** Design of CDCAs as novel Topo II-targeting anticancer agents.

Compound 3 showed modest cytotoxicity against cancer cell lines when used as a Topo II poison. These findings sparked a lot of interest in looking into carbazole derivatives as a new type of potential anticancer drug that targets Topo II. Chalcone's pharmacological activities, including anticancer, antioxidant, anti-inflammatory, and anti-infective activity, piqued researchers' interest in the twenty-first century. Compounds 4, 5, and 6 (Figure 6), which are naturally occurring and synthesized chalcone analogs, are now being studied as cytotoxic agents. In several cancer cell lines; these chemicals have been shown to suppress cancer cell proliferation and cause apoptosis. Tubulin polymerization inhibition, apoptosis induction, and Topo II inhibition have all been identified as modes of action for chalcone analogs. The mechanism of action of the most bioactive substances was investigated further. CDCAs appear to be non-intercalative Topo II catalytic inhibitors, certain CDCAs showed significant cytotoxic activity with low micromolar IC<sub>50</sub>.<sup>[18]</sup>

### **I.1.1.3 Finding a lead compound**

#### **I.1.1.3.1 Generation of Hits and Leads**

Once the target has been identified, the vast majority of drug development projects move on to the screening stage. Its goal is to identify a first group of active molecules, more commonly referred to as hits. During a screening test, a molecule must have a certain level of activity (usually in the micromolar range) in order to be identified as such. Because the precise value of the required level of activity is not absolute, a hit will be defined as a molecule that demonstrated moderate or strong activity during an experimental test. There are a variety of experimental methods available for identifying hits. Today, high-throughput screening (HTS) <sup>[39-41]</sup> is most likely the most widely used method in the pharmaceutical industry. There are two main types of experimental screening. <sup>[5, 42-44].</sup>

#### **I.1.1.3.2 Screening on the targets**

Molecules are tested on relatively small biochemical systems, usually for their affinity or ability to inhibit a certain protein. This is the most common sort of screening because it allows you to test many molecules in a short amount of time and

because it closely resembles the traditional pharmacological research paradigm: a target / a drug.

### **I.1.1.3.3 Phenotypical screening**

Molecules are tested on whole cells or animal models of a specific disease. They are slower and more expensive, but they allow researchers to study molecule activity in a cell-like environment and so achieve more goals. Several decades ago, this sort of screening was widely used. It has gradually been phased out in favor of target screening in order to save costs and shorten test times while increasing the number of molecules tested. Moreover, a number of authors have recently highlighted its benefits [42, 45, 46].

Once identified, the hits must be confirmed using more detailed testing, primarily to ensure that the observed activity is not due to artefacts related to the experimental method or the presence of impurities. A lead is a compound that has demonstrated a moderate or significant activity and is considered a good place to start looking for a potential drug candidate. After the effectiveness of the activity has been confirmed, more advanced tests will be conducted. These studies will aim to determine not only the activity of molecules (selectivity, low-concentration inhibition) but also their physico-chemical properties (solubility, lipophilic, metabolic stability, etc.) in order to select the most promising molecules. The selection of leads is a crucial step because the rest of the project will be focused on the few molecules that are obtained. Once a lead has been identified, and if it is successful, one or more molecules will be submitted to the optimization stage, representing as many paths as feasible for the discovery of a potential drug candidate.

### **I.1.1.4 Lead Optimization**

During this stage, medicinal chemists will begin an iterative process in which chemical alterations will be made to a few molecules obtained during screening in order to improve the activity and properties of future drug candidates. The goal of this step is to obtain some molecules with a high level of activity (the level of activity depends on the project and the goal, with the goal being to maximize the ratio of

activity to concentration) and appropriate Physicochemical, biological, and toxicological properties.

This is by far the most difficult step, as it necessitates optimizing both activity and other properties that will turn the molecule into a drug that is both effective and low (or non-toxic). In general, multi-objective optimization is discussed, and numerous studies have been conducted in this area, including in cheminformatics [47-49].

### **I.1.1.4.1 Rationalize the selection**

The elimination of false selection allows for a reduction in the number of unnecessary tests and hence significant cost savings. There are also methods for selecting more precisely the components to test in order to reduce the chances of success in relation to the project's goals.

#### **I.1.1.4.1.1 “Drug-like” compounds**

Ideally, only molecules with a high potential to become a drug should be tested: no toxicity, high therapeutic efficacy, good absorption for oral prescription drugs, and so on. In the absence of a universal definition or a perfect predictive method, numerous studies have attempted to distinguish between a biologically active molecule and a "drug-like" molecule that approaches the ideal drug [50-54].

Lipinski's [55] definition of the term "drug-like" is the most well-known. The molecules with the best probability of being absorbed by voice oral satisfy at least three of the following characteristics, based on compounds administered by voice oral that passed phase 2 of clinical tests successfully:

- Molecular weight < 500 Da,
- LogP < 5,
- Number of hydrogen bond acceptors < 10,
- Number of hydrogen bond donors < 5.

With a similar specific goal, Veber et al [56]:

- Polar surface area  $\leq 140 \text{ \AA}^2$  and  $\leq 10$  rotatable bonds

#### I.1.1.4.1.2 "lead-like" compounds

Despite being frequently associated with Lipinski's rules, the term "drug-like" is quite vague and has thus been repurposed to describe more specific classes of molecules. Numerous studies have been conducted, for example, in order to distinguish between the leads of pharmaceuticals and other molecules. Once again, the definition of a lead remains mostly speculative, and other studies have attempted to establish analogous rules to Lipinski's. The concept stems from the observation that molecules entering clinical trials are frequently more complicated and larger than the leads from which they were derived [57-60]. As a result, more restrictive filters for obtaining simpler compounds have been developed, the most famous of which is that of Hann and Oprea[59]:

Molecular weight < 460 Da ;

$-4 < \text{Log } P < 4, 2$  ;

$\text{Log } S_w \geq -5$  ;

rotatable bonds <10 ;

Number of hydrogen bond donors < 5 ;

Number of hydrogen bond acceptors <9 ;

Number of cycles <4 ;

Other criteria have recently been introduced as well. Hopkins et al.'s of "Ligand Efficiency" [61] suggest that the ratio between liaison energy and the number of heavy atoms is an effective measure for lead selection. It allows, for example, to distinguish between an active and complicated molecule and a molecule with a similar activity but a lower complexity, allowing for the selection of leads with a higher potential for further modification. Further groups have proposed other indices of this sort, this time taking into account the area of the polar topological surface or lipophilicity.

### I.1.2 Pre-clinical trials

After obtaining optimized "leads", the pre-clinical trials consist of numerous studies aimed at qualifying the drug candidate from a pharmacological, pharmacokinetic and toxicological point of view. The use of rational animal experiments will allow consideration of the administration of the candidate drug in humans during subsequent clinical trials. The aim of pharmacological studies is to validate the mechanism of action of the candidate drug and to measure its activity in experimental models of the pathology, *in vitro* and *in vivo* in animals. Pharmacokinetic studies can describe the fate of a compound, its distribution, absorption and metabolism, and then its elimination from the body. Toxicological studies are used to determine the toxic doses of the drug candidate in the organism studied (mainly mice or rats, more rarely cats, dogs, pigs, or primates) .[62, 63]

These data will help determine the doses to be administered to humans during clinical trials and constitute a first approach in the study of potential adverse effects of the candidate drug, allowing these effects to be monitored proactively. An ancillary part of the pre-clinical development also consists of the assessment of the environmental risk associated with the marketing of the candidate drug. All the information collected during the pre-clinical trials will be compiled in a marketing authorization application for the candidate drug. This will be closely studied by the competent health authorities (in France, this is the National Medicines Safety Agency (ANSM) and the People Protection Committee (CPP)), before authorizing, or no, the entry of the drug candidate into the clinical trial phase.[62, 63]

### I.1.3 Clinical tests

Clinical trials represent the most critical step in the drug design process, whether or not validating several years of pre-clinical and extremely expensive research. They are divided into four phases. The first three make it possible to establish the efficacy and safety of the drug candidate in order to obtain Marketing Authorization, while the fourth consists of the monitoring of side effects throughout the period of marketing and use of the drug (pharmacovigilance phase ) .[64]The

supervision of clinical trials by health authorities is very strict. In France, the informed consent of volunteers is required and a national register kept by the ANSM lists all the subjects, the amount of their compensation (capped at 4,500 euros per year to avoid possible abuses), the date and duration of their protocols. During each phase, if adverse reactions are detected, the clinical study may be terminated and the drug candidate may be permanently discontinued.

Phase I is preliminary to the study of the efficacy of a drug candidate. It takes place on a small number of healthy volunteers (20 to 80) and its sole objective is to assess the tolerance or absence of any side effects associated with the administration of the candidate drug. However, these trials can be offered to patients with treatment failure, for whom the studied treatment represents the only chance of survival. Approximately 54% of the compounds tested in phase I will advance to the next phase.[65] Phase II aims to determine the optimal dosage, the efficacy of the drug candidate at this dosage and its short-term tolerance. It is generally carried out on a homogeneous group of 100 to 200 patients. Only 18% of the clinical trials started go on to phase III.[65] These trials, on a larger scale, are carried out on several thousand patients representative of the patient population for which the treatment is intended. These are controlled trials in which the drug in development is compared either with an effective treatment already on the market or with a placebo.

Phase III trials are most often carried out double-blind and with random draw:

the treatments or placebo are randomly assigned to patients and to the doctors in charge of monitoring, without them being informed of what assignment they have been subject to. This method avoids biases related to the patient management process, commonly known as the "placebo effect". The complete clinical trial process results in a Marketing Authorization being obtained for 11% of the drug candidates.[6, 65]

When Marketing Authorization is granted, the marketing and application of the treatment can begin. Phase IV of clinical trials, also called pharmacovigilance, then consists of monitoring the potential side effects of the treatment on all the patients who benefit from it (large and heterogeneous population). In this context, physicians have

the obligation to report the adverse effects described by their patients, which makes it possible to quickly identify the emergence of new effects which would not have been detected during clinical trials and guarantees greater safety. of use to patients.

### I.2. Limitations and failures

Pharmaceutical research therefore faces major challenges, mainly scientific, but also financial and political. The success rate of the clinical trial phases is about 11%, all types of pathologies combined.[6, 65] This varies according to the types of pathologies, from around 5% for those involving the central nervous system to around 20% for cardiovascular disease (Figure 7) .[6]

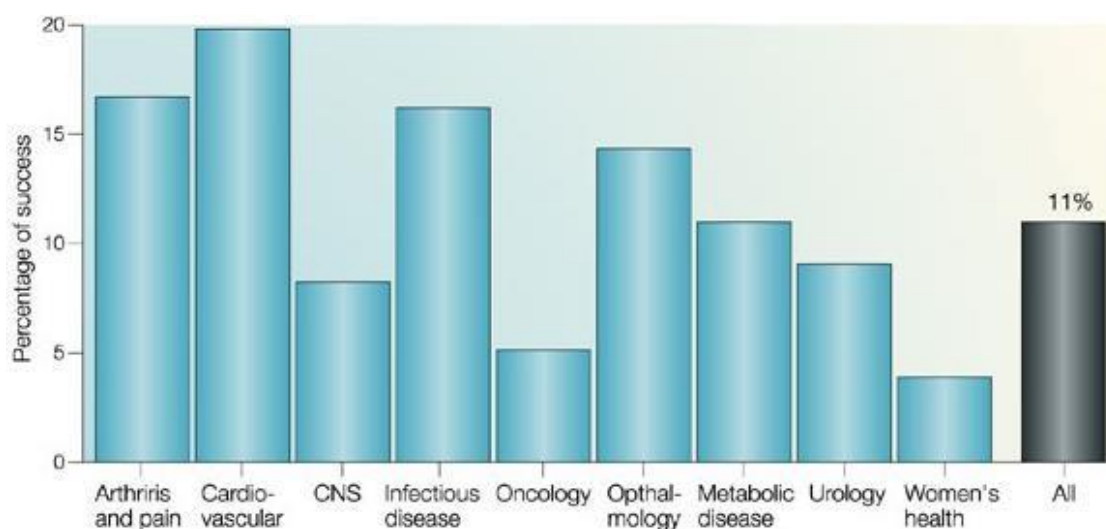


**Figure. 7.** Success rate of phase I clinical trials in obtaining marketing authorization for the ten largest pharmaceutical companies between 1991 and 2000. The success rate varies according to the pathologies targeted.

These low success rates can be explained in several ways: pharmaceutical research is currently focused on pathologies of great complexity (cancer, AIDS, etc.), competition between different pharmaceutical companies is increasing in parallel with standards of care and health authorities are becoming more demanding. In 1991, poor pharmacokinetic characteristics of drug candidates were the leading cause of clinical trial failure (40%). In 2000, pharmacokinetic problems represented only 10% of

clinical trial failures. Today, the main causes of failure during clinical trial phases are the lack of efficacy of compounds (30%) and their toxicity (30%). [6] The failures linked to the lack of efficacy of compounds are more frequent when the animal models used are not very predictive, in particular for pathologies of the central nervous system and cancers, inducing high failure rates in phases II and III (Figure 7) .[6]

### **I.3. Medicinal Chemists Today**

Medicinal chemists today are facing a serious challenge because of the increased cost and enormous amount of time taken to discover a new drug ,and also because of fierce competition amongst different drug companies.

Pharma Industry development became one of the important targets for different Governments in the last three decades, especially with the tremendous achievements of the multinational companies in this area of industry.

Challenges of this industry in third world have been increased; the discovery of a new active marketed molecule costs millions of USD, which increase the problem we are facing. Many worldwide companies have been merged to increase their ability in new drug discovery area. Most of them on the other hand adopted new technologies to discover and develop new drug entities, among these are computational and modeling techniques, which help in decreasing the time and cost of discovery researches, that's why importance of Computer Aided Drug Design and Molecular Modeling is increasing nowadays[6].

### **I.4 Conclusion**

It was discovered that chemical libraries were at the heart of the process of developing drug candidates. With the passage of time and ever-increasing storage capacities, the size of chemical libraries and the number of molecules available have grown significantly. The management and analysis of such a large amount of data necessitate the use of computer systems capable of implementing various data analysis and composition selection strategies. In the following section, we will introduce the field of discussing methods for responding to the issues raised in the previous section, putting the work of this thesis into context.

## References

- [1] C.P. Adams, V.V.J.H.a. Brantner, Estimating the cost of new drug development: is it really \$802 million?, 25 (2006) 420-428.
- [2] J.A.J.P. DiMasi, The value of improving the productivity of the drug development process, 20 (2002) 1-10.
- [3] J.A. DiMasi, R.W. Hansen, H.G.J.J.o.h.e. Grabowski, The price of innovation: new estimates of drug development costs, 22 (2003) 151-185.
- [4] C.P. Adams, V.V.J.H.e. Brantner, Spending on new drug development 1, 19 (2010) 130-141.
- [5] R.M.J.R.W.D.D. Rydzewski, Project Considerations, (2008) 175.
- [6] I. Kola, J.J.N.r.D.d. Landis, Can the pharmaceutical industry reduce attrition rates?, 3 (2004) 711-716.
- [7] H. Hernandez Guevara, F. Hervas, A. Tuebke, The 2011 EU Industrial R&D Investment Scoreboard, in, Joint Research Centre (Seville site), 2011.
- [8] S. Maslov, I.J.P.o.t.N.A.o.S. Ispolatov, Propagation of large concentration changes in reversible protein-binding networks, 104 (2007) 13655-13660.
- [9] H. Kitano, Towards a theory of biological robustness, in, John Wiley & Sons, Ltd Chichester, UK, 2007.
- [10] A.L.J.N.c.b. Hopkins, Network pharmacology: the next paradigm in drug discovery, 4 (2008) 682-690.
- [11] M. Soulie, G. Portier, L.J.P.e.u.j.d.l.A.f.d.u.e.d.l.S.f.d.u. Salomon, Oncological principles for local control of primary tumor, 25 (2015) 918-932.
- [12] M. Gérin, P. Gosselin, S. Cordier, C. Viau, P. Quénel, La référence bibliographique de ce document se lit comme suit: Gérin M, Band P (2003) Cancer. In: Environnement et santé publique-Fondements et.
- [13] H. Sung, J. Ferlay, R.L. Siegel, M. Laversanne, I. Soerjomataram, A. Jemal, F.J.C.a.c.j.f.c. Bray, Global cancer statistics 2020: GLOBOCAN estimates of incidence and mortality worldwide for 36 cancers in 185 countries, 71 (2021) 209-249.

## References

- [14] E. Apretna, F. Thiessard, G. Miremont-Salamé, F.J.O. Haramburu, *Pharmacovigilance, cancer et médicaments anticancéreux*, 6 (2004) 66-71.
- [15] N.T. Mason, N.I. Khushalani, J.S. Weber, S.J. Antonia, H.L. McLeod, Modeling the cost of immune checkpoint inhibitor-related toxicities, in, *American Society of Clinical Oncology*, 2016.
- [16] T.J. Yang, A.J.J.T.l.c.r. Wu, Cranial irradiation in patients with EGFR-mutant non-small cell lung cancer brain metastases, 5 (2016) 134.
- [17] A.D. McNaught, A. Wilkinson, *Compendium of chemical terminology. IUPAC recommendations*, (1997).
- [18] P.-H. Li, H. Jiang, W.-J. Zhang, Y.-L. Li, M.-C. Zhao, W. Zhou, L.-Y. Zhang, Y.-D. Tang, C.-Z. Dong, Z.-S.J.E.j.o.m.c. Huang, Synthesis of carbazole derivatives containing chalcone analogs as non-intercalative topoisomerase II catalytic inhibitors and apoptosis inducers, 145 (2018) 498-510.
- [19] A.M. Rahman, S.-E. Park, A.A. Kadi, Y.J.J.o.m.c. Kwon, Fluorescein hydrazones as novel nonintercalative topoisomerase catalytic inhibitors with low DNA toxicity, 57 (2014) 9139-9151.
- [20] M.D. Galsky, N.M. Hahn, B. Wong, K.M. Lee, P. Argiriadi, C. Albany, K. Gimpel-Tetra, N. Lowe, M. Shahin, V.J.C.c. Patel, *pharmacology*, Phase 2 trial of the topoisomerase II inhibitor, amrubicin, as second-line therapy in patients with metastatic urothelial carcinoma, 76 (2015) 1259-1265.
- [21] G. Capranico, J. Marinello, G.J.J.o.m.c. Chillemi, Type I DNA topoisomerases, 60 (2017) 2169-2192.
- [22] P. Meresse, E. Dechaux, C. Monneret, E.J.C.m.c. Bertounesque, *Etoposide: discovery and medicinal chemistry*, 11 (2004) 2443-2466.
- [23] B. Li, Z.-Z. Yue, J.-M. Feng, Q. He, Z.-H. Miao, C.-H.J.E.j.o.m.c. Yang, Design and synthesis of pyrido [3, 2- $\alpha$ ] carbazole derivatives and their analogues as potent antitumour agents, 66 (2013) 531-539.

## References

- [24] A.K. McClendon, N.J.M.R.F. Osheroff, M.M.o. Mutagenesis, DNA topoisomerase II, genotoxicity, and cancer, 623 (2007) 83-97.
- [25] N.J. Winick, R.W. McKenna, J.J. Shuster, N.R. Schneider, M.J. Borowitz, W.P. Bowman, D. Jacaruso, B.A. Kamen, G.R.J.J.o.c.o. Buchanan, Secondary acute myeloid leukemia in children with acute lymphoblastic leukemia treated with etoposide, 11 (1993) 209-217.
- [26] M.S. Christodoulou, F. Calogero, M. Baumann, A.N. García-Argáez, S. Pieraccini, M. Sironi, F. Dapiaggi, R. Bucci, G. Broggin, S.J.E.j.o.m.c. Gazzola, Boehmeriasin A as new lead compound for the inhibition of topoisomerases and SIRT2, 92 (2015) 766-775.
- [27] M.S. Christodoulou, N. Fokialakis, D. Passarella, A.N. García-Argáez, O.M. Gia, I. Pongratz, L. Dalla Via, S.A.J.B. Haroutounian, m. chemistry, Synthesis and biological evaluation of novel tamoxifen analogues, 21 (2013) 4120-4131.
- [28] M.S. Christodoulou, M. Zarate, F. Ricci, G. Damia, S. Pieraccini, F. Dapiaggi, M. Sironi, L.L. Presti, A.N. García-Argáez, L.J.E.j.o.m.c. Dalla Via, 4-(1, 2-diarylbut-1-en-1-yl) isobutyranilide derivatives as inhibitors of topoisomerase II, 118 (2016) 79-89.
- [29] N. Ferri, T. Radice, M. Antonino, E.M. Beccalli, S. Tinelli, F. Zunino, A. Corsini, G. Pratesi, E.M. Ragg, M.L.J.B. Gelmi, m. chemistry, Synthesis, structural, and biological evaluation of bis-heteroarylmaleimides and bis-heterofused imides, 19 (2011) 5291-5299.
- [30] H. Matsumoto, M. Yamashita, T. Tahara, S. Hayakawa, S.-i. Wada, K. Tomioka, A.J.B. Iida, m. chemistry, Design, synthesis, and evaluation of DNA topoisomerase II-targeted nucleosides, 25 (2017) 4133-4144.
- [31] M.S. Islam, S. Park, C. Song, A.A. Kadi, Y. Kwon, A.M.J.E.j.o.m.c. Rahman, Fluorescein hydrazones: A series of novel non-intercalative topoisomerase II $\alpha$  catalytic inhibitors induce G1 arrest and apoptosis in breast and colon cancer cells, 125 (2017) 49-67.
- [32] L. S. Tsutsumi, D. Gündisch, D.J.C.t.i.m.c. Sun, Carbazole scaffold in medicinal chemistry and natural products: a review from 2010-2015, 16 (2016) 1290-1313.
- [33] V.R. PO, M.P. Tantak, R. Valdez, R.P. Singh, O.M. Singh, R. Sadana, D.J.R.a. Kumar, Synthesis and biological evaluation of novel carbazolyl glyoxamides as anticancer and antibacterial agents, 6 (2016) 9379-9386.

## References

- [34] B. Maji, K. Kumar, M. Kaulage, K. Muniyappa, S.J.J.o.m.c. Bhattacharya, Design and synthesis of new benzimidazole–carbazole conjugates for the stabilization of human telomeric DNA, telomerase inhibition, and their selective action on cancer cells, 57 (2014) 6973-6988.
- [35] W. Wang, X. Sun, D. Sun, S. Li, Y. Yu, T. Yang, J. Yao, Z. Chen, L.J.C. Duan, Carbazole aminoalcohols induce antiproliferation and apoptosis of human tumor cells by inhibiting topoisomerase I, 11 (2016) 2675-2681.
- [36] A.J.E.j.o.m.c. Głuszyńska, Biological potential of carbazole derivatives, 94 (2015) 405-426.
- [37] Y. Funayama, K. Nishio, K. Wakabayashi, M. Nagao, K. Shimoi, T. Ohira, S. Hasegawa, N.J.M.R.F. Saijo, M.M.o. Mutagenesis, Effects of  $\beta$ - and  $\gamma$ -carboline derivatives on DNA topoisomerase activities, 349 (1996) 183-191.
- [38] Y. Hajbi, C. Neagoie, B. Biannic, A. Chilloux, E. Vedrenne, B. Baldeyrou, C. Bailly, J.-Y. Mérour, S. Rosca, S.J.E.j.o.m.c. Routier, Synthesis and biological activities of new furo [3, 4-b] carbazoles: Potential topoisomerase II inhibitors, 45 (2010) 5428-5437.
- [39] R. Macarron, M.N. Banks, D. Bojanic, D.J. Burns, D.A. Cirovic, T. Garyantes, D.V. Green, R.P. Hertzberg, W.P. Janzen, J.W.J.N.r.D.d. Paslay, Impact of high-throughput screening in biomedical research, 10 (2011) 188-195.
- [40] J.W.J.I.J.H.T.S. Noah, New developments and emerging trends in high-throughput screening methods for lead compound identification, 1 (2010) 141-149.
- [41] L.M. Mayr, D.J.C.o.i.p. Bojanic, Novel trends in high-throughput screening, 9 (2009) 580-588.
- [42] D.C. Swinney, J.J.N.r.D.d. Anthony, How were new medicines discovered?, 10 (2011) 507-519.
- [43] A. Golebiowski, S.R. Klopfenstein, D.E.J.C.o.i.c.b. Portlock, Lead compounds discovered from libraries: part 2, 7 (2003) 308-325.
- [44] A. Golebiowski, S.R. Klopfenstein, D.E.J.C.o.i.c.b. Portlock, Lead compounds discovered from libraries, 5 (2001) 273-284.

## References

- [45] S. Heller, A.J.J.o.C. McNaught, The status of the InChI project and the InChI trust, 2 (2010) 1-1.
- [46] D.C. Ince, L. Hatton, J.J.N. Graham-Cumming, The case for open computer programs, 482 (2012) 485-488.
- [47] S. Pickett, Multi-objective approaches to screening collection design and analysis of HTS data, in: ABSTRACTS OF PAPERS OF THE AMERICAN CHEMICAL SOCIETY, AMER CHEMICAL SOC 1155 16TH ST, NW, WASHINGTON, DC 20036 USA, 2005, pp. U770-U771.
- [48] S. Ekins, J.D. Honeycutt, J.T.J.D.d.t. Metz, Evolving molecules using multi-objective optimization: applying to ADME/Tox, 15 (2010) 451-460.
- [49] S.J. Lusher, R. McGuire, R. Azevedo, J.-W. Boiten, R.C. van Schaik, J.J.D.d.t. de Vlieg, A molecular informatics view on best practice in multi-parameter compound optimization, 16 (2011) 555-568.
- [50] M.S. Lajiness, M. Vieth, J.J.C.o.i.d.d. Erickson, development, Molecular properties that influence oral drug-like behavior, 7 (2004) 470-477.
- [51] I.J.M.r.r. Muegge, Selection criteria for drug-like compounds, 23 (2003) 302-321.
- [52] G. Vistoli, A. Pedretti, B.J.D.d.t. Testa, Assessing drug-likeness—what are we missing?, 13 (2008) 285-294.
- [53] M.-Q. Zhang, B.J.C.o.i.b. Wilkinson, Drug discovery beyond the ‘rule-of-five’, 18 (2007) 478-488.
- [54] P.D. Leeson, B.J.N.r.D.d. Springthorpe, The influence of drug-like concepts on decision-making in medicinal chemistry, 6 (2007) 881-890.
- [55] C.A. Lipinski, F. Lombardo, B.W. Dominy, P.J.J.A.d.d.r. Feeney, Experimental and computational approaches to estimate solubility and permeability in drug discovery and development settings, 23 (1997) 3-25.
- [56] D.F. Veber, S.R. Johnson, H.-Y. Cheng, B.R. Smith, K.W. Ward, K.D.J.J.o.m.c. Kopple, Molecular properties that influence the oral bioavailability of drug candidates, 45 (2002) 2615-2623.

## References

- [57] M.M. Hann, A.R. Leach, G.J.J.o.c.i. Harper, c. sciences, Molecular complexity and its impact on the probability of finding leads for drug discovery, 41 (2001) 856-864.
- [58] T.I. Oprea, A.M. Davis, S.J. Teague, P.D.J.J.o.c.i. Leeson, c. sciences, Is there a difference between leads and drugs? A historical perspective, 41 (2001) 1308-1315.
- [59] M.M. Hann, T.I.J.C.o.i.c.b. Oprea, Pursuing the leadlikeness concept in pharmaceutical research, 8 (2004) 255-263.
- [60] G.M. Keserü, G.M.J.n.r.D.D. Makara, The influence of lead discovery strategies on the properties of drug candidates, 8 (2009) 203-212.
- [61] A.L. Hopkins, C.R. Groom, A.J.D.d.t. Alex, Ligand efficiency: a useful metric for lead selection, 9 (2004) 430-431.
- [62] J.P. Hughes, S. Rees, S.B. Kalindjian, K.L.J.B.j.o.p. Philpott, Principles of early drug discovery, 162 (2011) 1239-1249.
- [63] A. Bender, J. Scheiber, M. Glick, J.W. Davies, K. Azzaoui, J. Hamon, L. Urban, S. Whitebread, J.L.J.C. Jenkins, Analysis of pharmacology data and the prediction of adverse drug reactions and off-target effects from chemical structure, 2 (2007) 861-873.
- [64] D. Wang, A. Bakhai, Clinical trials: a practical guide to design, analysis, and reporting, Remedica, 2006.
- [65] S.M. Paul, D.S. Mytelka, C.T. Dunwiddie, C.C. Persinger, B.H. Munos, S.R. Lindborg, A.L.J.N.r.D.d. Schacht, How to improve R&D productivity: the pharmaceutical industry's grand challenge, 9 (2010) 203-214.

## **Chapter II**

### **Part I: Computer in medicinal chemistry**

All theoretical research is underpinned by two essential motivations: understanding and forecasting, that is, understanding what has already been done and forecasting what may be achievable. The forecast answers questions like: "What would happen if ...?", Or "Can we do ...?" or "What would be the value of...?". The traditional answer would be to experiment. But at a time when the price of computer calculations is continually falling, while chemicals, devices, skilled labor, etc. continues to grow, it is increasingly interesting to exploit theoretical models of all kinds to help design new chemical species [1].

The ambition of a theoretical chemist is to be able to predict, confirm or reinterpret the experiment using molecular modeling. Indeed, the perseverance of researchers, and above all the power of their computer resources, play in favor of theoretical chemistry, and its field of application.

The research and synthesis of new chemical and biochemical compounds is often associated today with a study by molecular modeling. Molecular modeling is a commonly used methodology. For a little over thirty years, it has gradually established itself as a tool of choice for the discovery and oriented design of new active molecules. Previously, only systematic biological tests were performed on a large number of molecules and, often, only luck made it possible to highlight an interesting lead [2].

Molecular modeling is a tool for researchers concerned with the structure and reactivity of molecules. Knowing the structure of molecular edifices makes it possible to understand what is achieved in a physical, chemical or biological transformation. It can also make it possible to predict such transformations. Both understanding and forecasting are greatly facilitated when one can visualize the structures. A molecule is correctly described by its geometry and its thermodynamic properties. The visualization must account for all of these characteristics. The essential question is to represent a molecule on the screen as close as possible to "reality" [3].

### II.1 Theoretical Background for Quantum Mechanical Calculations

The goal of this chapter is to go over some uses of quantum mechanical calculations in medicinal chemistry and drug design. These introductions, on the other hand, will be kept to a bare minimum, focusing on the key differences between methodologies and their known strengths and shortcomings in respect to medicinal chemistry applications, with only one mathematical equation, probably to the relief of the majority of readers.

The Schrödinger equation is the foundation of quantum mechanics, and it has a simple eigenvalue problem form:

$$H\psi = E\psi$$

Even with today's computing power, this famous equation cannot be solved directly for anything greater than hydrogen. As a result, a number of assumptions were devised to allow for the quantum mechanical treatment of molecules of more immediate concern to most chemists.

For example, the Born–Oppenheimer approximation treats atom nuclei as fixed, and the Hartree–Fock (HF) approximation replaces the genuine electron–electron potential description with an effective potential, thus eliminating electron correlation. Another is the use of basis sets instead of actual electron integrals, which are designed to approximate the structure of orbitals. For ab initio computations, the quality of these basis sets is critical, and the larger they are and the more individual Gaussian functions they contain, the better. The utility and correctness of calculations based on these approximations are typically confirmed by comparison with experiment, especially for molecular geometries and properties such as dipole moments, and the findings are often surprisingly exact despite the use of these simplifications.

Some approximations, on the other hand, are more dubious, and the magnitude of inaccuracy imposed is frequently unknown. Despite the use of a variety of approximations, quantum mechanical calculations are often quite accurate and useful in answering questions and defining molecule structures, characteristics, and interactions that are crucial in medicinal chemistry. It should also be noted that some

of these questions, such as those relating to chemical reactivity, molecular properties such as nucleophilicity, electrophilicity, charge distribution, spin-orbit coupling, dipole, and higher multipole moments relating to polarizability, infrared, Raman, and NMR chemical shifts, circular dichroism, and magnetic susceptibility [4], must be answered in the affirmative, the computational and medicinal chemist's only choice for obtaining reliable predictions is quantum mechanical computations.

In contrast to molecular mechanics, quantum mechanical calculations are obtained directly from the physical rules that affect molecular structure through an approximate solution of the Schrödinger equation. Ab initio, DFT, and semiempirical approaches are the three types of methodologies available. While ab initio and density functional approaches do not need parametrization to solve the Schrödinger equation, semiempirical methods use parameters to avoid having to compute some of the time-consuming integrals that ab initio and DFT computations require. Furthermore, semiempirical approaches only consider the valence electrons, and despite having significantly fewer parameters than molecular mechanics methods, are also less comprehensible. All three approaches (ab initio, DFT, and semiempirical) produce a wave function that may be used to calculate all electrical properties [5].

### II.1.1 Molecularmechanics

#### II.1.1.1 Introduction

Molecular modellers usually have a different goal in mind: they want a force field that can be transmitted from molecule to molecule so that they may anticipate (for example, the shape of a new molecule) using data from other molecules. They use the bond notion and appeal to classical chemists' ideas that a molecule is made up of a collection of bonded atoms; a large molecule contains the same qualities as small molecules, and in various combinations [6].

Because of non-bonded van der Waals and Coulombic interactions, molecules are described in terms of "bonded atoms," which have been distorted from some idealized shape. The success of molecular mechanics models is determined by the geometrical parameters' great transferability from one molecule to the next, as well as the parameters' predictable dependency on atomic hybridization.

## Computer in medicinal chemistry

Carbon-carbon single bond lengths, for example, are typically in the tiny range of 1.45 to 1.55, and grow in length as the “p character” of the carbon hybrids increases. As a result, if the molecule has already been represented in terms of a certain valence structure, it is possible to make a pretty accurate “guess” about molecular geometry in terms of bond lengths, bond angles, and torsion angles. This group includes the vast majority of organic compounds.

The “energy” of a molecule in molecular mechanics is described as a sum of contributions from distortions in “ideal” bond distances (stretch contributions), bond angles (bond contributions), and torsion angles (torsion contributions), as well as contributions from “non-bonded” (van der Waals and Coulombic) interactions.

$$E = \sum_{\text{bonds}} \frac{k_l}{2} (l_i - l_{i,0})^2 + \sum_{\text{angles}} \frac{k_\theta}{2} (\theta_i - \theta_{i,0})^2 + \sum_{\text{torsions}} \frac{V_n}{2} (1 + \cos(n\omega - \gamma)) \\ + \sum_{i=1}^N \sum_{j>i}^N \left( 4\epsilon_{ij} \left[ \left( \frac{\sigma_{ij}}{r_{ij}} \right)^{12} - \left( \frac{\sigma_{ij}}{r_{ij}} \right)^6 \right] + \frac{q_i q_j}{4\pi\epsilon_0 r_{ij}} \right)$$

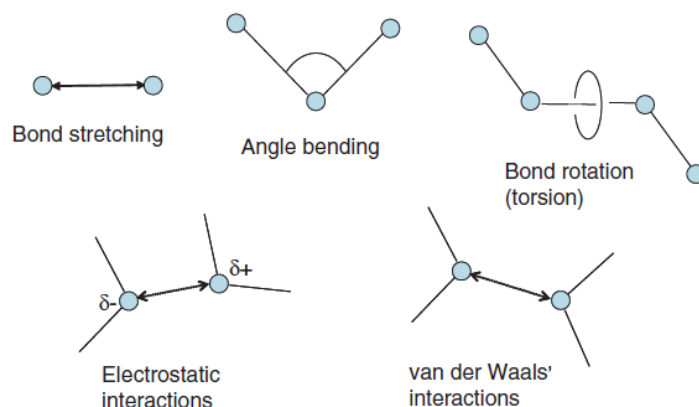


**Figure .8.** An illustration of the various terms that contribute to a typical force field.

### II.1.1.1.1 Elongation energy

Bonds between atoms in a molecular structure often tend to elongate or contract (Figure 9).

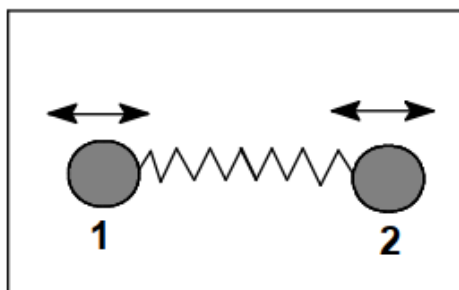


**Figure.9.** Elongation between two atoms.

This deformation is governed as a first approximation by the “Hooke” law of spring elongation. We can thus associate it with an energy of elongation of the form:

$$E(L) = 1/2[K_1(L-L_0)^2]$$

Where  $K_1$ : is the constant of elongation or constant of Hooke

$L_0$ : the length of the reference link.

$L$ : the length of the link in the model.

All of these elongation terms are summed over all of the bonds in the molecule.

A cubic term  $(L-L_0)^3$  is generally added for large deformations. The computation of this energy thus imposes to know at least the two indissociable parameters ( $K_1$  and  $L_0$ ) which represent a subset of the force field. Indeed, it emerges from the serial development of the mathematical expression of the Morse curve reflecting the existing interaction between two atoms according to their respective distance [7].

### II.1.1.1.2. Bending energy

The fluctuation of atoms around their equilibrium position generates a deformation of the valence angles (figure 10) [7].

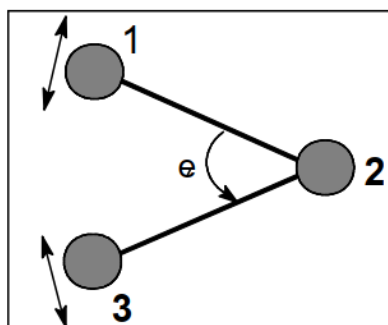


Figure.10. Deformation of valence angles.

This phenomenon is governed by a bending energy which can be expressed in the same forms as above, namely, to put it simply:

$$E(\theta) = 1/2[K_f(\theta - \theta_0)^2]$$

**K<sub>f</sub>**: bending constant

**θ<sub>0</sub>**: reference valence angle

**θ**: valence angle in the molecule

The pair (**K<sub>f</sub>**, **θ<sub>0</sub>**) represents here again a subset of the force field.

### II.1.1.1.3. Torsional energy

It concerns the dihedral angle formed by atoms 1-2-3-4. It notably takes into account the 3D structure of the molecule (figure 11) [7].

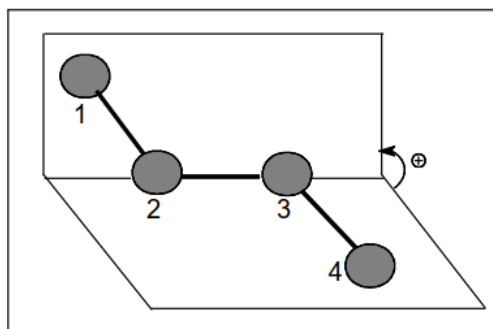


**Figure.11.** Dihedral angle formed by atoms 1-2-3-4.

The evaluation of this energy  $E(f)$  is done by a function developed in Fourier series.

$$E(f) = 1/2 [V_1(1+\cos f)+V_2(1 - \cos 2f)+V_3(1+\cos 3f)]$$

The dihedral angle ( $f$ ) defines the twist around link 2-3.

$V_1, V_2, V_3$  are the constants of the potential of torsional energy.

#### II.1.1.1.4. Van der Waals energy

This energy concerns atoms not linked to each other and not linked to a common atom [8]. It consists of two parts, one repellent and the other attractive, and can be expressed by the following equation[7]:

$$E(\text{vdw})= e^*[- C_1(r^*/r)^6 +C_2 \exp(-C_3(r/r^*))]$$

$e^*$  :energy parameter which characterizes the depth of the potential well at the distance  $r^*$ , also called "hardness".

$r^*$ : sum of the VdW radii of the interacting atoms.

$r$ : interatomic distance.

$C_1, C_2, C_3$ : constants of the force field.

We can therefore represent this energy as a function of the interatomic distance " $r$ " as follows:

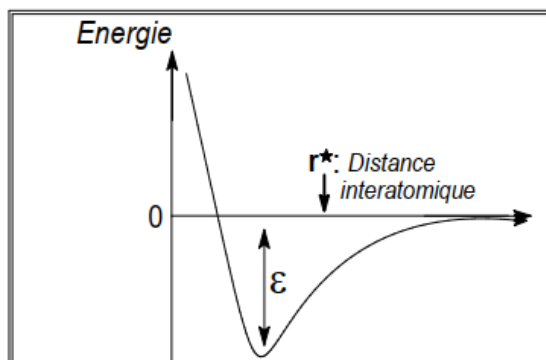


**Figure.12.** Van der Waals energy curve.

#### II.1.1.1.5. Electrostatic energy

The electrostatic interactions can, in certain cases, take on a considerable importance, in particular in the case of molecules comprising two or more heteroatoms, Meyer et al [9], have proposed to introduce an electrostatic term even for hydrocarbons. It can be expressed from the atomic charges or the dipole moments of each bond [7].

In the first case:

$$E(e) = \frac{q_1 q_2}{D \cdot d_{12}}$$

**D:** local dielectric constant of the medium

**$q_1 q_2$ :** atomic partial charges of atoms 1,2

**$d_{12}$ :** interatomic distance.

In the second:

$$E(e) = \frac{\mu_1 \mu_2 (\cos X - 3 \cos a_1 \cos b_2)}{D \cdot r^3}$$

**r**: distance between the midpoints of the two links

**$\mu_1$ ,  $\mu_2$** : respectively represent the dipole moments of the two bonds.

**X**: the angle between the two moment vectors.

**$a_1$ ,  $b_2$** : angles formed respectively between  $\mu_1$  and  $r$  and  $\mu_2$  and  $r$

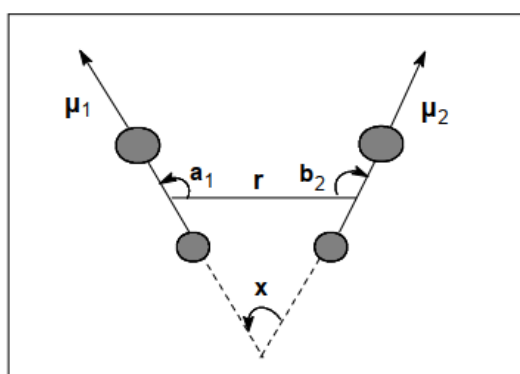


**Figure.13.**Electrostatic interactions between two atoms.

### II.1.1.2 Force Fields

Models of molecular mechanics differ in terms of the number and nature of terms they include, as well as the details of their parameterization. The combination of functional form and parameterization is known as a force field.

We have been vague so far about which variables are the ‘correct’ ones to take.

Chemists visualize molecules in terms of bond lengths, bond angles and dihedral angles, yet this information is also contained in the set of Cartesian coordinates for the constituent atoms. Both are therefore ‘correct’; it is largely a matter of personal choice and professional training.

Spectroscopists have developed systematic simplifications to the force fields in order to make as many as possible of the small terms vanish. If the force field contains only ‘chemical’ terms such as bond lengths, bond angles and dihedral angles, then it is referred to as a valence force field (VFF). There are other types of force fields in the literature, intermediate between the VFF and the general force field[10].

With these principles in mind, many different force fields were build in professional molecular modelling programs such as :Dreiding, MM1, MM2, Amber, OPLS...etc.

### II.1.1.3 Limitations of Molecular Mechanics

The primary advantage of molecular mechanics models, is their simplicity. Except for very small systems, computation cost is completely dominated by evaluation of non-bonded van der Waals and Coulombic terms, the number of which is given by the square of the number of atoms.

However, the magnitude of these terms falls off rapidly with increasing interatomic distance and, in practice, computation cost scales linearly with molecular size for sufficiently large molecules.

Molecular mechanics calculations may easily be performed on molecules comprising several thousand atoms. Additionally, molecular mechanics calculations are sufficiently rapid to permit extensive conformational searching on molecules containing upwards of 100-200 atoms.

The fact that molecular mechanics models are parameterized may also be seen as providing an advantage over quantum chemical models. It is possible, at least in principle, to construct molecular mechanics models which will accurately reproduce known experimental data, and hopefully will anticipate (unknown) data on closely-related systems.

There are important limitations of molecular mechanics models. First, they are limited to the description of equilibrium geometries and equilibrium conformations. Because the mechanics “strain energy” is specific to a given molecule (as a measure of how far this molecule deviates from its “ideal arrangement”). Two important exceptions are: calculations involving isomers with exactly the same bonding, e.g., comparison of cis and trans-2-butene, and conformational energy comparisons, where different conformers necessarily have exactly the same bonding.

In addition, molecular mechanics calculations reveal nothing about bonding or, more generally, about electron distributions in molecules. As will become evident later,

information about electron distributions is key to modeling chemical reactivity and selectivity. There are however, important situations where purely steric effects are responsible for trends in reactivity and selectivity, and here molecular mechanics would be expected to be of some value.

Finally, it needs to be noted that molecular mechanics is essentially an interpolation scheme, the success of which depends not only on good parameters, but also on systematics among related molecules. Molecular mechanics models would not be expected to be highly successful in describing the structures and conformations of “new”) unfamiliar (molecules outside the range of parameterization [11].

### II.1.2 Quantum Mechanics

#### II.1.2.1 Introduction

There are two approaches to quantum mechanics. One is to follow the historical development of the theory from the first indications that the whole fabric of classical mechanics and electrodynamics should be held in doubt to the resolution of the problem in the work of Planck, Einstein, Heisenberg, Schrödinger, and Dirac. The other is to stand back at a point late in the development of the theory and to see its underlying theoretical structure[12]. Quantum mechanics can be thought of roughly as the study of physics on very small length scales, although here are also certain macroscopic systems it directly applies to. In quantum mechanics, particles have wave like properties, and a particular wave equation, the Schrodinger equation, governs how these waves behave.

What are we looking for in quantum mechanics? we search to solve the equation of Schrödinger of an electron using Born-Oppenheimer approximations. We can use the Born- Oppenheimer approximation to construct an electronic Hamiltonian, which neglects the kinetic energy term of the nuclei since the weight of a typical nucleus is thousands of times greater than that of an electron.

$$\hat{H} = -\frac{\hbar^2}{2m_e} \nabla_i^2 + \sum_l \sum_{j < l} \frac{z_l z_j e^2}{r_{lj}} - \sum_l \sum_j \frac{z_l e^2}{r_{lj}} + \sum_j \sum_{i > j} \frac{e^2}{r_{ij}} \dots \dots \dots (8)$$

This Hamiltonian is used in the Schrödinger equation describing the motion of the electrons in the field of the fixed nuclei:

$$\hat{H}_{ele} \Psi_{ele} = E_{eff} \Psi_{ele} \dots\dots\dots (9)$$

Solving this equation for the electronic wave function will produce the effective nuclear potential function  $E_{eff}$  that depends on the nuclear coordinates and describes the potential energy surface of the system.

For bond electronic problem, should satisfy two requirements: antisymmetry and normalization. should change sign when two electrons of the molecule interchange and the integral of overall space should be equal to the number of electrons of the molecule [13].

### II.1.2.2 HF and DFT Methods

Many aspects of molecular structure and dynamics can be modeled using classical methods in the form of molecular mechanics and dynamics. The classical force field is based on empirical results, averaged over a large number of molecules. Because of this extensive averaging, the results can be good for standard systems, but there are many important questions in chemistry that cannot at all be addressed by means of this empirical approach. If one wants to know more than just structure or other properties that are derived only from the potential energy surface, in particular properties that depend directly on the electron density distribution, one has to resort to a more fundamental and general approach: quantum chemistry. The same holds for all non-standard cases for which molecular mechanics is simply not applicable [14]. In these methods, we use a set of basic functions from which we define all the molecular orbitals of the chemical system studied by LCAO approximation (linear combination of atomic orbitals).

The choice of basic orbital is essential for quantum chemistry calculations. There are two types of basic functions mainly used in electronic structure calculations: The Orbital Type Slater (STO) and those of Gaussian type (GTO).

The question here is, what basis to choose? Is it the biggest possible?

The answer is: all depend of your studied system.

With the increase in computing power, the minimum size of a calculation base is currently around 6-31G (d).

- Double zeta at least.
- With polarization at least on the heavy atoms.
- Diffuse functions in the case of an anion or a system performing hydrogen bonds or a system having free doublets.
- A good basis: 6-31G\*\* (or 6-31++G\*\*).
- A very good basis: 6-311 ++ G (2df,2p).

### II.1.2.3. Semi-empirical methods

In ab-initio methods almost all of the computation time is consumed by the calculations of the integrals, and in order to reduce this computation time, it is necessary to simplify the Roothann equations.

A semi-empirical method is a method in which part of the calculations necessary for Hartree-Fock calculations are replaced by parameters fitted to experimental values (the Hamiltonian is always parameterized by comparison with references). In general, all these methods are very precise for given families of products similar to those used for parameterization. Depending on the nature of the approximations used [15], there are several variants:

- **CNDO / 2:** (Complete Neglect of Differential Overlap) 1st semi-empirical method, it was proposed by Pople, Segal and Santry in 1965. Method presenting certain defects among others: it does not take into account Hund's rule.
- **INDO:** (Intermediate Neglect of Differential Overlap) Proposed by Pople, Beveridge and Dobosh in 1967. It distinguishes between singlet states and triplet states of a system by keeping the exchange integrals.
- **NDDO:** method (Neglect of Diatomic Differential Overlap): proposed by Pople in 1965. All bicenter bi-electronic integrals are retained.

- **MINDO / 3:** Proposed by Bingham, Dewar and Lo in 1975. Parameterization carried out with reference to experimental results and not to initial results, moreover the optimization algorithm used is very efficient (DavidonFletcher-Powell). However, it overestimates the heat of formation of unsaturated systems and underestimates that of molecules containing neighboring atoms with free pairs.
- **MNDO:** (Modified Neglect of Diatomic Overlap) Proposed by Dewar and Thiel in 1977. Methods based on the NDDO (Neglect of Diatomic Differential Overlap) approximation which consists in neglecting the differential overlap between atomic orbitals on different atoms. This method does not deal with transition metals and presents difficulties for conjugate systems.
- **AM 1:** (Austin Model 1) Proposed by Dewar in 1985. He tried to correct the flaws of MNDO.
- **PM 3:** (Parametric Method 3) Proposed by Stewart in 1989. Presents many points in common with AM1, moreover there is still a debate concerning the relative merits of parametrization of each of them.
- **SAM 1:** (Semi-ab initio Model 1) The most recent method proposed by Dewar in 1993. It includes electronic correlation.

### II.1.2.4 Limitations of Quantum Mechanics

However, these methods draw back calculations could be sometimes very long, the size of the system studied is limited and there must be very good calculation equipment.

One of the major challenges for computer-aided drug design is that it is not governed by the clear-cut rules of design in engineering, and hence, these methods do not produce a finished product by a fully prescribed procedure. The limitations of the rational computer aided drug design approach arise because of the complexity of the biological processes involved in drug actions and metabolism at the molecular level and the level of approximation that must be used in describing molecular properties.[5] However, there is clear evidence in the literature that molecular modeling and computer-aided drug design methods and also data analysis and chemoinformatics

approaches have become very important tools for drug discovery and that they have been successfully applied to medicinal chemistry,[16]particularly hit and lead generation as well as at the lead development stages.[17-19] Accepting that molecular modeling and chemoinformatics are useful techniques does however not sufficiently explain why one needs quantum mechanical methods. This has been done by Clark in a recent review, where he indicates that calculational techniques used to describe molecules should be able to describe the intermolecular interactions adequately.

[20]He points out that this can only be achieved if the molecular electrostatics and the molecular polarizability are described well. The former is responsible for strong interactions and the latter is directly related to dispersion and other weak interactions. Therefore, following this argument, molecular interactions of any type can only be described adequately and accurately by using quantum mechanical calculations.

We will divide the application of quantum mechanical calculations to answer medicinal chemistry related questions in a drug design environment into a total of four sections on:

- (1)the accurate calculation of molecular structure,
- (2) the calculation of quantum mechanical descriptors for prediction of molecular propertiesand QSAR, [21, 22]
- (3) applications to chemical reactivity and the investigation of enzyme mechanisms, and
- (4) the calculation of interactions and binding energies of small molecules with proteins.

This selection of topics is meant to reflect the main areas of interest to medicinal chemists working in the field of drug discovery. It is noted that although there are a great number of publications on the use of quantum mechanical calculations to medicinal chemistry, however, a large number of them are retrospective studies concerned with the validation of new technology rather than the prospective application to problem solving and design of new chemical entity (NCEs).

### II.2 Choice of method

The method of calculation chosen depends on what calculation needs to be done, as well as the size of the molecule. As far as size of molecule is concerned, ab initio calculations are limited to molecules containing tens of atoms, semi-empirical calculations on molecules containing hundreds of atoms, and molecular mechanics on molecules containing thousands of atoms.

Molecular mechanics is useful for the following operations or calculations: [23]

- Energy minimization ;
- Identifying stable conformations;
- Energy calculations for specific conformations;
- Generating different conformations;
- Studying molecular motion.

Quantum mechanical methods are suitable for calculating the following:

- Molecular orbital energies and coefficients;
- Heat of formation for specific conformations;
- Partial atomic charges calculated from molecular orbital coefficients;
- Electrostatic potentials;
  
- Dipole moments;
- Transition state geometries and energies;
- Bond dissociation energies.

### II.3 Minima search method

#### II.3.1 Introduction

Minimization sometimes results in hydrogens and doublets arranged around the atom in impossible structural positions. This is often due to improper initial movement of these light atoms when a strongly distorted structure is introduced.

This can also happen if you start with a planar structure. This is why the program performs a "second pass" of minimization after having repositioned the light atoms.

## Computer in medicinal chemistry

Another difficulty of minimization concerns the problem of the local minimum. The constrained optimization routines indeed have the unfortunate tendency to find a minimum energy closest to the input structure [24].

In general, bond distances and angles are properly minimized, so the local minimum problem can boil down to optimizing dihedral angles (it takes a lot more energy to deform a bond or valence angle by compared to a dihedral angle). The following approaches aim to extract the molecule from its potential well.

Almost all minimization methods have at least one point in common: we start at a given place in the hypersurface and work our way down to the nearest minimum, without knowing whether this minimum is local or absolute. We must therefore present to the computer several starting conformations, in the form of internal coordinates, taking inspiration from molecular models [7].

### II.3.2 Minimization algorithms

For a molecule comprising  $N$  atoms, the function to be minimized therefore comprises  $3N$  variables. Such a function generally comprises a global minimum and local minima.

From the initial geometry, we look for the set of Cartesian coordinates which reduces to a minimum the sum of all the energy contributions.

In principle, it suffices to take the first derivative of the steric energy with respect to each of the degrees of freedom of the molecule and to find the place on the energetic hypersurface where, for each coordinate  $r_i$ ,  $(dE / dr_i) = 0$ .

The procedures to achieve this goal are of two types: Some use only the slope of the surface (first derivative), others, both this slope and the curvature of the surface (the first and second derivatives).

#### II.3.2.1 The "steepest descent" method

The first minimization program that can perform geometry optimization is due to Wiberg[25] and uses the steepest descent method. After having calculated the energy

corresponding to an initial geometry, we move each atom individually according to its three Cartesian coordinates and we recalculate the energy after each displacement. This amounts to calculating the first derivative only. Then we move all the atoms over a distance that depends on  $(dE / dri)$ , and so on. This algorithm will therefore follow the direction imposed by the dominant interatomic forces.

This is why it proves to be very effective in removing bad contacts or the main stereochemical problems which exist in the coarse coordinates of a crystalline or modeled structure, while disturbing the latter very little.

However, this random method is generally long towards the end of each minimization cycle and convergence becomes very slow beyond the first cycles (oscillating phenomena, energy rise).

In fact, the method consists in finding the direction of the greatest slope during which the objective function  $F(x)$  decreases the most rapidly. The direction followed will be that indicated by the opposite of the energy gradient, i.e. the direction of the greatest slope of the energy function, which is the direction in which the energy decreases the fastest, at least locally.

### II.3.2.2. The conjugate gradient method

This method, based on the same principle as the previous one (direction opposite to the energy gradient), also takes into account the previous steps, in order to more precisely determine the direction and the pitch. For a quadratic energy surface, function of  $3N$  variables, this method converges in  $3N$  not [26].

It retains good efficiency, but is more costly in computation time (a factor of 2 compared to "steepest descent"). The step is adjusted at each cycle to obtain the best reduction in energy. The interest of this algorithm is to avoid an oscillatory behavior around the minimum and to accelerate the convergence. However, it turns out to be less efficient or even unusable (no convergence) for structures which present a lot of bad contacts, such as structures averaged over the trajectory of a molecular dynamic.

### **II.3.2.3. The Newton-Raphson method.**

An additional improvement of convergence can still be obtained by having recourse to a quadratic approximation  $Q$  of the function  $F$ , obtained by development in series of Taylor [27].

The method consists in seeking at each step the minimum of the development at order 2 of the function  $F$ . This method known as "Newton-Raphson", uses the second derivatives. Now we use this optimization technique instead. It evaluates the second derivatives of molecular energy with respect to the geometric parameters and therefore converges more quickly.

In summary, the complete optimization according to the Newton Raphson method requires calculating the complete matrix of second derivatives (matrix of force constants). This matrix contains  $3N \times 3N$  elements for a molecule of  $N$  atoms. The  $3N$  dimensions correspond to the three degrees of motion for each atom.

The optimization of the geometry however requires only  $3N-6$  degrees of freedom since the three translations and the three rotations are not accompanied by changes of energy. The force constants are then manipulated in the form of a matrix of second derivatives.

### **II.3.2.4. The simulated annealing method.**

The methods that we have just described have the particularity of making the function  $F$  decrease at each step; these methods cannot thus escape the local minimum close to the starting structure and consequently have a radius of convergence always restricted. The "anneal" simulated annealing method, developed by Kirkpatrick [28], allows the  $F$  function to increase momentarily in order to cross energy barriers and fall back to a deeper minimum.

The crossing of these barriers makes it possible to go beyond the local minima in the vicinity of the initial structure to explore more extensively the accessible

conformational space, in order to discover deeper minima and more distant from the initial structure than the minima. local.

In conclusion, a minimizer is a mathematical black box which remains an important tool in the search for a minimum of energy. In general, several minimizers are used. We go to a second or a third if it does not converge quickly enough. Everything also depends on the number of variables or the number of variations in the connection angle introduced.

### II.4 Molecular Modeling

#### II.4.1 Elements of Computational Chemistry

##### II.4.1.1 Drawing chemical structures

Various software packages, such as ChemDraw, Hyperchem, MarvinSketch, ChemWindow, and IsisDraw, are available which can be used to construct diagrams quickly and to a professional standard.

For example, the diagrams in this thesis have all been prepared using the Hyperchem package. Some drawing packages are linked to other items of software which allow quick calculations of various molecular properties. For example, the following properties for '**adrenaline**' were obtained using Hyperchem and, gaussian: the structure's correct IUPAC chemical name, molecular formula, molecular weight, exact mass, and theoretical elemental analysis. It was also possible to get calculated predictions of the compound's  $^1\text{H}$  and  $^{13}\text{C}$  nuclear magnetic resonance (NMR) chemical shifts, Energies of the HOMO and LUMO, melting point, freezing point, log *P* value, molar refractivity, and heat of formation ect...( Fig.14)

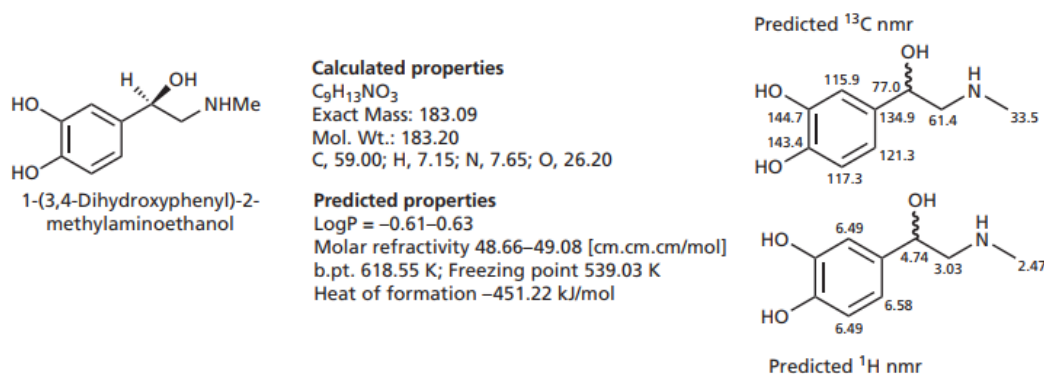


Figure .14. Drawing chemical structures.

A vast number of organic molecules are known. In order to distinguish one from another, chemists give them names. There are two kinds of names: trivial and systematic. Trivial names are often brand names (such as adrenaline). Trivial names don't give any real clue as to the structure of a molecule, unless you are the recipient of divine inspiration. The IUPAC systematic name for **adrenaline** is 1-(3,4-dihydroxyphenyl)-2-methylaminoethanol. Any professional scientist with training in chemistry would be able to translate the systematic name into (Figure 14).

There are various conventions that we can follow when drawing chemical structures, but the conventions are well understood amongst professionals. First of all, we haven't shown the hydrogen atoms attached to the benzene ring (or indeed the carbon atoms within), and we have taken for granted that we understand that the normal valence of carbon is four. Everyone understands that hydrogens are present, and so we needn't clutter up an already complicated drawing.

In the Figure 14 the benzene ring as alternate single and double bonds, yet we understand that the C—C bonds in benzene are all the same. This may not be the case in the molecule shown; some of the bonds may well have more double bond character than others and so have different lengths, but once again it is a well-understood convention. Sometimes a benzene ring is given its own symbol Ph or  $\Phi$ . Then again, we drawn the NHMe and the OH groups as 'composites' rather than showing the

individual O–H and N–H bonds, and so on. We followed to some extent the convention that all atoms are carbon atoms unless otherwise stated.

Much of this is personal preference, but the important point is that no one with a professional qualification in chemistry would mistake this drawing for another molecule. Equally, given the systematic name, no one could possibly write down an incorrect molecule.

The aim of this chapter is to show how chemistry is a well-structured science, with a vast literature. There are a number of important databases that contain information about syntheses, crystal structures, physical properties and so on. Many databases use a molecular structure drawing as the key to their information, rather than the systematic name. Structure drawing is therefore a key chemical skill.

### II.4.1.2 Three-dimensional structures

Molecular modelling software allows the chemist to construct a three-dimensional (3D) molecular structure on the computer. There are several software packages available, such as Chem3D, Alchemy, Sybyl, Hyperchem, Discovery Studio Pro, Spartan, and CAChe. The 3D model can be made by constructing the molecule atom by atom, and bond by bond. It is also possible to automatically convert a two-dimensional (2D) drawing into a 3D structure, and most molecular modelling packages have this facility. For example, the 2D structure of adrenaline in Fig. 15 was drawn in ChemDraw, then copied and pasted into Chem3D, resulting in the automatic construction of the 3D model shown. The 3D structures of a large number of small molecules can also be accessed from the Cambridge Structural Database (CSD) and downloaded. This database contains over 200,000 molecules which have been crystallized and their structure determined by X-ray crystallography.

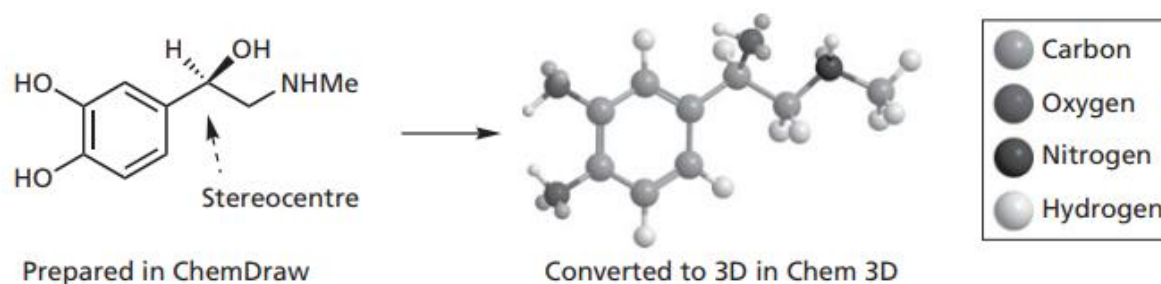


Figure .15. Conversion of a 2D drawing to a 3D model.

### II.4.1.3 Molecular Structure Databases

Molecular geometries can be determined for gas-phase molecules by microwave spectroscopy and by electron diffraction. In the solid state, the field of structure determination is dominated by X-ray and neutron diffraction and many crystal structures are known. Also, nuclear magnetic resonance (NMR) also has a role to play, especially for proteins.

Over the years, a vast number of molecular structures have been determined and there are several well-known structural databases. One is the Cambridge Structural Database (CSD)(<http://ccdc.cam.ac.uk>), which is supported by the Cambridge Crystallographic Data Centre (CCDC). The CCDC was established in 1965 to undertake the compilation of a computerized data base containing comprehensive data for organic and metal-organic compounds studied by X-ray and neutron diffraction. At the time of writing, there are some 272 000 structures in the database[29].

CCDC  FIZ Karlsruhe  
Leibniz Institute for Information Infrastructure

CSD Entry: ABAFOA Sign In

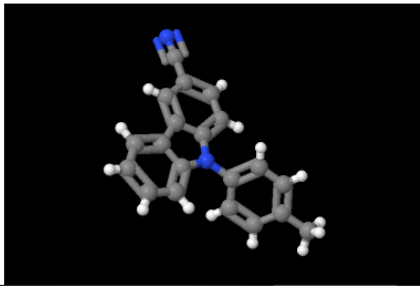
Simple Search | Structure Search | Unit Cell Search | Formula Search

Your query was: Compound name: carbazole and the search returned more than 30 records. Back to Search List | Modify Search | New Search

Results	
<input checked="" type="checkbox"/> Database Identifier	Deposition Number
<input checked="" type="checkbox"/> ABAFOA	850666
<input checked="" type="checkbox"/> ABEDOE	2082732
<input checked="" type="checkbox"/> ABEOFG	2087211
<input checked="" type="checkbox"/> ABEFUM	2087213
<input checked="" type="checkbox"/> ABEGEX	2087215
<input checked="" type="checkbox"/> ABEHAS	817867
<input checked="" type="checkbox"/> ABEJOK	2087216
<input checked="" type="checkbox"/> ABEPON	251749
<input checked="" type="checkbox"/> ABIWIU	1475008

ABAFOA : 9-(4-Methylphenyl)-9H-carbazole-3-carbonitrile  
Space Group: P  $\bar{1}$  (2), Cell: a 8.6031(3)Å b 8.8247(3)Å c 10.4609(4)Å,  $\alpha$  80.514(2)°  $\beta$  87.499(2)°  $\gamma$  72.114(2)°

3D viewer



Chemical diagram

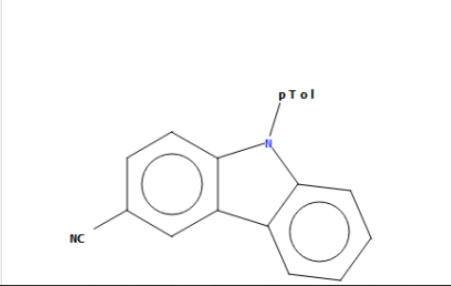


**Figure.16.** The Cambridge Crystallographic Data Centre (CCDC).

For each entry in the CSD, three types of information are stored. First, the bibliographic information: who reported the crystal structure, where they reported it and so on. Next comes the connectivity data; this is a list showing which atom is bonded to which in the molecule. Finally, the molecular geometry and the crystal structure. The molecular geometry consists of cartesian coordinates. The database can be easily reached through the Internet, but individual records can only be accessed on a fee-paying basis.

The Protein Data Bank (PDB) is the single worldwide repository for the processing and distribution of three-dimensional biological macromolecular structural data. It is operated by the Research Collaboratory for Structural Bioinformatics[30].

At the time of writing, there were 19749 structures in the data bank, relating to proteins, nucleic acids, protein–nucleic acid complexes and viruses. The databank is available free of charge to anyone who can navigate to their site

## Computer in medicinal chemistry

<http://www.rcsb.org/>. Information can be retrieved from the main website. A four-character alphanumeric identifier, such as 1PCN, represents each structure. The PDB database can be searched using a number of techniques, all of which are described in detail at the homepage.

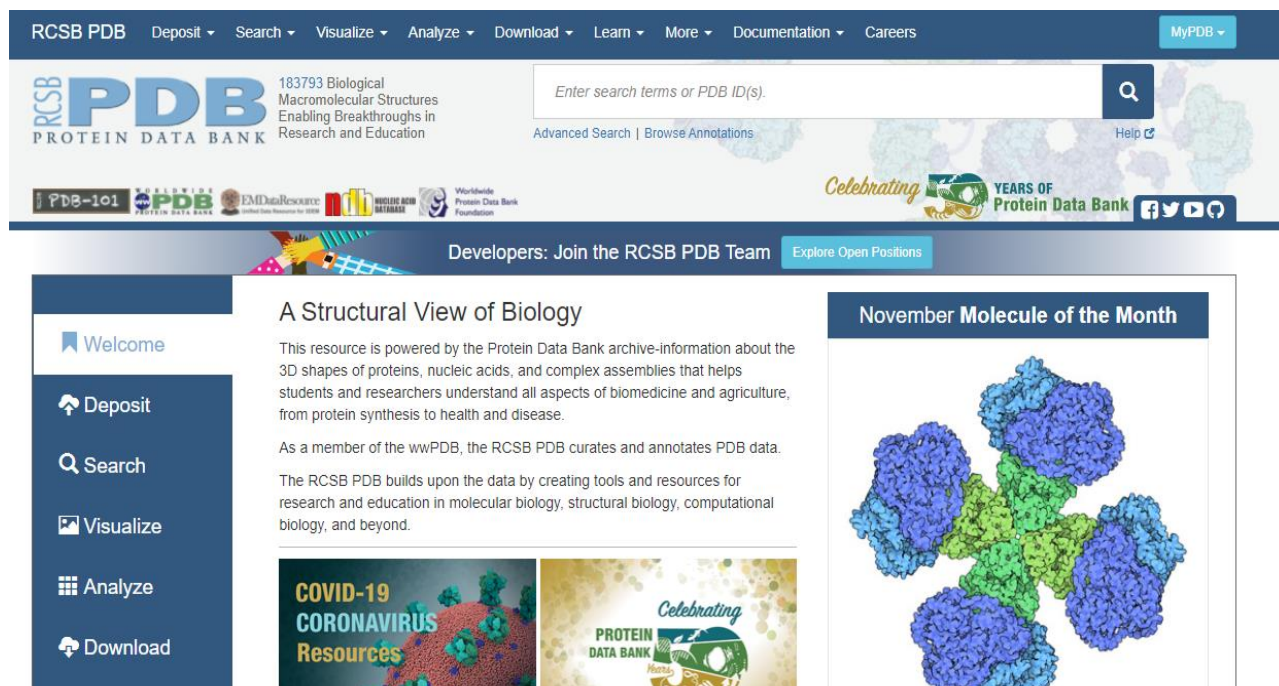


**Figure.17.**TheProteinDataBank(PDB).

### II.4.1.4 Energy minimization

Whichever software program is used to create a 3D structure, a process called energy minimization should be carried out once the structure is built. This is because the construction process may have resulted in unfavorable bond lengths, bond angles, or torsion angles. Unfavorable non-bonded interactions may also be present (i.e. atoms from different parts of the molecule occupying the same region of space).<sup>[14]</sup>The energy minimization process is usually carried out by a molecular mechanics program which calculates the energy of the starting molecule, then varies the bond lengths, bond angles, and torsion angles to create a new structure. The energy of the new structure is calculated to see whether it is energetically more stable or not. If the

starting structure is inherently unstable, a slight alteration in bond angle or bond length will have a large effect on the overall energy of the molecule resulting in a large energy difference ( $\Delta E$ ; Fig. 18 ).

The program will recognize this and carry out more changes, recognizing those which lead to stabilization and those which do not. Eventually, a structure will be found where structural variations result in only slight changes in energy—an energy minimum. The program will interpret this as the most stable structure and will stop at that stage.

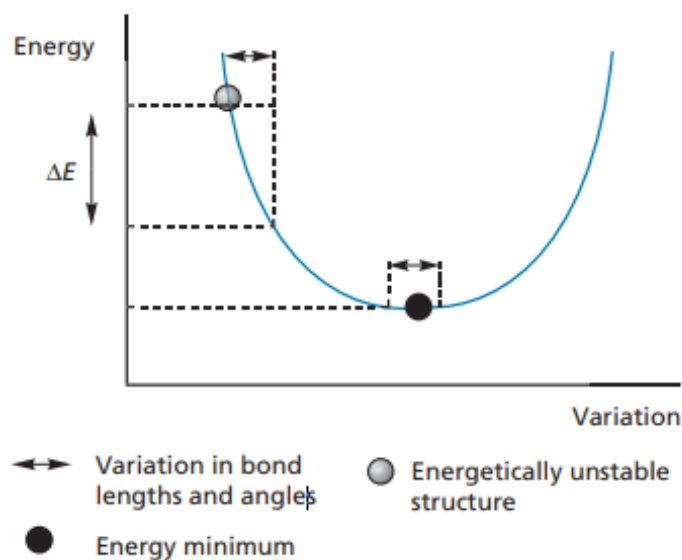


**Figure .18.** Diagram of energy minimization.

### II.3.1.5 Molecular dimensions

Once a structure has been energy minimized, it can be rotated in various axes to study its shape from different angles. It is also possible to display the structure in different formats (i.e. cylindrical bonds, wire frame, ball and stick, space-filling; Fig. 19).

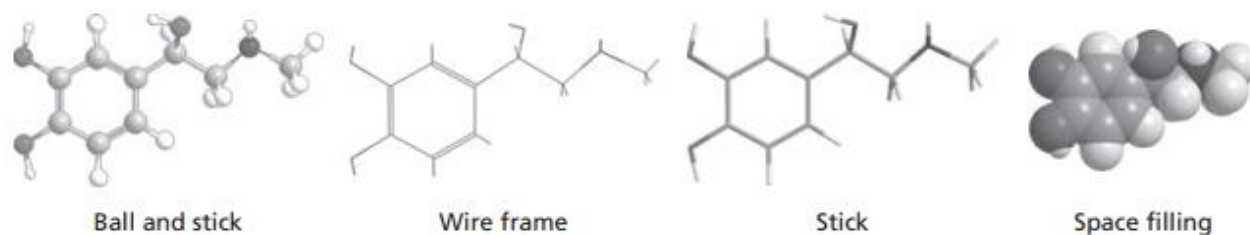


**Figure .19.** Different methods of visualizing molecules.

Once a 3D model of a structure has been constructed, it is a straightforward procedure to measure all of its bond lengths, bond angles, and torsion (or dihedral) angles. These values can be read from tables or by highlighting the relevant atoms and bonds on the structure itself. The various bond lengths, bond angles, and torsion angles measured for adrenaline are illustrated in Fig. 20. It is also a straightforward process to measure the separation between any two atoms in a molecule.

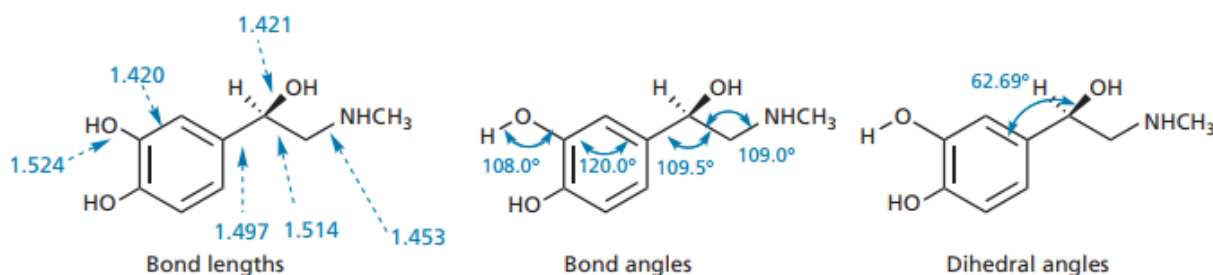


**Figure .20.** Molecular dimensions for adrenaline (3D Hyperchem).

### II.4.2 Molecular properties

Various properties of the 3D structure can be calculated once it has been built and minimized. For example, the steric energy is automatically measured as part of the minimization process and takes into account the various strain energies within the molecule, such as bond stretching or bond compression, deformed bond angles, deformed torsion angles, non-bonded interactions arising from atoms which are too

close to each other in space, and unfavorable dipole–dipole interactions. The steric energy is useful when comparing different conformations of the same structure, but the steric energies of different molecules should not be compared.

### II.4.2.1 Geometric Parameters

#### II.4.2.1.1 Bond length

Is the distance between atomic centers involved in a chemical bond. The notion of bond length is defined differently in various experimental methods of determination of molecular geometry; this leads to small (usually 0.01 – 0.02 Å) differences in bond lengths obtained by different techniques. For example, in gas-phase electron-diffraction experiments, the bond length is the interatomic distance averaged over all occupied vibrational states at a given temperature. In an X-ray crystal structural method, the bond length is associated with the distance between the centroids of electron densities around the nuclei. In gas-phase microwave spectroscopy, the bond length is an effective inter atomic distance derived from measurements on a number of isotopic molecules, etc[31].

#### II.4.2.1.2 Valence angle

The shape of a molecule is determined by its Valence angles, the angles made by the lines joining the nuclei of the atoms in the molecule. The bond angles of a molecule, together with the bond lengths, define the shape and size of the molecule. In Figure 21, we can see that there are six bond angles Cl-C ClinCCl<sub>4</sub>, all of which have the same value. That bond angle, 109.5°, is characteristic of a tetrahedron. In addition, all four C-Cl bonds are of the same length (1.78 Å). Thus, the shape and size of CCl<sub>4</sub> are completely described by stating that the molecule is tetrahedral with C-Cl bonds of length 1.78 Å[31].

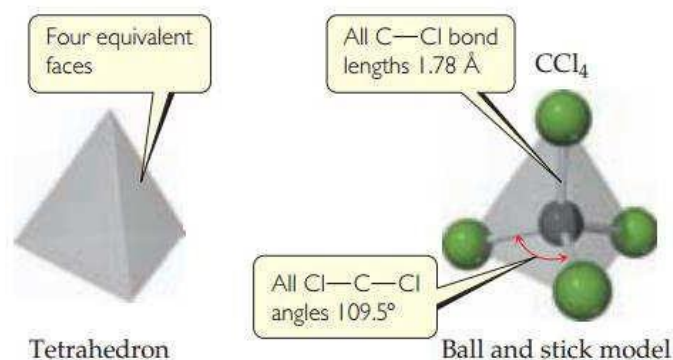


Figure .21. Tetrahedral shape of CCl<sub>4</sub>.

### II.4.2.1.3 Dihedral Angle (Torsion angle)

In a chain of atoms A-B-C-D, the dihedral angle between the plane containing the atoms A,B,C and that containing B,C,D. In a Newman projection (Fig.22) the torsion angle is the angle (having an absolute value between 0° and 180°) between bonds to two specified (fiducial) groups, one from the atom nearer (proximal) to the observer and the other from the further (distal) atom. The torsion angle between groups A and D is then considered to be positive if the bond A-B is rotated in a clockwise direction through less than 180° in order that it may eclipse the bond C-D: a negative torsion angle requires rotation in the opposite sense[31].

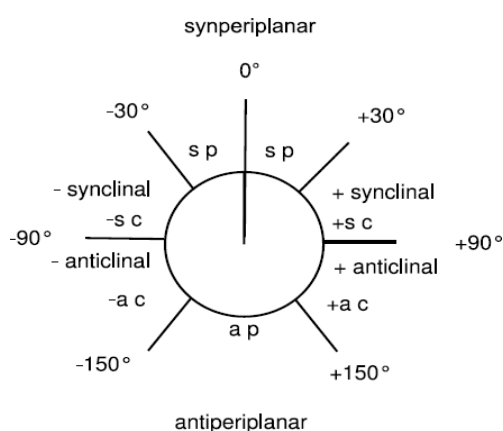


Figure .22. Newman projection.

Other properties for the structure can be calculated, such as Atomic charges, the predicted electrostatic potential, Fukui function, and infrared vibrational frequencies. Some of these are described in the following sections:

### II.4.3 Electronic Parameters

#### II.4.3.1 Atomic charges

A main problem in comparing different point-charge models is the missing of clear criterion for the quality of the charges. This is probably the reason why so many charge models have been suggested such as:

- CHelpG: Produce charges fit to the electrostatic potential at points selected according to the CHelpG scheme.
- NBO: Requests a full Natural Bond Orbital analysis.
- Mulliken: retains only the density terms involving pairs of basic functions on different centers. HLY: Hu, Lu, and Yang charge fitting method.

Furthermore, different applications put different demands on the charges. For example, in molecular dynamics, molecules move, so the charges must be able to describe the electrostatics properly in all accessible points in the phase space, and they should also be invariant to changes in the internal coordinates of the molecule [32-34].

#### II.4.3.2 Molecular electrostatic potentials

The molecular electrostatic potential (MESP) surface which is a plot of electrostatic potential mapped onto the iso-electron density surface [35], the importance of the MESP lies in the fact that it simultaneously displays the molecular size and shape as well as positive, negative and neutral electrostatic potential regions in terms of the electrostatic surface, which explain the investigation of the molecular structure with its physiochemical property relationships also be useful in identifying how compounds with different structures might line up to interact with corresponding electron rich and electron-poor areas in a binding site [36, 37].

An example of how electrostatic potentials have been used in drug design can be seen in the design of the **cromakalim** analogue (II; Fig.23), where the cyano aromatic ring

was replaced by a pyridine ring. This was part of a study looking into analogues of **cromakalim** which would have similar antihypertensive properties, but which might have different pharmacokinetics. In order to retain activity, it was important that any replacement heteroaromatic ring was as similar in character to the original aromatic ring as possible. Consequently, the MEPs of various bicyclic systems were calculated and compared with the parent bicyclic system (III; Fig. 24).

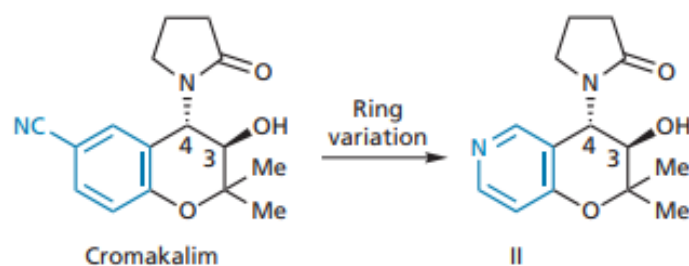


**Figure .23.** Ring variation on cromakalim.

In order to simplify the analysis, the study was carried out in 2D within the plane of the bicyclic systems, and maps were created showing areas of negative potential (Fig.25). The contours represent the various levels of the MEP and can be taken to indicate possible hydrogen bonding regions around each molecule. The analysis demonstrated that the bicyclic system (IV) had similar electrostatic properties to (III), resulting in the choice of structure (II) as an analogue.

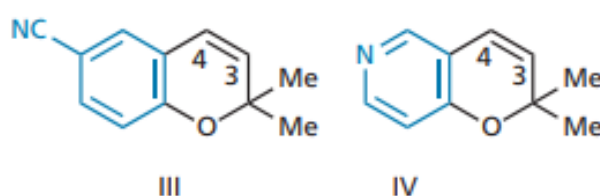


**Figure .24.** Bicyclic models in cromakalim study.

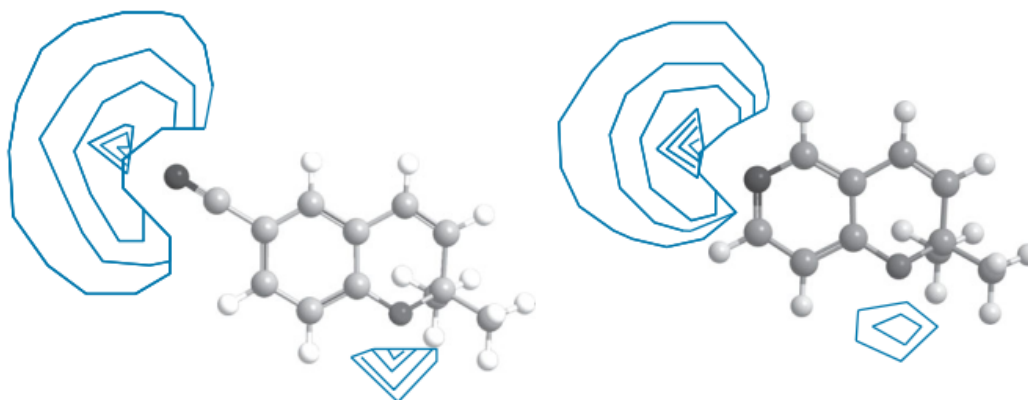


**Figure 25.** Molecular electrostatic potentials (MEPs) of bicyclic models (III) and (IV).

### II.4.3.3 Molecular orbitals

The most important orbitals in a molecule are the frontier molecular orbitals, called highest occupied molecular orbital (HOMO) which explains the ionization energy and lowest unoccupied molecular orbital (LUMO) which explains the electron affinity in a molecule.

These orbitals determine the way the molecule interacts with other species including the interactions between a ligand and its receptor [38]. Whereas, electrophilic and nucleophilic attack will most likely occur at atoms where the coefficients of the corresponding atomic orbitals in HOMO and LUMO, respectively, are large [39]. For example, ethene can be shown to have 12 molecular orbitals. The highest occupied molecular orbital (HOMO) and lowest unoccupied molecular orbital (LUMO) are shown in Fig. 26.

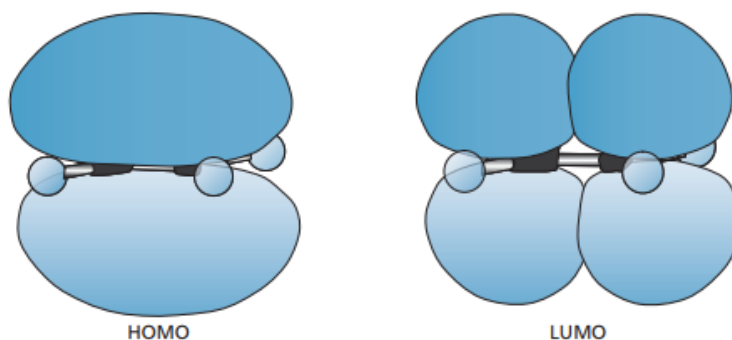


**Figure .26.**HOMO and LUMO molecular orbitals for ethene.

#### II.4.3.4 Fukui functions

The Fukui functions are some of these indexes. They represent a local reactivity of the studied compounds. They are given by [40]:

$$\vec{f}(r) = \left( \frac{\partial \rho(r)}{\partial N} \right) v(r)$$

where  $\rho(r)$  is the electronic density,  $N$  is the number of electrons and  $v(r)$  is a constant external potential. The reactivity of an atom  $k$  in a molecule can be described, by a condensed Fukui function  $f_k$ . As  $\rho(r)$  is a discontinuous function of  $N$ , Yang and Parr [41, 42] have proposed approximated atomic indices  $f_k$  by applying the finite difference approximation to the condensed electronic population on any atom. Three indices were defined to describe nucleophilic, electrophilic, and radical attack. These can be written respectively as:

$$f_+(A) = [q_{N+1}(A) - q_N(A)]$$

$$f_-(A) = [q_N(A) - q_{N-1}(A)]$$

$$f_0(A) = [q_{N+1}(A) - q_{N-1}(A)] / 2$$

$q_k(N)$ : electronic population of  $k$  atom in neutral molecule.

$q_k(N+1)$ : electronic population of  $k$  atom in anionic molecule.

$q_k(N-1)$ : electronic population of  $k$  atom in cationic molecule.

In this approximation, the indices depend widely on the used population analysis approach. The electronic population around an atom  $k$  can be evaluated using Mulliken[43], Hirshfield[44], or natural orbital [45]approximations. These indices are some of the widely used local density functional descriptors to model chemical reactivity and site selectivity [41, 46]. The atom with the highest Fukui indices is the most reactive compared to the other atoms in the molecule.

### II.5. Studies of vibrational properties

#### II.5.1. Introduction

Molecular modeling is essential for the interpretation and understanding of experimental observations. In the molecular domain, all properties are related to the nature and shape of the molecule. Being able to optimize the geometry of a molecule by a theoretical model (quantum chemistry methods) is to approach its molecular conformation observed experimentally [47, 48].

The object of this part of our work, which was oriented towards the search for a molecular conformation of the calculated indole similar to that given by the experiment, is to make a contribution to the understanding of the structural, vibrational properties and electronics to exhibit the most stable molecular conformation and also the arrangement and atomic environment of carbazole.

#### II.5.2. Theoretical aspects of infrared vibration spectroscopy

The movements of atoms in a molecule can be classified into three categories:

translations, rotations and vibrations. Nowadays, studies by vibrational spectroscopy are, more and more, supplemented by calculations of quantum chemistry [49, 50].

In this case, the contribution of molecular modeling is very important to understand reaction mechanisms or have access to chemical properties. Indeed, the methods of quantum chemistry make it possible to model a very large number of quantities characteristic of atomic or molecular systems or to simulate a wide variety

of reaction processes. Also, the combination of these two techniques is proving to be very powerful in explaining mechanistic details at the molecular level [51].

The main purpose of vibrational spectroscopy is the determination of the vibrational frequencies of a molecule. These frequencies depend on the mass of the atoms involved in the normal mode of vibration as well as the strength of the interatomic bonds. Therefore, precise information about the structure of a molecule can be deduced from a vibrational spectrum [52, 53].

Molecular vibrations take place at different frequencies ( $\nu$  vib) which depend on the nature of the bonds as well as their environment. These frequencies correspond to the infrared range of electromagnetic radiation [54].

### II.5.3. Principle of infrared spectroscopy

#### II.5.3.1. Electromagnetic radiation

Electromagnetic radiation consists of a beam of particles: photons, the movement of which is described by means of equations of wave mechanics.

The latter has shown that light participates in both wave and particle properties. When it collides with matter, it can be thought of as discrete packets of energy (quanta) called photons [55]. The interactions between matter and a radiation to which it is subjected are numerous. The most interesting and the most studied involve absorption phenomena (molecules can absorb the energy quanta of certain radiations). In this case, their fundamental energy states are altered by transition, or transition, to excited states of higher energy. Each state of matter is quantified and excitation takes place by absorption of a discrete amount of energy  $\Delta E$  [56]. To be absorbed, the radiation must be at the same frequency corresponding to this quantity of energy either: the recording of the energy absorbed or transmitted according to the frequency or the wavelength, constitutes the absorption spectrum of the compound in the spectral region of interest [55, 57]. The frequency  $\nu$  of an electromagnetic wave is related to its wavelength by the relation [56, 57]:

$$\nu = C/\lambda$$

## Computer in medicinal chemistry

where  $C$  represents the speed of light propagation in vacuum and  $\lambda$  the wavelength.

The energy  $E$  of the radiation or photon is directly proportional to the frequency of the electromagnetic wave or the field wave.

It is written: 
$$E = h\nu$$

Normally, a spectrum should appear as a succession of fine lines. In fact, there is for a molecule a succession of energetic states close to each other.

Hence the obtaining of more or less broad peaks or absorption bands even with equipment with high resolving power. The purpose of studying infrared spectra is most often to characterize compounds or to verify their compliance with a reference sample. Absorption in the infrared spectral region corresponds to transitions in the energies of molecular vibrations.

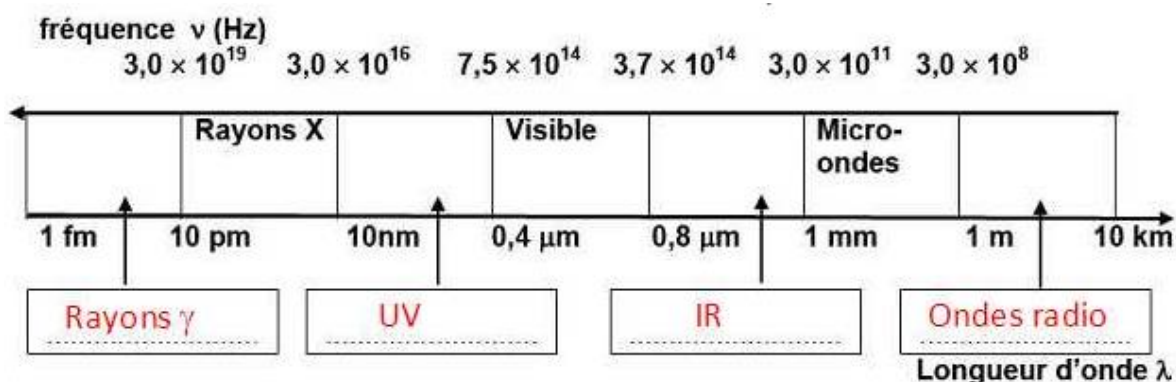


**Figure .27.** The various spectral domains of electromagnetic radiation.

Quantum mechanics shows us that only vibrational transitions in which there is variation in the dipole moment of the molecule, can cause an absorption peak in IR to appear. Many lines are due to the different modes of vibration of the bonds.

### II.5.3.2. Infrared

Understood between the visible and the microwaves, the infrared is subdivided into three parts: the near infrared located between 13,000 and 4,000  $\text{cm}^{-1}$ , the medium infrared located between 4,000 and 200  $\text{cm}^{-1}$ , and the far infrared located between 200 and 10  $\text{cm}^{-1}$  [56]. Infrared spectroscopy is based on the study of the reactions between matter and electromagnetic radiation. The latter can be defined by its frequency  $\nu$  expressed in hertz (Hz) or by its wave number,  $\tilde{\nu}$  is usually expressed in  $\text{cm}^{-1}$  or in kayser. It represents the number of waves contained in the interval of 1 cm [57]. In our investigation, we limited ourselves to the mid-infrared range (in the region of 4000 to 600  $\text{cm}^{-1}$ ), this corresponds to energies ranging from 4 to 40  $\text{kJ}\cdot\text{mol}^{-1}$ .

An infrared spectrum is complex. This complexity can be increased by the appearance of additional bands due to the harmonics of the fundamental absorption frequencies  $\nu_f$  of lower intensity. They can be observed at  $2\nu_f$ ,  $3\nu_f$ , or at frequency combination bands, which correspond to the sum of two fundamental frequencies.

Fundamental bands may not appear in the following cases: the vibration does not cause a variation in the dipole moment of the molecule, which often occurs in the case of compounds with a very symmetrical structure; vibrations occur at very close frequencies or at the same frequency; absorption is too low for the band to be visible.

### II.5.3.3. Infrared absorption

Any molecule excited by electromagnetic radiation absorbs an amount of energy and goes into an excited state. According to the mechanics, the absorption process is quantified and only particular frequencies can be absorbed by the molecule.

Vibrational excitation can be considered simply by considering two atoms  $A_1$  and  $A_2$  united by a bond as being two masses connected by a spring (figure 28) which stretches and relaxes at a certain frequency  $\nu$ .

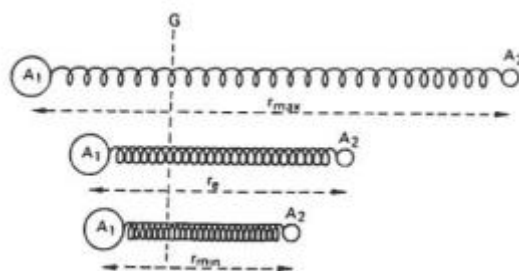


**Figure.28.** Movement of atoms during the phenomenon of vibration

In this representation, the frequency of vibrations between the two atoms depends both on the bond strength between them and on their atomic masses. It can be shown that it is governed by the following Hooke's law which describes the motions of a spring.

$$\bar{\nu} = k \sqrt{f \frac{(m_1+m_2)}{m_1 \cdot m_2}}$$

$\bar{\nu}$  : vibrational frequency in wavenumbers ( $\text{cm}^{-1}$ )

**K:** constant

**f:** force constant, indicating the stiffness of the spring (of the connection)

**m1 and m2:** values of the masses attached to the spring (masses of the united atoms)

This equation could lead us to think that each individual bond in a molecule gives rise to a specific absorption band in the infrared spectrum. Which is not the case.

The energies of radiation absorption correspond to movements of elongation, or deformation of most of the covalent bonds of molecules. In the process of absorption, the frequencies of infrared radiation coincide with those of the natural vibrational frequencies of molecules [58]. Not all bonds are capable of absorbing infrared energy even if their frequency coincides perfectly with that of movement of the bond. Only groups whose dipole moment varies during vibration are bonds which admit a dipole movement are able to absorb infrared radiation [57].

A bond must have an electric dipole which must oscillate at the same frequency as that of the excitation radiation, so that energy can be transferred.

In the case of infrared spectroscopy the molecule absorbs infrared light if and only if the dipole moment of the molecule changes during vibration [58].

The advantage with infrared is that it avoids unwanted photochemical or luminescence reactions. Electromagnetic radiation in the infrared (located in the region of 10,000 to 20  $\text{cm}^{-1}$ ), causing a change in the vibrational level nevertheless leaves the molecule at its fundamental electronic level [58, 59]. To understand the phenomenon of atomic vibration, it must be visualized as the interaction of two particles linked together by a spring [58]. When this spring is pulled and released, the two particles enter into a stretching motion. The amplitude of their movement is not only a function of the mass of the particles but also of the force of the spring (see figure 28). During the vibration phenomenon, other movements can be described: stretching, folding, twisting, swaying, shearing. In biological membranes, these movements become all the more complex as the chemical structures of the membrane constituents are more elaborate.

### II.5.4. Theoretical aspects

#### II.5.4.1. Internal vibration modes

In a polyatomic molecule comprising  $N$  atoms, the atoms can perform oscillating movements around their position of equilibrium. The rather weak oscillations of the molecule cause small displacements of the atoms formed. In this case the harmonic oscillation model is adapted to describe the movements of the atoms of the molecule. In a molecule made up of  $N$  atoms, each atom is assigned three coordinates to define its position. There by; an atom has three independent degrees of freedom of movement in the three directions of space. This results in  $3N$  degrees of freedom to describe the motion of an entire molecule (Table 2). Of these  $3N$  degrees of freedom, three are the coordinates that define the position of the center of mass of the molecule (translational degrees of freedom), and three other coordinates necessary to specify the molecular orientation around the center of gravity. These represent the degrees of freedom of

rotation. Note that a linear molecule has only two degrees, since rotation around the molecular axis does not cause the nuclei to shift. In conclusion, a molecule with  $N$  atoms has  $3N-6$  ( $3N-5$  for a linear molecule) degrees of freedom, responsible for all changes in the shape of the molecule without moving or rotating the center of gravity of the molecule [60, 61].

**Table.2.** Molecular degrees of freedom

	Degrés de liberté	Translation	Rotation	Vibration
Atome	3	-	-	-
Molécule linéaire ( $N$ atomes)	$3N$	3	2	$3N-5$
Molécule non linéaire ( $N$ atomes)	$3N$	3	3	$3N-6$

### II.5.4.2. Classification of vibration modes

Vibrations can be classified into two categories: in-plane and out-of-plane [62, 63].

- In the plane: we distinguish the elongation ( $\nu$ ) and the angular deformation ( $\delta$ ) which can be either symmetrical ( $\delta_s$  and  $\nu_s$ ), or antisymmetric ( $\delta_{as}$  and  $\nu_{as}$ ). Symmetric and antisymmetric angular deformations correspond to shearing or rotational movements of three atoms forming the angle  $\theta$  (Figure 29).
- Out of plane: these are angular deformations outside a molecular plane that can induce collective movement of the molecule corresponding to torsion ( $\tau$ ) or sway ( $\gamma$ ) movements.

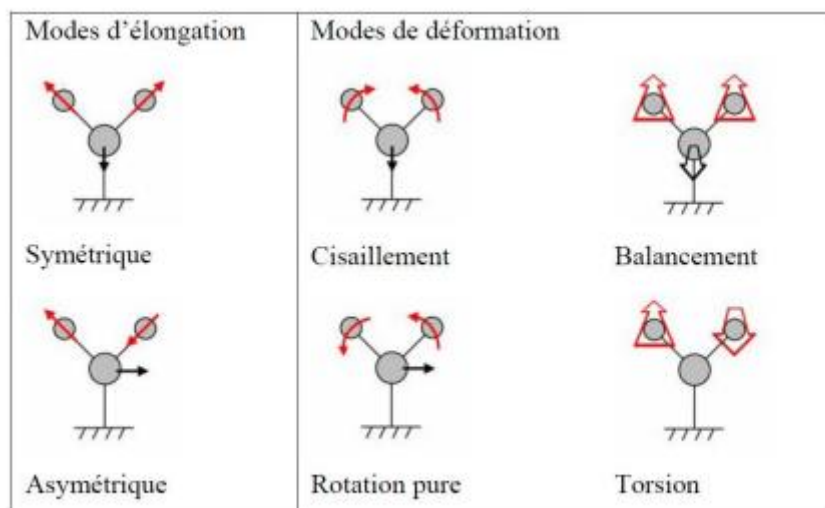


**Figure.29.** Movements associated with normal modes of vibration of a molecule containing 3 atoms.

### II.5.4.3. Factors that influence vibration frequencies

Analysis of an IR spectrum most often carried out in solution or in the solid state shows that a number of factors influence the vibration frequencies as well as their intensities.

The intensity of the bands depends on the nature and polarity of the bond. The vibration frequency, for its part, depends on the atoms constituting the bond, the multiplicity of the bond and its environment. Generally speaking, bonds between light atoms vibrate at a higher frequency than bonds between heavier atoms. The higher the constant  $K$  (bond strength constant), the higher the vibration frequency.

The link environment can have an electronic or mechanical impact on the vibration of this frequency. We will cite a few examples:

- ✓ **Electrical effects:** The effects of electronegativity and conjugation can cause significant shifts in vibration frequencies.
- ✓ **Hydrogen bond:** For some functions such as  $-OH$ ,  $-NH$ ,  $-SH$ , there is the possibility of hydrogen bond formation when they perceive in their molecular neighborhood the presence of an electronegative atom. This results in an elongation of the  $X-H$  bond and therefore a weakening of its force constant.

- ✓ **Steric Effects:** The frequency of a vibration depends on the steric constraints associated with this vibrator. The vibration  $\nu$  (C = O) occurs at a frequency so much higher as the valence angle COC is small.

Mechanical coupling: When in a molecule vibration of the same nature are found in the vicinity of one another, having an atom in common for example, they do not vibrate independently of one another. As a result, the frequencies are affected compared to those generally observed. This phenomenon is due to the existence of a mechanical coupling.

### II.5.5. Application

Infrared spectrometry [64] thus provides detailed information on:

- The chemical structure of macromolecules and the composition of the polymer: identification of the basic unit, branches, analysis of chain ends, determination of the nature and concentration of additives, structural defects, impurities.
- Intra- or intermolecular interactions, chain conformation, polymer crystallinity, orientation of macromolecules.
- Infrared spectrometry is also an effective tool for studying the structural modifications of polymers resulting from chemical treatments, degradations or aging of various origins.

### II.6 Conclusion

Chemoinformatics and molecular modeling methods are among the recent techniques now routinely applied in the research phases and in particular for the management and analysis of chemical libraries. They certainly arouse as much hope as they do criticism, but nevertheless constitute a very active line of research over the past two decades. In this chapter, we have presented most of the methods used in chemoinformatics for the analysis of chemical libraries. All of these concepts were used during this thesis in order, on the one hand, to make our own contribution through the creation of new methods allowing to characterize the chemical libraries and on the other hand, to develop a software allowing to implement some of these methods.

**Part II:**

**Computer-Assisted Drug Design**

What is computer-assisted drug design (CADD), and why is it important? There is no clear definition, although a consensus view has emerged. Simply, CADD is the coalescence of information on chemical structures, their properties, and their interactions with biological macromolecules. Further, these data are transformed into knowledge intended to aid in making better decisions for drug discovery and development.

These are representative of some questions facing the current drug-design community and significant applications of CADD.

Of the compounds included in our dataset, how many could be predicted to lack drug likeproperties based on similarity in properties to known orally active drugs?

How many would be predicted to be inactive based on the known structure–activity dataavailable on topoisomerase II inhibitors?

Given the structure–activity relationships (SARs) available on the inhibitors, what could one determine regarding the active site of topoisomerase II?

What novel classes of compounds could be suggested based on the SAR of inhibitors, or based on the new crystal structure of the complex?

Do the most potent compounds share a set of properties that can be identified and used to optimize a novel lead structure?

Can a predictive equation relating properties and affinity for the isolated enzyme be established?

### II.1 Predictive Quantitative Structure–Activity Relationship Modeling

At the beginning of its over 40 years of existence as an independent area of research, quantitative structure–activity relationship (QSAR) modeling was viewed strictly as analytical physical chemical approach applicable only to small congeneric series of molecules. The technique was first introduced by Hanschet al.[65] on the basis of implications from linear free energy relationships in general and the Hammett equation in particular. [66]

It is based upon the assumption that differences in physicochemical properties account for the differences in biological activities of compounds. According to this approach,

## Computer-Assisted drug design

the changes in physicochemical properties that affect the biological activities of a set of congeners are of three major types: electronic, steric, and hydrophobic.[67]

The quantitative relationships between biological activity (or chemical property) and the structural parameters could be conventionally obtained using multiple linear regression (MLR) analysis. The fundamentals and applications of this method in chemistry and biology have been summarized by Hansch and Leo.[67] This traditional QSAR approach has generated many useful and, in some cases, predictive QSAR equations and led to several documented drug discoveries.[68-70]

Many years of active research in QSAR have dramatically changed the breadth and the depth of this field in all its components including the diversity of target properties, descriptor types, data modeling approaches, and applications. The most important changes in QSAR deal with a substantial increase in the size of data sets available for the analysis and an increasing use of QSAR models as virtual screening tools to discover biologically active molecules in chemical databases and virtual chemical libraries.

### II.2. Principle of QSPR / QSAR methods

The principle of the QSPR / QSAR methods is to establish a mathematical relationship linking in a quantitative manner molecular properties, called descriptors, with a macroscopic observable (biological activity, toxicity, physicochemical property, etc.), for a series of similar chemical compounds. using data analysis methods. The general form of such a model is as follows:

$$\text{Property / Activity} = f(\text{D1, D2, ..., Dn, ,...})$$

**D1, D2, Dn** are descriptors of molecular structures.

The aim of such a method is to analyze structural data in order to detect the determining factors for the property / activity being measured. To do this, different types of statistical tools can be used:

- Simple and multiple linear regressions [71],
- Partial least squares regressions (PLS) [72],

## Computer-Assisted drug design

- Decision trees [73],
- Neural networks [74-76],
- Genetic algorithms[77],
- Machine Vectors [76],

Once this relationship is established and validated, it can then be employed for the prediction of the property / activity of new molecules, for which experimental values are not available. Such models can also be used to better understand mechanisms and modes of action.

### II.3 Key Quantitative Structure–Activity Relationship Concepts

An inexperienced user or sometimes even an avid practitioner of QSAR could be easily confused by the diversity of methodologies and naming conventions used in QSAR studies. 2D or three-dimensional (3D) QSAR, variable selection or artificial neural network (ANN) methods, Comparative molecular field analysis (CoMFA), or binary QSAR present examples of various terms that may appear to describe totally independent approaches, which cannot be generalized or even compared to each other. In fact, any QSAR method can be generally defined as an application of mathematical and statistical methods to the problem of finding empirical relationships (QSAR models) of the form  $P_i = k(D_1, D_2, \dots, D_n)$ , where  $P_i$  are biological activities (or other properties of interest) of molecules,  $D_1, D_2, \dots, D_n$  are calculated (or, sometimes, experimentally measured) structural properties (molecular descriptors) of compounds, and  $k$  is some empirically established mathematical transformation that should be applied to descriptors to calculate the property values for all molecules.

The relationship between values of descriptors  $D$  and target properties  $P$  can be linear (e.g., MLR as in the Hansch QSAR approach), where target property can be predicted directly from the descriptor values, or nonlinear (such as ANNs or classification QSAR methods) where descriptor values are used in characterizing chemical similarity between molecules, which in turn is used to predict compound activity.

## Computer-Assisted drug design

The differences in various QSAR methodologies can be understood in terms of the types of target property values, descriptors, and optimization algorithms used to relate descriptors to the target properties and generate statistically significant models.

**A- Target properties**(regarded as dependent variables in statistical data modeling sense) can generally be of three types:

- (1) continuous, i.e., real values covering certain range, e.g., IC<sub>50</sub>, MIC values, or binding constants.
- (2) categorical related, classes of target properties covering certain range of values, e.g., active and inactive compounds, frequently encoded numerically for the purpose of the subsequent analysis as 1 (for active) or 0 (for inactive), or adjacent classes of metabolic stability such as unstable, moderately stable, and stable.
- (3) categorical unrelated, classes of target properties that do not relate to each other in any continuum, e.g., compounds that belong to different pharmacological classes, or compounds that are classified as drugs versus non drugs.

**B- Chemical descriptors**(or independent variables in terms of statistical data modeling) can be typically classified into two types:

- (1) continuous (i.e., range of real values, e.g., as simple as molecular weight or many molecular connectivity indices); or
- (2) categorical related (i.e., classes corresponding to adjacent ranges of real values, e.g., counts of functional groups or binary descriptors indicating presence or absence of a chemical functional group or an atom in a molecule).

Descriptors can be generated from various representations of molecules, e.g., 2D chemical graphs or 3D molecular geometries, giving rise to the terms of 2D or 3D QSAR, respectively.

**C- Correlation methods**(which can be used either with or without variable selection) can be classified into two major categories:

- (1) linear (e.g., linear regression (LR), or principal component regression (PCR), or partial least squares (PLS)) or
- (2) nonlinear (e.g., k nearest neighbor (kNN), recursive partitioning (RP), ANNs, or support vector machines (SVMs)). [78]

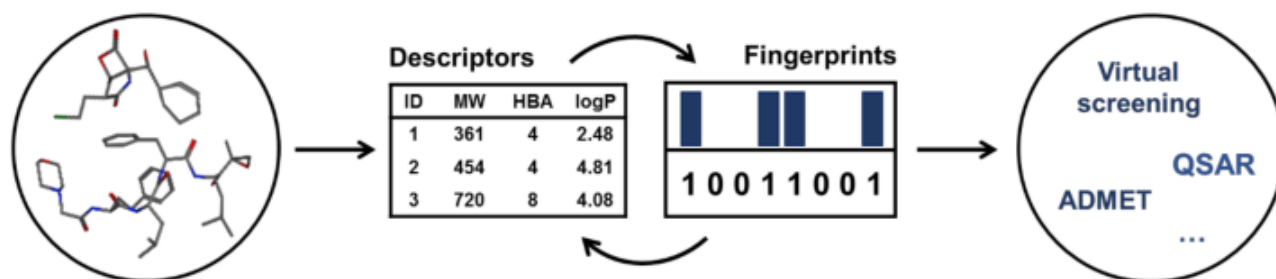


**Figure .30.** Molecular descriptors and fingerprints are examples of strategies that allow researchers to extract important information about compounds that can be used in additional computer-aided drug design techniques, such as virtual screening, quantitative-structure-activity relationship (QSAR).

In some cases, the types of biological data, the choice of descriptors, and the class of optimization methods are closely related and mutually inclusive. For instance, MLR can only be applied when a relatively small number of molecular descriptors are used (at least five to six times less than the total number of compounds) and the target property is characterized by a continuous range of values. The use of multiple descriptors makes it impossible to use MLR due to a high chance of spurious correlation [79] and requires the use of PLS or nonlinear optimization techniques.

### II.3.1 Molecular Descriptors

Theoretical descriptors derived from physical and physico-chemical theories show some natural overlap with experimental measurements. Several quantum chemical descriptors, surface areas, and volume descriptors are examples of such descriptors also having an experimental counterpart.

With respect to experimental measurements, the greatest recognized advantages of the theoretical descriptors are usually (but not always) in terms of cost, time, and availability.

Each molecular descriptor takes into account a small part of the whole chemical information contained in to the real molecule and,asaconsequence,the number of descriptors

## Computer-Assisted drug design

is continuously increasing with the increasing request of deeper investigations on chemical and biological systems. Different descriptors have independent methods or perspectives to view a molecule, taking into account the various features of chemical structure. Molecular descriptors have now become some of the most important variables used in molecular modeling, and, consequently, managed by statistics, chemometrics, and chemoinformatics [80].

There are many different descriptors and many different kinds of classification based on the effect (steric, hydrophobic, electronic, etc.) or based on its dimension that called Descriptors Block, whereas we find four types of molecular descriptors 0D, 1D, 2D and 3D [80].

- Molecular descriptors 0D, 1D: contains numbers of atoms, functional groups, molecules properties, and charges (eg. Molecular Weight, Molecular Refractivity, etc.).
- Molecular descriptors 2D: contains simple descriptors and other derivatives of algorithms applied to a topological representation (eg. Number of Cl atoms, presence of hydroxyl group, etc.).
- Molecular descriptors 3D: contains descriptors derived from a geometric representation also called geometric descriptors (eg. Molecular volume, Surface area, etc.).

### II.3.3 Quantitative Structure–Activity Relationship Modeling Approaches

#### II.3.3.1 General Classification

Many different approaches to QSAR have been developed since Hansch's seminal work. As briefly discussed above, the major differences between these methods can be analyzed from two viewpoints:

- (1) the types of structural parameters that are used to characterize molecular identities starting from different representation of molecules, from simple chemical formulas to 3D conformations, and
- (2) the mathematical procedure that is employed to obtain the quantitative relationship between these structural parameters and biological activity.

## Computer-Assisted drug design

Based on the origin of molecular descriptors used in calculations, QSAR methods can be divided into three groups.

One group is based on a relatively small number (usually many times smaller than the number of compounds in a data set) of physicochemical properties and parameters describing hydrophobic, steric, electrostatic, etc. effects. Usually, these descriptors are used as independent variables in multiple regression approaches. In the literature, these methods are typically referred to as Hansch analysis.

A more recent group of methods is based on quantitative characteristics of molecular graphs (molecular topological descriptors). Since molecular graphs or structural formulas are 'two dimensional,' these methods are described as 2D QSAR. Most of the 2D QSAR methods are based on graph theoretical indices. Although these structural indices represent different aspects of molecular structures, and, what is important for QSAR, different structures provide numerically different values of indices, their physicochemical meaning is frequently unclear.

The third group of methods is based on descriptors derived from spatial (3D) representation of molecular structures. Correspondingly, these methods are referred to as 3D QSAR; they have become increasingly popular with the development of fast and accurate computational methods for generating 3D conformations and alignments of chemical structures. Perhaps the most popular example of 3D QSAR is CoMFA, developed by Cramer et al.,[\[81\]](#) which has combined the power of molecular graphics and PLS technique and has found wide applications in medicinal chemistry and toxicity analysis.[\[82\]](#)

### II.3.3.2. General Methodology of a QSPR / QSAR study

The general methodology of a QSAR / QSPR study is as follows:

- a-** Build up a database from reliable experimental measurements of the property or activity of each compound.
- b-** Select the descriptors in relation to the property or activity studied.
- c-** Divide this database, randomly, into a training set which generally contains 2/3 of the database and a test series (test set) consisting of the remaining 1/3.

## Computer-Assisted drug design

**d-** Establish mathematical models using the learning series.

**e-** Characterize the models developed by their internal validation indices and check their robustness by a randomization test (Randomization) of the dependent variable Y (response).

**f-** Validate the models developed using the test series and calculate their statistical parameters for external validation.

### II.3.3.3 Transforming the Bioactivities

The main advantage of transforming data is to guarantee linearity, to achieve normality, or to stabilize the variance. Several simple nonlinear regression relationships can be made linear through the appropriate transformations. The simplest and most common method of transforming [83] bioactivity data is to take the log or negative log of the bioactivities to reduce the range of the data.

The method of creating Training and Test Sets that are representative of the population is to choose molecules that represent all the molecules of interest based on molecular structure and bioactivity. The number of molecules in the Test Set is determined (20% of the total molecules in this study) and then all the molecules are placed in a table and ordered based on bioactivities. With the table prepared, the extraction of the molecules for the Test Set can begin through an iterative process starting at the top of the table.

### II.3.3.4 Determination of the Best Set of Descriptors Approaches

Both 2D and 3D QSAR studies have focused on the development of optimal QSAR models through variable selection. This implies that only a subset of available descriptors of chemical structures, which are the most meaningful and statistically significant in terms of correlation with biological activity, is selected. The Stepwise Method Search selects a model by adding or removing individual descriptors, a step at a time, based on their statistical significance. The end result of this process is a single regression model, which makes it nice and simple. The p-value for each term tests the null hypothesis that the coefficient is equal to zero (no effect). A low p-value ( $< 0.05$ ) indicates that you can reject the null hypothesis. In other words, a descriptor that has a low p-value is likely to be a meaningful addition to

your model because changes in the descriptor's value are related to changes in the response variable (bioactivity). Conversely, a larger (insignificant) p-value suggests that changes in the descriptor are not associated with changes in the response.

### **II.4. Building Predictive Quantitative Structure–Activity Relationship Models: The Approaches to Model Validation**

#### **II.4.1. Data analysis methods**

To develop a QSPR / QSAR model we need a data analysis method, this method allows to quantify the relationship between the property / Activity and the Structure (descriptors).

There are several methods to build a model and analyze its statistical data, some are linear such as multiple linear regression (MLR), partial least squares (PLS) regression, others are nonlinear such as trees of decisions, neural networks... these methods are available in software such as, Excel, Origin Microcal, Minitab, Statistica, SPSS, JMP, R,...

The method used in our studies is the Multiple Linear Regression (MLR) and Neural Networks (ANN) method.

##### **II.4.1.1. Neural networks**

The formal neural networks initiated in 1943 by Mc Culloch and Pitts are analogous to biological nervous systems.[84]

Formal neurons (Figure 31) perform a linear combination of the inputs received(descriptors), then apply to this value an activation function  $f$ , generally nonlinear (sigmoidal, tangent, hyperbolic). The obtained value  $Y$  (biological activity) is the output of the neuron.[85]

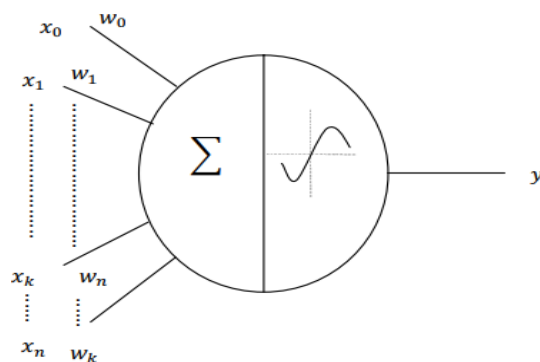


Figure.31. Representation of a formal neuron.

$X_k$  (where  $k = 1, 2, \dots, n$ ) are the input neurons (descriptors) and  $W_k$  (where  $k = 0, 1, 2, \dots, n$ ) are the weights.  $W_0$  is the weight associated with an entry set at 1, called bias. The neuron equation looks like this:

$$y = f\left(W_0 + \sum_{k=1}^n W_k X_k\right)$$

Neurons alone perform fairly simple functions, and it is their combinations, called neural networks, that make it possible to construct particularly interesting functions (Figure 31).

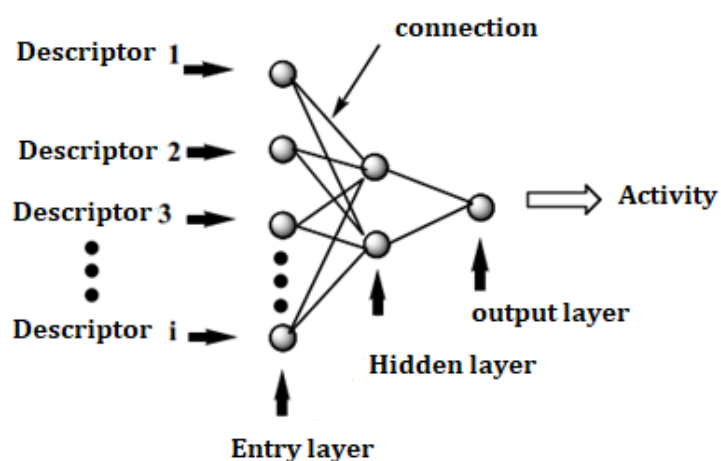


Figure.32. Architecture of neural networks.

## Computer-Assisted drug design

The architecture of neural networks consists of three layers:

- An input layer: made up of input neurons, their number is equal to the number of input variables (descriptors) plus one (bias). Each neuron is connected to the hidden neurons.
- A hidden layer: made up of a variable number of neurons. For each hidden neuron, the network performs a weighted sum operation with the different weights of each input neuron.
- An output layer: where the number of output neurons is equal to the number of properties (activities) to be modeled.

Each connection between the neurons of the different layers is associated with a weight. The number of weights then depends on the number of neurons in the hidden layer, so it is possible to vary the complexity of the network by increasing or decreasing the number of hidden neurons. To do this, data presentation cycles are established via a learning algorithm. The one used in our approach is a backpropagation algorithm.[86]

The principle of the back-propagation algorithm is to minimize the difference between the calculated output (calculated activity) and the experimental values of the activity.

Defined in two stages, the algorithm propagates in a first stage the inputs (descriptors) forward until obtaining an output (biological activity) calculated by the network. In a second step, the calculated output is compared with the experimental value. The error obtained by this comparison is then propagated back to the input layer by modifying the weights of the neurons. This process is repeated until a negligible error is obtained.[87]

### II.4.1.2 Multiple linear regression

Multiple linear regression is the simplest statistical modeling method and the most applied in studies of the structure-activity relationship [88]. The method was popularized by Hanch by relating biological activity to experimental lipophilic, electronic and steric properties for series of compounds.[89]

## Computer-Assisted drug design

The RLM method is based on the assumption that there is a linear relationship between a dependent variable  $Y$  (in our case the biological activity) and a series of  $n$  independent variables  $X_i$  (here, the molecular descriptors)[90]. The objective is to arrive at a mathematical equation of the form:

$$y = a_0 + a_1x_1 + a_2x_2 + \dots + a_nx_n$$

Where  $a_i$  ( $i = 0, 1, \dots, n$ ) are the coefficients of the regression.

Determining the equation from a data set of  $p$  samples is like solving a system of  $p$  equations.

$$y_1 = a_0 + a_1x_{1,1} + a_2x_{2,1} + \dots + a_nx_{n,1} + b_1$$

$$y_2 = a_0 + a_1x_{1,2} + a_2x_{2,2} + \dots + a_nx_{n,2} + b_2$$

⋮

$$y_p = a_0 + a_1x_{1,p} + a_2x_{2,p} + \dots + a_nx_{n,p} + b_p$$

Or:

The residuals  $b_i$  ( $i = 1, 2, \dots, p$ ) represent the model error,

$y_i$  ( $i = 1, 2, \dots, p$ ) represent the dependent variables (activities),

$x_i$  ( $i = 1, 2, \dots, p$ ) represent the independent variables (descriptors),

$a_i$  ( $i = 1, 2, \dots, p$ ) represent the coefficients of the regression.

This set of equations can be written in the following matrix form:

$$\begin{pmatrix} y_1 \\ y_2 \\ \vdots \\ \vdots \\ y_p \end{pmatrix} = \begin{pmatrix} 1 & x_{1,1} & x_{2,1} & \cdots & \cdots & x_{n,1} \\ 1 & x_{1,2} & x_{2,2} & \cdots & \cdots & x_{n,2} \\ \vdots & \vdots & & & & \\ \vdots & \vdots & & & & \\ 1 & x_{1,p} & x_{2,p} & \cdots & \cdots & x_{n,p} \end{pmatrix} \begin{pmatrix} a_0 \\ a_1 \\ \vdots \\ \vdots \\ a_p \end{pmatrix} + \begin{pmatrix} b_1 \\ b_2 \\ \vdots \\ \vdots \\ b_p \end{pmatrix}$$

Or in a condensed way:

$$\mathbf{Y} = \mathbf{XA} + \mathbf{B}$$

Where  $\mathbf{Y}$ ,  $\mathbf{X}$ ,  $\mathbf{A}$ , and  $\mathbf{B}$  represent the property vector, the attribute matrix (descriptors), the coefficient matrix, and the regression error matrix, respectively.

The RLM method then consists in choosing the coefficients  $a_i$  so as to minimize the sum of the squares of the differences between the calculated values of the property and the experimental ones, the equation of the model therefore becomes:

$$\hat{y}_i = \hat{a}_0 + \hat{a}_1 x_{1,i} + \hat{a}_2 x_{2,i} + \cdots + \hat{a}_n x_{n,i}$$

Or in matrix form:

$$\mathbf{X} \cdot \mathbf{A} = \mathbf{Y}$$

The coefficients can be obtained from the following matrix equation:

$$\mathbf{A} = (\mathbf{X}^T \cdot \mathbf{X})^{-1} \mathbf{X}^T \cdot \mathbf{Y}$$

#### II.4.1.2.1. Randomization test

The randomization test is used by the modeler to assert that the good correlations, between descriptors and activity, presented by the QSAR model are not due to luck. To do this, the observations are randomly disorganized, for example ten times, by randomly changing the activity column, but the descriptor columns remain unchanged[91]. We therefore obtain ten models with specific statistical characteristics. If the randomization of the observations leads to weak forecast models, this means that

the predictive capacities of the constructed QSAR model are not due to the correlations of luck.[92]

### II.4.2. Interpretation and validation of a QSPR / QSAR model

Once developed, the model must be interpreted by analyzing all the statistical parameters of this model, its quality must also be studied, this quality is checked by what is called validation. Its robustness, ie the influence of the compounds of the training series on the model, is estimated by internal validation methods. In order to estimate its predictive power, additional experimental data is needed to determine the ability of the model to predict these values, this is called external validation. Finally, it is important to know which type of molecules used with which model.

#### II.4.2.1. The Importance of Validation

The process of QSAR model development is divided into three key steps: (1) data preparation, (2) data analysis, and (3) model validation. The implementation and relative merit of these steps is generally determined by the researcher's interests and experience, and the availability of software. The resulting models are then frequently employed, at least in theory, to design new molecules based on chemical features or trends found to be statistically significant with respect to underlying biological activity.

The first stage includes the selection of a data set for QSAR studies and the calculation of molecular descriptors. The second stage deals with the selection of a statistical data analysis technique, either linear or nonlinear such as MLR, PLS or ANN. A variety of different algorithms and computer software are available for this purpose. In all approaches, descriptors are considered as independent variables, and biological activities as dependent variables.

Typically, the final part of QSAR model development is model validation, [93, 94] in which estimates of the predictive power of the model are calculated. This predictive power is one of the most important characteristics of QSAR models.

Ideally, it should be defined as the ability of the model to predict accurately the target property (e.g., biological activity) of compounds that were not used in model

development.

Here, we are going to discuss about the validation parameters for the QSAR models which are developed by multiple linear regression (MLR). Four tools of assessing validity of QSAR models [95] are (i) cross-validation, (ii) bootstrapping, (iii) randomization of the response data, and (iv) external validation. Where we are using the data that created the model (an internal method) and using a separate data set (an external method).

The methods of least squares fit ( $R^2$ ), cross validation ( $Q^2$ ) [96, 97], adjusted  $R^2$  ( $R^2_{adj}$ ), chisquared test ( $\chi^2$ ), rootmean-squared error (RMSE), bootstrapping and scrambling (YRandomization) [98, 99] are internal methods of validating a model. The best method of validating a model is an external method, such as evaluating the QSAR model on a test set of compounds.

### II.4.2.1.1. Internal Validation

#### II.4.2.1.1.1. Least Squares Fit

The most common internal method of validating the model is least squares fitting. This method of validation is similar to linear regression and is the  $R^2$  (squared correlation coefficient) for the comparison between the predicted and experimental activities. An improved method of determining  $R^2$  is the robust straight line fit, where data points are away from the central data points (essentially data points a specified standard deviation away from the model) are given less weight when calculating the  $R^2$ . An alternative to this method is the removal of outliers (compounds from the training set) from the dataset in an attempt to optimize the QSAR model and is only valid if strict statistical rules are followed. The difference between the  $R^2$  and  $R^2_{adj}$  value is less than 0.3 indicates that the number of descriptors involved in the QSAR model is acceptable. The number of descriptors is not acceptable if the difference is more than 0.3.

$$R^2 = 1 - \frac{PRESS}{\sum_{i=1}^n (y_i - y_m)^2}$$
$$PRESS = \sum_{i=1}^n (\hat{y}_i - y_i)^2$$

## Computer-Assisted drug design

Where,  $y$  and  $\hat{y}$  are the experimental and predicted bioactivity for an individual compound in the training set,  $y_m$  is the mean of the experimental bioactivities, and  $n$  is the number of molecules in the set of data being examined. *PRESS* is the predictive residual sum of the squares.

### II.4.2.1.1.2 Fit of the Model

Fit of the QSAR models can be determined by the methods of chi-squared ( $\chi^2$ ) and root-mean squared error (*RMSE*). These methods are used to decide if the model possesses the predictive quality reflected in the  $R^2$ . The use of *RMSE* shows the error between the mean of the experimental values and predicted activities. The chi squared value exhibits the difference between the experimental and predicted bioactivities:

$$\chi^2 = \sum_{i=1}^n \left( \frac{(y_i - \hat{y}_i)^2}{\hat{y}_i} \right)$$
$$RMSE = \sqrt{\sum_{i=1}^n \frac{(y_i - y_m)^2}{n - 1}}$$

Large chi-square or *RMSE* values ( $\geq 0.5$  and  $1.0$ , respectively) reflect the model's poor ability to accurately predict the bioactivities even the model is having large  $R^2$  value ( $\geq 0.7$ ).

For good predictive model the chi and *RMSE* values should be low ( $< 0.5$  and  $< 0.3$ , respectively). These methods of error checking can also be used to aid in creating models and are especially useful in creating and validating models for nonlinear data sets, such as those created with Artificial Neural Network (ANN) [100]. However, excellent values of  $R^2$ ,  $\chi^2$  and *RMSE* are not sufficient indicators of model validity. Thus, alternative parameters must be provided to indicate the predictive ability of models. In principle, two reasonable approaches of validation can be envisaged one based on prediction and the other based on the fit of the predictor variables to rearranged response variables.

### II.4.2.1.2 External validation

Several authors have suggested that the only way to estimate the true predictive power of a QSAR model is to compare the predicted and observed activities of an (sufficiently large) external test set of compounds that were not used in the model development [94, 101-104]. The problem in external validation is how can we select the training and test set? Roy et al. clearly discussed that how we can solve this problem in one of their article. [105]

To estimate the predictive power of a QSAR model, Golbraikh and Tropsha recommended use of the following statistical characteristics of the test set [93]: (i) correlation coefficient R between the predicted and observed activities; (ii) coefficients of determination ( $R^2$ ) (predicted vs. observed activities  $r_0^2$ , and observed vs. predicted activities  $r_0'$ ); (iii) slopes k and k' of the regression lines through the origin. They consider a QSAR model is predictive, if the following conditions are satisfied [93]:

$$R_{test}^2 > 0.6 ;$$

$$r^2 - \frac{r_0^2}{r'^2} < 0.1 \quad ; \quad r'^2 - \frac{r_0'^2}{r^2} < 0.1 \quad \text{and}$$

$$0.85 \leq k \leq 1.15 \quad \text{or} \quad 0.85 \leq k' \leq 1.15$$

The predictive ability of the selected model was also confirmed by external  $R^2_{test}$ . A value of  $R^2_{test}$  is greater than 0.6 may be taken as an indicator of good external predictability.

$$R_{test}^2 = 1 - \frac{\sum_{i=1}^{test} (y_{exp} - y_{pred})^2}{\sum_{i=1}^{test} (y_{exp} - \bar{y}_{tr})^2}$$

Where  $\bar{y}_{tr}$  is the average value for the dependent variable for the training set. Kubinyi et al [94], Novellino et al. [102], Norinder [103], and Golbraikh and Tropsha [93] demonstrated that all of the above-mentioned criteria are necessary to adequately assess the predictive ability of a QSAR model. Norinder suggest [103] that the external test set must contain at least five compounds, representing the whole range of both descriptor and activities of compounds included into the training set.

### II.5. Application of QSAR

There are a large number of applications of QSAR models in industry, in university research, in economics, in weather forecasting, ...etc.

We report below some possible applications of QSAR models:

- Rational identification of new leads with: optimization of pharmacological, biocidal or pesticide activity.
- Rational design of many products such as surfactants, perfumes, dyes and fine chemicals.
- The identification of dangerous compounds in the early stages of development.
- Prediction of toxicity and side effects of new compounds.
- The selection of compounds with optimal pharmacokinetic properties, be it stability or availability in biological systems.

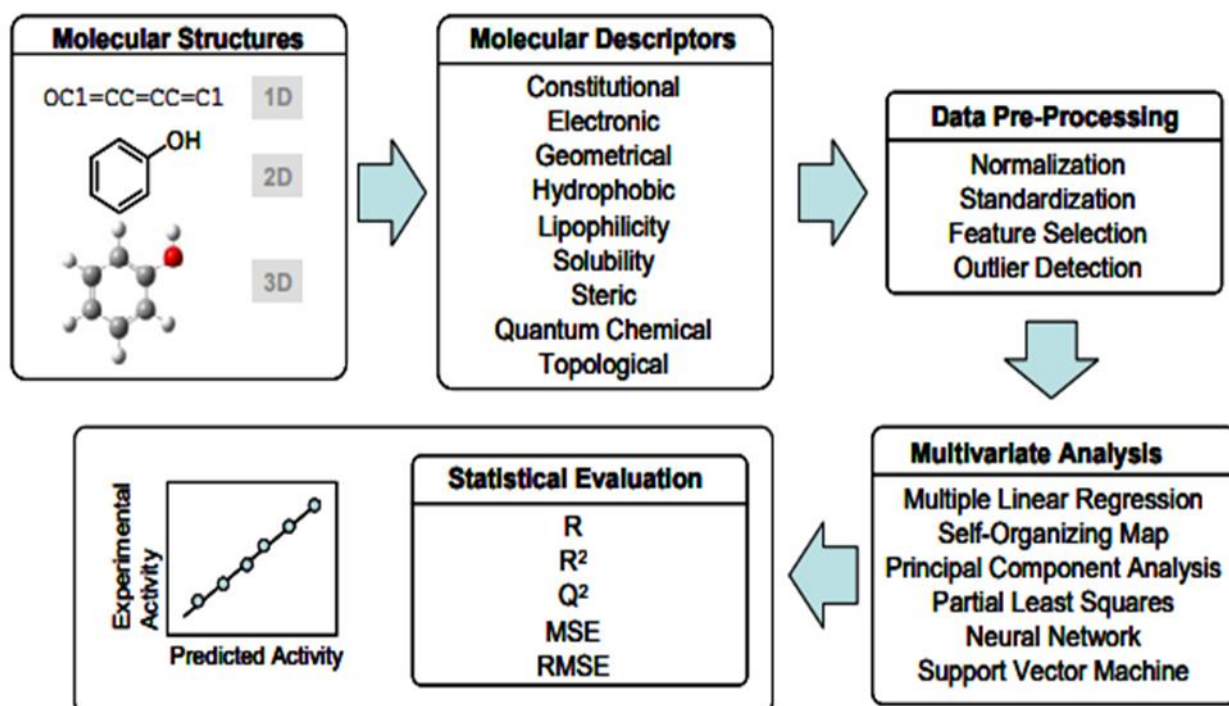


**Figure.33.** Schematic overview of the QSAR process.

## References

- [1] C. Larive, Apports combinés de l'expérimentation et de la modélisation à la compréhension de l'alcali-réaction et de ses effets mécaniques, in, Ecole nationale des ponts et chaussées, 1997.
- [2] A. Hamdouch, M.-H. Depret, Spatial Scales, Proximity and Institutional Logics: Outline of an Evolutionary Approach of Technological Change Dynamics in Pharmaceuticals and Biotechnology (Echelles spatiales, formes de proximité et logiques institutionnelles: Esquisse d'une approche co-evolutionnaire des dynamiques de changement technologique dans la pharmacie et les biotechnologies), (2008).
- [3] F. Lerbet-Sereni, Expériences de la modélisation, modélisation de l'expérience, Harmattan, 2004.
- [4] Y. Yamaguchi, H.F. Schaefer, Y. Osamura, J. Goddard, A New Dimension to Quantum Chemistry: Analytic Derivative Methods in Ab Initio Molecular Electronic Structure Theory, Oxford University Press, 1994.
- [5] G.H. Loew, H.O. Villar, I.J.P.r. Alkorta, Strategies for indirect computer-aided drug design, 10 (1993) 475-486.
- [6] A. Hinchliffe, Molecular modelling for beginners, John Wiley & Sons, 2003.
- [7] S. Belaidi, Nouvelle approche de la stéréosélectivité dans les macrolides antibiotiques dissymétriques, par la modélisation moléculaire, in, Batna, Université El Hadj Lakhder. Faculté des sciences, 2002.
- [8] N.L. Allinger, X. Zhou, J.J.J.o.M.S.T. Bergsma, Molecular mechanics parameters, 312 (1994) 69-83.
- [9] A. Meyer, F.J.J.o.c.c. Forrest, Towards the convergence of molecular-mechanical force fields, 6 (1985) 1-4.
- [10] R. Thomsen, M.H.J.J.o.m.c. Christensen, MolDock: a new technique for high-accuracy molecular docking, 49 (2006) 3315-3321.
- [11] W.J. Hehre, A guide to molecular mechanics and quantum chemical calculations, Wavefunction Irvine, CA, 2003.
- [12] P.W. Atkins, R.S. Friedman, Molecular Quantum Mechanics, OUP Oxford, 2011.
- [13] A. KERASSA, Etude par la modélisation moléculaire des relations structures-propriétés de quelques séries hétérocycliques bioactives, in, Université Mohamed Khider-Biskra, 2015.

## References

- [14] N.L. Allinger, Y.H. Yuh, J.H.J.J.o.t.A.C.S. Lii, Molecular mechanics. The MM3 force field for hydrocarbons. 1, 111 (1989) 8551-8566.
- [15] H.J.A.t.e.p. Dugas, quatrième édition, Librairie de l'Université de Montréal, Principes de base en modélisation moléculaire, (1996).
- [16] F.J.C.m.c. Ooms, Molecular modeling and computer aided drug design. Examples of their applications in medicinal chemistry, 7 (2000) 141-158.
- [17] K.H. Bleicher, H.-J. Böhm, K. Müller, A.I.J.N.r.D.d. Alanine, Hit and lead generation: beyond high-throughput screening, 2 (2003) 369-378.
- [18] G.J.D.D.T.T. Klebe, Lead identification in post-genomics: computers as a complementary alternative, 1 (2004) 225-230.
- [19] G.R. Marshall, T.I. Oprea, M.M.H.A.R. Leach, D.V. Green, M.R.C.L.H. Matter, D.H.B.M.R. Gozalbes, F.B.S.L. Rogalski, I.M.G.W.J. Alvarez, C.L.C.D.M. Schnur, A.J. Tebben, Chemoinformatics in drug discovery, Wiley Online Library, 2004.
- [20] R. Clark, D. Sprous, J.J.P.S. Leonard, Barcelona, Rational Approaches to Drug Design, HD Höltje, W, (2001) 475-485.
- [21] C.J.D.D.R. Hansch, The physicochemical approach to drug design and discovery (QSAR), 1 (1981) 267-309.
- [22] C.J.A.o.c.r. Hansch, Quantitative structure-activity relationships and the unnamed science, 26 (1993) 147-153.
- [23] G.L. Patrick, An introduction to medicinal chemistry, Oxford university press, 2013.
- [24] V. Brenner, Modelisation des forces intermoleculaires et caracterisation des hypersurfaces d'energie potentielle. Applications a de petits agregats de van der waals, in, Paris 11, 1993.
- [25] K.B.J.J.o.t.A.C.S. Wiberg, A scheme for strain energy minimization. Application to the cycloalkanes1, 87 (1965) 1070-1078.
- [26] W.H. Press, W.T. Vetterling, S.A. Teukolsky, B.P. Flannery, Numerical recipes, Cambridge university press Cambridge, 1986.
- [27] A. Warshel, S.J.T.J.o.C.P. Lifson, Consistent force field calculations. II. Crystal structures, sublimation energies, molecular and lattice vibrations, molecular conformations, and enthalpies of alkanes, 53 (1970) 582-594.

## References

- [28] V.N. Viswanadhan, A.K. Ghose, J.N.J.B.e.B.A.-P.S. Weinstein, M. Enzymology, Mapping the binding site of the nucleoside transporter protein: a 3D-QSAR study, 1039 (1990) 356-366.
- [29] Cambridge Crystallographic Data Centre (CCDC) database, <http://www.ccdc.cam.ac.uk>, in.
- [30] Official website of Protein Data Bank (PDB) : [www.rcsb.org/pdb](http://www.rcsb.org/pdb).
- [31] A.D. McNaught, A. Wilkinson, Compendium of chemical terminology. IUPAC recommendations, (1997).
- [32] K.B. Wiberg, P.R.J.J.o.C.C. Rablen, Comparison of atomic charges derived via different procedures, 14 (1993) 1504-1518.
- [33] J.G.J.C.p.l. Ángyán, Choosing between alternative MP2 algorithms in the self-consistent reaction field theory of solvent effects, 241 (1995) 51-56.
- [34] E. Sigfridsson, U.J.J.o.C.C. Ryde, Comparison of methods for deriving atomic charges from the electrostatic potential and moments, 19 (1998) 377-395.
- [35] O. Prasad, L. Sinha, N.J.J.A.M.S. Kumar, Theoretical Raman and IR spectra of tegafur and comparison of molecular electrostatic potential surfaces, polarizability and hyperpolarizability of tegafur with 5-fluoro-uracil by density functional theory, 1 (2010) 201-214.
- [36] C. Ai, Y. Li, Y. Wang, Y. Chen, L.J.B. Yang, m.c. letters, Insight into the effects of chiral isomers quinidine and quinine on CYP2D6 inhibition, 19 (2009) 803-806.
- [37] R.K. Srivastava, V. Narayan, O. Prasad, L.J.J.C.P.R. Sinha, Vibrational, Structural and Electronic properties of 6-methyl nicotinic acid by Density Functional Theory, 4 (2012) 3333-3341.
- [38] H.B. Broughton, I.A.J.J.o.M.G. Watson, Modelling, Selection of heterocycles for drug design, 23 (2004) 51-58.
- [39] I. Lessigiarska, Development of structure-activity relationships for pharmacotoxicological endpoints relevant to European Union legislation, in, Liverpool John Moores University, 2006.
- [40] G. Petersson, M.A.J.T.J.o.c.p. Al-Laham, A complete basis set model chemistry. II. Open-shell systems and the total energies of the first-row atoms, 94 (1991) 6081-6090.
- [41] R.G. Parr, W.J.J.o.t.A.C.S. Yang, Density functional approach to the frontier-electron theory of chemical reactivity, 106 (1984) 4049-4050.

## References

- [42] W. Yang, W.J.J.J.o.t.A.C.S. Mortier, The use of global and local molecular parameters for the analysis of the gas-phase basicity of amines, 108 (1986) 5708-5711.
- [43] R.S.J.T.J.o.C.P. Mulliken, Electronic population analysis on LCAO–MO molecular wave functions. I, 23 (1955) 1833-1840.
- [44] F.L.J.T.c.a. Hirshfeld, Bonded-atom fragments for describing molecular charge densities, 44 (1977) 129-138.
- [45] A.E. Reed, F.J.T.J.o.c.p. Weinhold, Natural bond orbital analysis of near-Hartree–Fock water dimer, 78 (1983) 4066-4073.
- [46] K.J.s. Fukui, Role of frontier orbitals in chemical reactions, 218 (1982) 747-754.
- [47] F. Maseras, K.J.J.o.C.C. Morokuma, IMOMM: A new integrated ab initio+ molecular mechanics geometry optimization scheme of equilibrium structures and transition states, 16 (1995) 1170-1179.
- [48] S. Humbel, S. Sieber, K.J.T.J.o.c.p. Morokuma, The IMOMO method: Integration of different levels of molecular orbital approximations for geometry optimization of large systems: Test for n-butane conformation and SN 2 reaction: RCl+ Cl–, 105 (1996) 1959-1967.
- [49] E.B. Wilson, J.C. Decius, P.C. Cross, Molecular vibrations: the theory of infrared and Raman vibrational spectra, Courier Corporation, 1980.
- [50] X. Zhou, L. Wang, P.J.J.o.C. Qin, T. Nanoscience, Free vibration of micro-and nano-shells based on modified couple stress theory, 9 (2012) 814-818.
- [51] É. Biémont, Spectroscopie moléculaire: structures moléculaires et analyse spectrale, De Boeck Supérieur, 2008.
- [52] I. Taleb, Apport de la spectroscopie vibrationnelle, infrarouge et Raman, appliquée au sérum pour le diagnostic de carcinome hépatocellulaire chez les patients atteints de cirrhose, in, Reims, 2013.
- [53] A.C.E.Z.J.C.d.p. CIHLA, 12C 160, MAURICE KIBLER: NIVEAUX D'ÉNERGIE DES IONS 3d<sup>n</sup> PLACÉS DANS UN CHAMP CRISTALLIN DE SYMÉTRIE Caro Mlle FRANÇOISE CALENDINI ET GUY MESNARD: NIVEAUX D'ÉNERGIE DE L'ION Ti<sup>3+</sup> DANS UN CHAMP CRISTALLIN DE SYMÉTRIE Cero, 21 (1966) 96.
- [54] M. Dalibart, Spectroscopie Dans l'infrarouge, Ed. Techniques Ingénieur, 2000.
- [55] J. Darnell, Biologie moléculaire de la cellule, (1993).

## References

- [56] Z. Szafran, R. Pike, M.J.I.N. Singh, *Microscale Inorganic Chemistry*, J. Wiley&Sons, (1991).
- [57] F. BEAUDOIN, 1) *Chimie organique expérimentale*, (1991).
- [58] M. Hamel, *Influence de la variation de la température ambiante sur les vibrations induites par effet de couronne*, Université du Québec à Chicoutimi, 1991.
- [59] M. Lutz, W.J.C. Mäntele, *Vibrational spectroscopy of chlorophylls*, (1991) 855-902.
- [60] S.W. Shaw, C.J.J.o.s. Pierre, *vibration, Normal modes of vibration for non-linear continuous systems*, 169 (1994) 319-347.
- [61] T. Eicher, S. Hauptmann, A. Speicher, *The chemistry of heterocycles: structures, reactions, synthesis, and applications*, John Wiley & Sons, 2013.
- [62] Y. Morino, K.J.T.J.o.C.P. Kuchitsu, *A note on the classification of normal vibrations of molecules*, 20 (1952) 1809-1810.
- [63] Z. Konkoli, D.J.I.j.o.q.c. Cremer, *A new way of analyzing vibrational spectra. I. Derivation of adiabatic internal modes*, 67 (1998) 1-9.
- [64] J. Bartol, P. Comba, M. Melter, M.J.J.o.c.c. Zimmer, *Conformational searching of transition metal compounds*, 20 (1999) 1549-1558.
- [65] C. Hansch, R.M. Muir, T. Fujita, P.P. Maloney, F. Geiger, M.J.J.o.t.A.C.S. Streich, *The correlation of biological activity of plant growth regulators and chloromycetin derivatives with Hammett constants and partition coefficients*, 85 (1963) 2817-2824.
- [66] L.P.J.C.r. Hammett, *Some relations between reaction rates and equilibrium constants*, 17 (1935) 125-136.
- [67] C. Hansch, A. Leo, D. Hoekman, *Exploring QSAR: fundamentals and applications in chemistry and biology*, American Chemical Society Washington, DC, 1995.
- [68] D.B. Boyd, K.J.R.i.C.C. Lipkowitz, *The computational chemistry literature*, 2 (1991) 461-479.
- [69] U. Norinder, T.J.A.p.n. Högberg, *A quantitative structure-activity relationship for some dopamine D2 antagonists of benzamide type*, 4 (1992) 73-78.
- [70] H. Van de Waterbeemd, N. El Tayar, B. Testa, H. Wikstroem, B.J.J.o.m.c. Largent, *Quantitative structure-activity relationships and eudismic analyses of the presynaptic dopaminergic activity and*

## References

dopamine D2 and. sigma. receptor affinities of 3-(3-hydroxyphenyl) piperidines and octahydrobenzo [f] quinolines, 30 (1987) 2175-2181.

[71] J. Ghasemi, S. Saaidpour, S.D.J.J.o.M.S.T. Brown, QSPR study for estimation of acidity constants of some aromatic acids derivatives using multiple linear regression (MLR) analysis, 805 (2007) 27-32.

[72] P. Geladi, B.R.J.A.c.a. Kowalski, Partial least-squares regression: a tutorial, 185 (1986) 1-17.

[73] A.J. Myles, R.N. Feudale, Y. Liu, N.A. Woody, S.D.J.J.o.C.A.J.o.t.C.S. Brown, An introduction to decision tree modeling, 18 (2004) 275-285.

[74] A.F. Duprat, T. Huynh, G.J.J.o.c.i. Dreyfus, c. sciences, Toward a principled methodology for neural network design and performance evaluation in QSAR. Application to the prediction of logP, 38 (1998) 586-594.

[75] I.V. Tetko, A.E.J.N.P.L. Villa, An enhancement of generalization ability in cascade correlation algorithm by avoidance of overfitting/overtraining problem, 6 (1997) 43-50.

[76] J. Gasteiger, J.J.A.C.I.E.i.E. Zupan, Neural networks in chemistry, 32 (1993) 503-527.

[77] R.J.J.o.C.A.J.o.t.C.S. Leardi, Genetic algorithms in chemometrics and chemistry: a review, 15 (2001) 559-569.

[78] A. Kovatcheva, A. Golbraikh, S. Oloff, Y.-D. Xiao, W. Zheng, P. Wolschann, G. Buchbauer, A.J.J.o.c.i. Tropsha, c. sciences, Combinatorial QSAR of ambergris fragrance compounds, 44 (2004) 582-595.

[79] J.G. Topliss, R.P.J.J.o.M.C. Edwards, Chance factors in studies of quantitative structure-activity relationships, 22 (1979) 1238-1244.

[80] J.J.N.F.C.S. Leszczynski, Challenges and advances in computational chemistry and physics, (2006) 1-680.

[81] R.D. Cramer, D.E. Patterson, J.D.J.J.o.t.A.C.S. Bunce, Comparative molecular field analysis (CoMFA). 1. Effect of shape on binding of steroids to carrier proteins, 110 (1988) 5959-5967.

[82] H. Kubinyi, G. Folkers, Y.C. Martin, 3D QSAR in Drug Design: Volume 2: Ligand-Protein Interactions and Molecular Similarity, Springer Science & Business Media, 1998.

[83] S. Chatterjee, A. Hadi, B.J.I. Price, New York, Regression analysis by example John Wiley & Sons, (2000).

## References

- [84] W.S. McCulloch, W.J.T.b.o.m.b. Pitts, A logical calculus of the ideas immanent in nervous activity, 5 (1943) 115-133.
- [85] L. Douali, A. Schmitzer, D. Villemin, A. Jarid, D.J.P. Cherqaoui, c. news, Neural networks and their applications in chemistry and biology, (2007) 131-144.
- [86] D.W. Salt, N. Yildiz, D.J. Livingstone, C.J.J.P.s. Tinsley, The use of artificial neural networks in QSAR, 36 (1992) 161-170.
- [87] I.J.M.p.l.o.d.d.d.M.e.M. Ghania, Université Mentouri, Constantine, Faculté des Sciences Exactes., Publié le, Régression et modélisation par les réseaux de neurones, (2009) 49.
- [88] R.J.R.l.b.e.p. Rakotomalala, Université Lumière Lyon, Pratique de la régression logistique, 2 (2011) 258.
- [89] J. Confais, M. Le Guen, Premiers pas en régression linéaire avec SAS®, (2007).
- [90] K. Roy, P.P.J.E.j.o.m.c. Roy, Comparative chemometric modeling of cytochrome 3A4 inhibitory activity of structurally diverse compounds using stepwise MLR, FA-MLR, PLS, GFA, G/PLS and ANN techniques, 44 (2009) 2913-2922.
- [91] L. Eriksson, J. Jaworska, A.P. Worth, M.T. Cronin, R.M. McDowell, P.J.E.h.p. Gramatica, Methods for reliability and uncertainty assessment and for applicability evaluations of classification- and regression-based QSARs, 111 (2003) 1361-1375.
- [92] P.J.Q. Gramatica, c. science, Principles of QSAR models validation: internal and external, 26 (2007) 694-701.
- [93] A. Golbraikh, A.J.J.o.m.g. Tropsha, modelling, Beware of  $q^2$ !, 20 (2002) 269-276.
- [94] H. Kubinyi, F.A. Hamprecht, T.J.J.o.m.c. Mietzner, Three-dimensional quantitative similarity-activity relationships (3d qsar) from self similarity matrices, 41 (1998) 2553-2564.
- [95] A. Worth, T. Hartung, C.J.S. Van Leeuwen, Q.i.E. Research, The role of the European centre for the validation of alternative methods (ECVAM) in the validation of (Q) SARs, 15 (2004) 345-358.
- [96] A.R. Leach, A.R. Leach, Molecular modelling: principles and applications, Pearson education, 2001.
- [97] J.J.J.o.t.A.s.A. Shao, Linear model selection by cross-validation, 88 (1993) 486-494.

## References

- [98] W. Svante, M. Sjöström, L.J.E.C.C. Erikson, Partial least squares projections to latent structures (PLS) in chemistry, 3 (2002).
- [99] A. Yasri, D.J.J.o.c.i. Hartsough, c. sciences, Toward an optimal procedure for variable selection and QSAR model building, 41 (2001) 1218-1227.
- [100] G. Schneider, P.J.P.i.b. Wrede, m. biology, Artificial neural networks for computer-based molecular design, 70 (1998) 175-222.
- [101] R. Guha, P.C.J.J.o.c.i. Jurs, modeling, Determining the validity of a QSAR model– a classification approach, 45 (2005) 65-73.
- [102] E. Novellino, C. Fattorusso, G.J.P.A.H. Greco, Use of comparative molecular field analysis and cluster analysis in series design, 70 (1995) 149-154.
- [103] U.J.J.o.c. Norinder, Single and domain mode variable selection in 3D QSAR applications, 10 (1996) 95-105.
- [104] N.S. Zefirov, V.A.J.J.o.c.i. Palyulin, c. sciences, QSAR for boiling points of “small” sulfides. Are the “high-quality structure-property-activity regressions” the real high quality QSAR models?, 41 (2001) 1022-1027.
- [105] P.P. Roy, K.J.Q. Roy, C. Science, On some aspects of variable selection for partial least squares regression models, 27 (2008) 302-313.

## **Chapter III**

### **Results and Discussion**

## Result and discussion

Many researches have been carried out for the development of anticancer drugs; nevertheless, no drug could achieve a parasitological cure and some of them presented serious toxic side effects.

While, **RESEARCHES NEVER END WITH NOTHING**, some compounds were found to be important candidates as inhibitors against topoisomerase II and cytotoxic activity.

Therefore, following our interest in this field, we applied several computational methods on the most effective Topo II candidates in order to, study structures and properties of these ligands, evaluate their biological response and better understand topoisomerase II inhibition mode.

To simplify our ideas, we divide this chapter to three big titles as follow:

- **Molecular Geometry, Electronic Properties, MPO Methods and Structure Activity/Property Relationship Studies of carbazole derivatives containing chalcone Analogues (CDCAs).**

At first, we aim to study the Structure, spectroscopy and electronic properties of carbazole subunit using DFT methods, Afterward, we extend a dataset of Carbazole Derivatives containing Chalcone Analogues, in order to identify compounds with higher potency, we study physicochemical properties, descriptors and drug-likeness scoring.

- **Quantitative Structure-Activity Relationships of Topo II inhibition activity of carbazole derivatives containing chalcone analogues (CDCAs).**

Next, in this part we develop QSAR models of CDCAs analogues with respect to their topoisomerase II inhibition activities.

### III .1 Introduction

Carbazole is a tricyclic compound (figure 34) belonging to the general class of nitrogen heterocycles. It possesses photoluminescent properties and good thermal stabilities [1,2] due its extended  $\pi$ -conjugation and aromatic character. [1] Carbazole derivatives exhibit interesting biological activities, with high potential for use as antibacterial, antifungal, antiviral, antimalarial, anticancer and anti-Alzheimer agents. [3,4] Additionally, carbazole-based compounds have potential applications for the symptomatic and disease-modifying treatment of Parkinson's disease. [5] Some derivatives of carbazole, such as N-substituted carbazole-imidazole hybrids, N-substituted carbazole imidazolium salts [6], N-thioalkylcarbazoles [7] and carbazole aminoalcohols, [8] have shown anti-proliferative activity against several tumor cell lines by a variety of mechanisms based on the inhibition of topoisomerase I and II (Topo I and Topo II, respectively). Further, according to recent studies, [9,10] it has been found that the carbazole scaffold functionalized with small substitution groups leads to stabilization of the intramolecular G-quadruplex, thus inhibiting the telomerase activity.

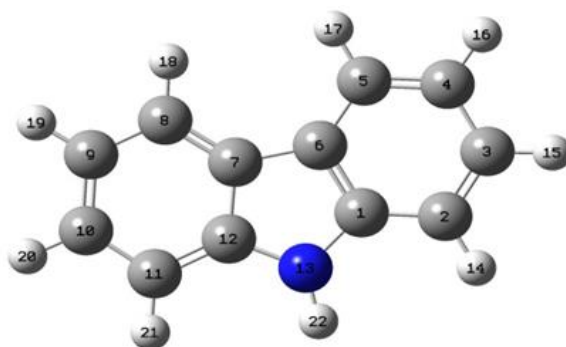


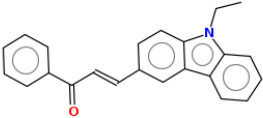
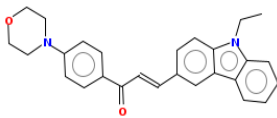
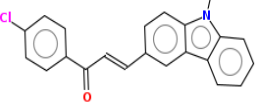
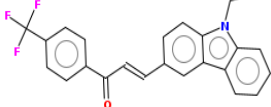
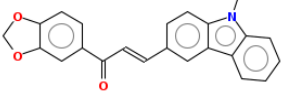
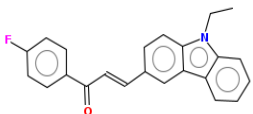
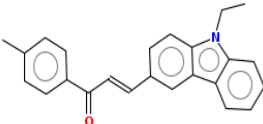
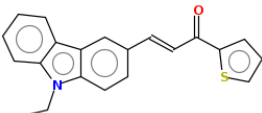
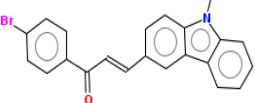
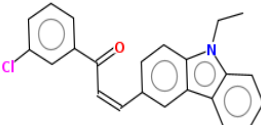
**Figure .34.**Chemical structure of carbazole with atom numbering.

A new set of Carbazole Derivatives containing Chalcone Analogues (CDCAs) was reported by Li et al in 2018. [11] All these compounds (from 1 to 24, see Table 3) possess a carbazole moiety connected to a chalcone group, with the only exception of

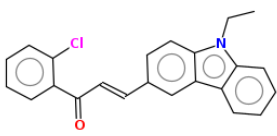
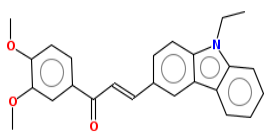
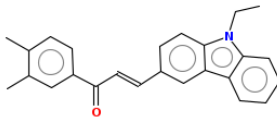
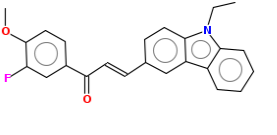
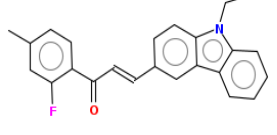
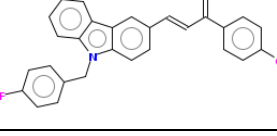
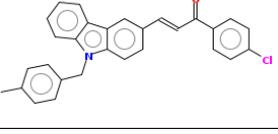
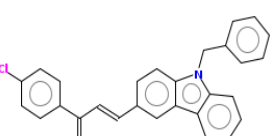
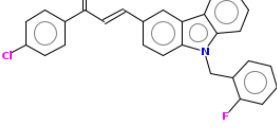
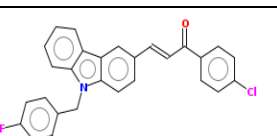
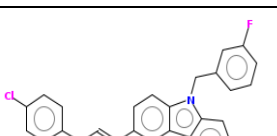
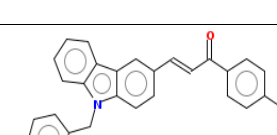
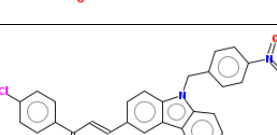
## Result and discussion

compound 8, in which the phenyl group of chalcone is replaced by a thiophene unit. Although etoposide (VP-16), here numbered as compound 25, is chemically different from the other compounds in Table 3, it was chosen as a reference drug. Indeed, its use as an efficient antineoplastic agent is well established since more than five decades. [12,13] Li et al. showed that the carbazole subunit in these compounds acts as a scaffold for Topo II inhibition, and that the chalcone moiety of CDCAs plays a key role in anticancer activity. This CDCAs series exhibits also a strong Topo II inhibitory and moderate cytotoxic activity against different tested cancer cell lines such as Hela, HL-60, A549, and PC-3. The different inhibitory activity shown by these molecules in laboratory studies is related to the differences in their molecular structures.

**Table 3:** Chemical structure and experimental activity ( $pIC_{50}$ [11]) of the CDCAs under study.  $pIC_{50}$  is  $\log_{10}(1/IC_{50})$ . \* denotes the compounds selected for external validation (test set).

N	Structure	$pIC_{50}$	N	Structure	$pIC_{50}$
1*		4.874	2		4.600
3		5.545	4*		5.209
5		4.574	6		4.888
7		6.658	8		4.787
9		4.623	10		5.038

## Result and discussion

11		5.144	12*		5.195
13		5.265	14		4.525
15		3.573	16		5.413
17		6.013	18		5.666
19		5.411	20		6.174
21		5.485	22		5.343
23		4.788	24*		5.903

Computational chemistry and modelling are useful tools in modern pharmacological and medicinal chemistry for both drug discovery and drug development. Indeed, their interplay with biological sciences have resulted in a better understanding of the mechanisms of action of drugs and body functions at the cellular and molecular levels. Consequently, most research projects in the pharmaceutical industry start by identifying a suitable target in the body and designing drugs able to interact with it. Knowledge of the structure and function of the target, as well as the mechanisms by which it interacts with drug molecules, is crucial to this approach. [14] In this respect, Density Functional Theory (DFT) [15-17] is a very elegant approach to describe the chemical processes and provides a powerful theoretical framework for the study of both reactivity and selectivity [17] of medium-sized molecular systems. In addition, the

## Result and discussion

Quantitative Structure-Activity Relationships (QSAR) approach attempts to establish a mathematical relation between the physicochemical and structural properties of a potential drug and its biological activity, [18] expressed in terms of  $pIC_{50}$ . Thus, it allows designing drug molecules with improved pharmacokinetic properties, reducing the number of compounds to be tested and limiting development failures. [14]

In this paper, we carried out several benchmark computations on the structure and spectroscopy of the carbazole subunit using the DFT technique. After comparison to experiments, it turns out that the B3LYP/6-311 G(d,p) level is accurate enough to derive accurate physicochemical properties and parameters for the 25 CDCA derivatives identified in the recent work by Li et al. [11] In order to predict the pharmacological activity of these compounds, we incorporated these parameters into quantitative models based on two statistical methods: Multiple Linear Regression (MLR) and Artificial Neural Network (ANN). As implemented, the present combined QSAR-DFT approach [19-23] for the calculation of descriptors allows us to build simpler (less parameterized) models, thus reducing the risk of over-parameterization, for an easier and more direct interpretation of the drug activity at the phenomenological level. In order to develop an accurate model capable of explaining the role of CDCAs derivatives in chemotherapy, we have performed drug-like calculations, evaluations of physicochemical properties and QSAR study of carbazole derivatives containing chalcone analogues targeting Topo II inhibition (Figure 35) and presenting strong cytotoxic activity. In addition, our model will facilitate the design of new CDCAs for this purpose.

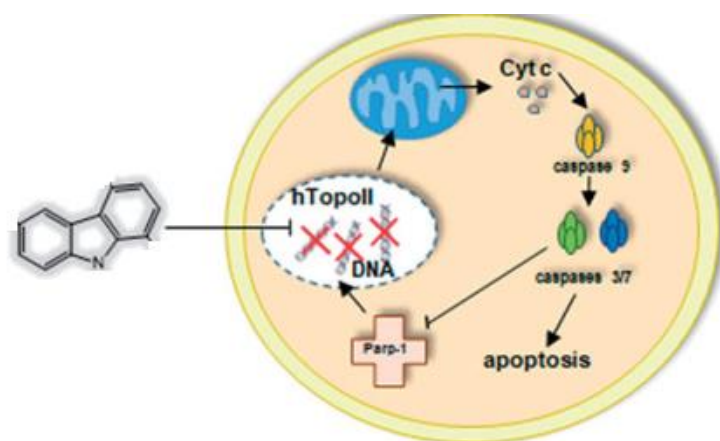


**Figure .35.** The Synthetic or natural carbazole derivatives induces cancer cells death triggering the intrinsic apoptotic pathway by inhibition of Topoisomerase II.

### III .2 Structure, spectroscopy and electronic properties of carbazole and its derivatives

The choice of the approach for electronic structure computations on a given molecular system is crucial to accurately describe its reactivity, selectivity and most stable molecular conformation. Indeed, the latter is closely connected to the identification of interactions between the drug and active site of the enzyme. Due to the relatively large size of drug molecules, post Hartree-Fock ab initio computations on these systems are out of reach. Instead, various studies showed that DFT calculations on large molecules yield good results on different systems (organic, inorganic, and organometallic ...) [23-26] at a reasonable computational cost. Indeed, DFT takes into account the dynamic correlation of electrons [27], which is mandatory for the accurate description of the structure and the spectroscopic properties of these compounds. Hence, in this study we opted for DFT-based approaches. For instance, computations were performed using gradient-corrected DFT with the Becke 3 exchange [28] and Lee-Yang-Parr correlation functions (B3LYP), in conjunction with three different basis sets 6-31G+(d,p), 6-311G and 6-311G(d,p), as implemented in GAUSSIAN 09 program package. [29]

#### III .2.1 Carbazole structure and properties

Prior to deriving the properties of the CDCAs of interest, we performed geometry optimizations of the carbazole subunit in its electronic ground state. We carried out these computations at the B3LYP/6-31G+(d,p), B3LYP/6-311G and B3LYP/6-311G(d,p) levels of theory in order to select an appropriate atomic basis set for the molecular systems studied herein. The results are listed in Table 2.

## Result and discussion

**Table 4:** Equilibrium Geometrical Parameters (Bond lengths in Å and angles in degrees) of carbazole in its electronic ground state. The numbering of the atoms is given in Figure 34.

Parameters	DFT/B3LYP			Exp. <sup>a)</sup>
	6-31G+(d,p)	6-311G	6-311G(d,p)	
C1-C2	1.398	1.397	1.395	1.393
C1-C6	1.421	1.424	1.419	1.401
C1-N13	1.388	1.396	1.385	1.387
C2-C3	1.395	1.395	1.390	1.373
C2-H14	1.087	1.082	1.085	1.00
C3-C4	1.408	1.408	1.404	1.379
C3-H15	1.086	1.082	1.084	0.96
C4-C5	1.394	1.395	1.390	1.379
C4-H16	1.086	1.082	1.084	1.02
C5-C6	1.402	1.400	1.398	1.388
C5-H17	1.087	1.082	1.085	1.01
C6-C7	1.450	1.454	1.449	1.415
C7-C8	1.402	1.400	1.398	1.388
C7-C12	1.421	1.424	1.419	1.401
C8-C9	1.394	1.395	1.390	1.379
C8-H18	1.087	1.082	1.085	1.01
C9-C10	1.408	1.408	1.404	1.379
C9-H19	1.086	1.082	1.084	1.02
C10-C11	1.395	1.395	1.390	1.373
C10-H20	1.086	1.082	1.084	0.96
C11-C12	1.398	1.397	1.395	1.393
C11-H21	1.087	1.082	1.085	1.00
C12-N13	1.388	1.396	1.385	1.387
N13-H22	1.007	1.003	1.057	0.98
C2-C1-C6	121.9	121.8	121.8	122.3
C2-C1-N13	129.6	129.8	129.7	128.7
C6-C1-N13	108.4	108.3	108.4	109
C1-C2-C3	117.6	117.7	117.7	116.7
C1-C2-H14	121.4	121.3	121.3	121
C3-C2-H14	120.9	120.8	120.9	122
C2-C3-C4	121.3	121.2	121.3	122

## Result and discussion

C2-C3-H15	119.2	119.3	119.2	119
C4-C3-H15	119.4	119.4	119.4	119
C3-C4-C5	120.7	120.7	120.7	121
C3-C4-H16	119.5	119.4	119.4	118
C5-C4-H16	119.8	119.8	119.8	121
C4-C5-C6	119.2	119.2	119.2	118.4
C4-C5-H17	120.3	120.3	120.3	124
C6-C5-H17	120.5	120.5	120.4	118
C1-C6-C5	119.2	119.2	119.2	119.7
C1-C6-C7	106.7	106.9	106.7	106.6
C5-C6-C7	134.0	133.9	134.1	133.7
C6-C7-C8	134.0	133.9	134.1	133.7
C6-C7-C12	106.7	106.9	106.7	106.6
C8-C7-C12	119.2	119.2	119.2	119.7
C7-C8-C9	119.2	119.2	119.2	118.4
C7-C8-H18	120.4	120.5	120.4	118
C9-C8-H18	120.3	120.3	120.3	124
C8-C9-C10	120.7	120.7	120.7	121
C8-C9-H19	119.8	119.8	119.8	121
C10-C9-H19	119.5	119.4	119.4	118
C9-C10-C11	121.3	121.2	121.3	122
C9-C10-H20	119.4	119.4	119.4	119
C11-C10-H20	119.2	119.3	119.2	119
C10-C11-C12	117.6	117.7	117.7	116.7
C10-C11-H21	120.9	120.8	120.9	122
C12-C11-H21	121.4	121.3	121.3	121
C7-C12-C11	121.9	121.8	121.8	122.3
C7-C12-N13	108.5	108.3	108.4	109
C11-C12-N13	129.6	129.8	129.7	128.7
C1-N13-C12	109.6	109.5	109.6	108.7
C1-N13-H22	125.2	125.2	125.8	125.65
C12-N13-H22	125.2	125.2	125.8	125.65

a. Ref. [30].

where a comparison is made between these theoretical data and the experimental results by Gerkin and Reppart. [30] As expected, the larger basis set (i.e.

## Result and discussion

6-311G(d,p)) performs better than the smaller ones. Indeed, a good agreement between the experimental data and those deduced using the 6-311G(d,p) basis set is found. For instance, deviations between the computed and measured distances are mostly in the range 0.002-0.2 Å. For the angles, the differences between the two sets are mostly less than 1°, except for a few ones that are 3.7° off. Such deviations may be related to the gas phase structure (here) and the crystal structure of carbazole determined in Gerkin and Reppart's experiments. Overall, this basis set is reliable enough for the study of the molecular and electronic structure of this molecule and of its derivatives. For further confirmation, we computed the anharmonic frequencies of carbazole. Table 3 gives the computed values for the 60 normal modes of vibration of carbazole, together with the comparison to the measured fundamentals by Bree and Zwarich. [31] Again, a good agreement is found between the two sets of data, where the differences between both sets are less than 30 cm<sup>-1</sup>, except for U<sub>1</sub> (NH stretching), for which we computed 3501 cm<sup>-1</sup>, while Bree and Zwarich measured 3421 cm<sup>-1</sup>. In sum, we conclude that B3LYP, in conjunction with the 6-311G(d, p) basis set, is accurate enough for investigating the carbazole derivatives. In the following, this level of theory will be used for the treatment of the structural and physicochemical properties of the CDCAs of interest.

**Table 5:** Comparison of the experimental and calculated anharmonic frequencies ( $\nu$ , in cm<sup>-1</sup>) of carbazole. Computed at the B3LYP/6-311G(d,p) level of theory and we give also the computing of IR intensity (I in (km/mol)). Abbreviations used:  $\nu$ , stretching;  $\nu_s$ , sym. stretching;  $\nu_{as}$ , asym. stretching;  $b$ , in-plane-bending;  $g$ , out-of-plane bending; Ben: Benzene; Pyr: pyrrole.

Sym	Calculated		Exp <sup>a)</sup> $\nu$	Assignment
	$\nu$	I		
a <sub>1</sub>	3501	41.0	3421	$\nu$ NH (Ben)
	3056	43.2	3084	$\nu_s$ CH (Ben)
	3051	2.3	3077	$\nu_s$ CH (Ben)
	3048	1.2	3055	$\nu_s$ CH (Ben)
	3046	55.6	3039	$\nu_{as}$ CH (Ben)
	1628	2.9	1625	$\beta$ CCC (Ben) + $\nu$ CC (Pyr)

## Result and discussion

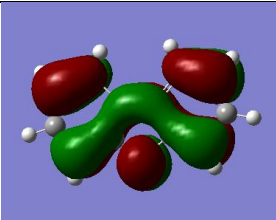
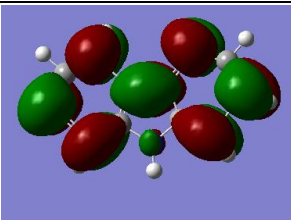
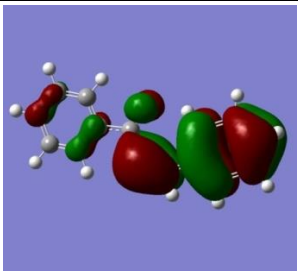
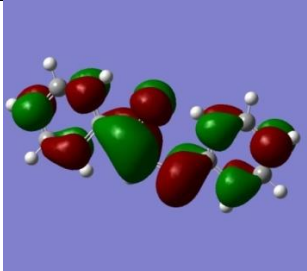
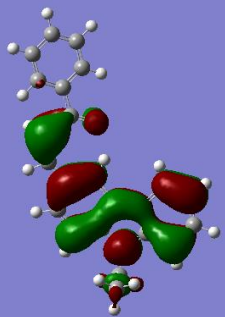
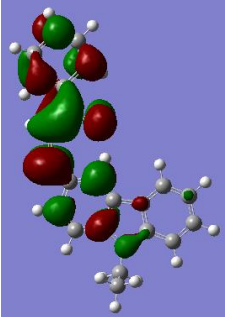
	1580	0.8	1576	$\nu$ C=C (Ben-Pyr)
	1486	0.0	1481	$\nu$ CC (Pyr)
	1449	27.1	1449	$\nu$ C=C (Ben-Pyr)
	1340	8.2	1334	$\beta$ CNC (Pyr) + $\nu$ C=C (Ben-Pyr)
	1312	0.1	1288	$\nu$ CC (Pyr) + $\nu$ C=C (Ben)
	1235	78.8	1205	$\nu$ C=C (Ben-Pyr) + $\nu$ CN (Pyr)
	1162	4.6	1136	$\nu$ C=C (Ben-Pyr)
	1113	2.3	1107	$\nu$ CC (Pyr) + $\beta$ CCC (Ben)
	1021	0.3	1012	$\nu$ C=C (Ben)
	932	3.6	910	$\gamma$ CH (Ben)
	851	0.0	856	$\gamma$ CH (Ben) + $\gamma$ CCC (Ben-Pyr)
	755	47.3	747	$\gamma$ CH (Ben) + $\gamma$ CNH (Pyr)
	642	0.5	658	$\beta$ CNC + $\beta$ CCC (Ben-Pyr)
	426	10.4	425	$\gamma$ CH (Ben) + $\gamma$ NH (Pyr)
	216	0.3	220	$\beta$ CCC (Ben-Pyr)
a <sub>2</sub>	969	0.0		$\gamma$ CH (Ben)
	968	0.0		$\gamma$ CH (Ben)
	846	2.7		$\beta$ CCN + $\beta$ CCC (Ben-Pyr)
	780	0.0		$\gamma$ CH (Ben) + $\gamma$ CCC (Pyr)
	580	0.0		$\gamma$ CH (Ben)
	429	1.0		$\beta$ CCC + CCN (Ben-Pyr)
	290	0.0		$\gamma$ ring Ben
	298	3.9	299	$\gamma$ CH (Ben) + $\gamma$ NH (Pyr)
b <sub>2</sub>	107	3.0	104	$\gamma$ CH (Ben)
	3059	0.3	3094	$\nu$ as CH (Ben)
	3048	10.6	3050	$\nu$ s CH (Ben)
	3027	5.5	3030	$\nu$ CH (Ben)
	3013	1.6	2940	$\nu$ CH (Ben)
	1582	1.5	1594	$\nu$ C=C (Ben-Pyr)
	1495	15.0	1490	$\nu$ C=C (Ben) + $\nu$ CN (Pyr)
	1465	30.0	1452	$\nu$ C=C (Ben-Pyr)
	1395	21.2	1380	$\nu$ C=C (Ben) + $\nu$ CN (Pyr)
	1324	29.4	1320	$\nu$ C=C (Ben-Pyr)
	1281	1.7	1233	$\nu$ CN (Pyr)
	1216	6.4	1204	$\nu$ C=C (Ben) + $\nu$ CN (Pyr)
	1207	6.0	1158	$\nu$ C=C (Ben-Pyr)
	1126	5.6	1118	$\nu$ C=C (Ben)
	1031	0.3	1022	$\nu$ C=C (Ben)
	1002	6.4	995	$\beta$ CCC (Ben)+ $\beta$ CH (Ben)
	844	1.3	835	$\gamma$ CH (Ben)
	741	0.0	737	$\gamma$ CH (Ben)
	627	5.9	616	$\beta$ CCC (Ben-Pyr)
	559	0.1	548	$\beta$ CCC (Ben)
b <sub>1</sub>	510	3.5	505	$\beta$ ringPyr
	1605	23.7		$\beta$ CCC (Pyr) + $\nu$ C=C (Ben)
	1169	0.5	1152	$\nu$ C=C (Ben)
	937	0.1	926	$\gamma$ CH (Ben)
	882	0.2	880	$\beta$ CNC + $\beta$ CCC (Ben-Pyr)
	749	0.1	741	$\beta$ CCC (Ben)
	731	87.5	722	$\gamma$ CH (Ben)
	569	6.6	566	$\gamma$ CH (Ben) + $\gamma$ NH (Pyr)
	444	0.0	445	$\gamma$ CH (Ben) + $\gamma$ CCC (Ben-Pyr)
	342	70.7	310	$\gamma$ NH (pyr)
	149	0.0	139	$\gamma$ CH (Ben)

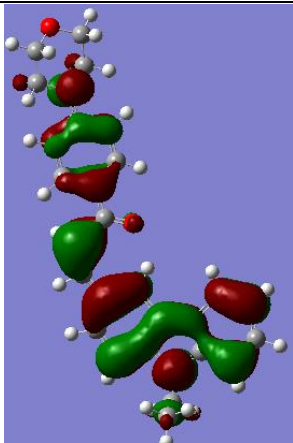
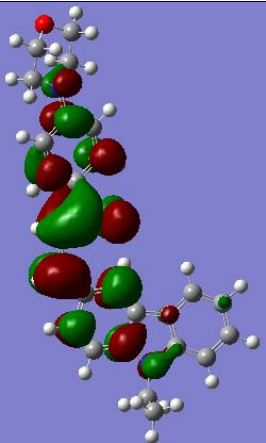
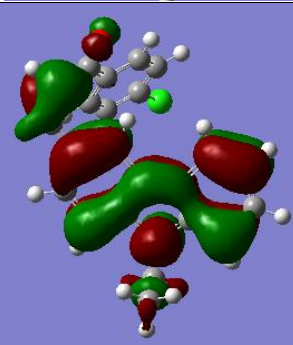
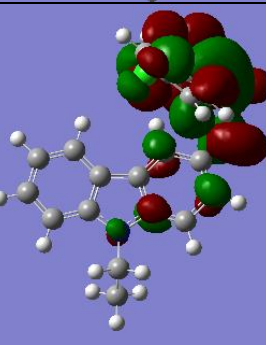
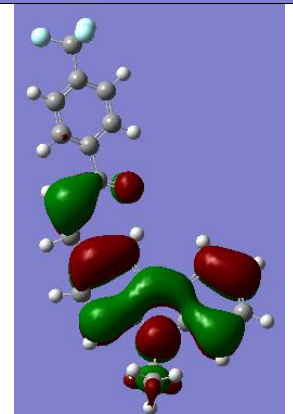
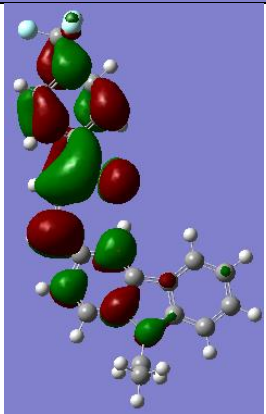
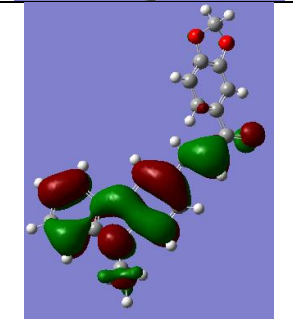
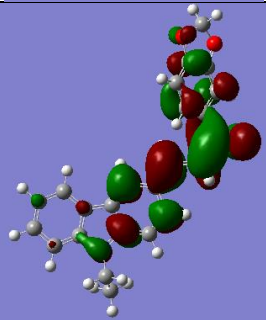
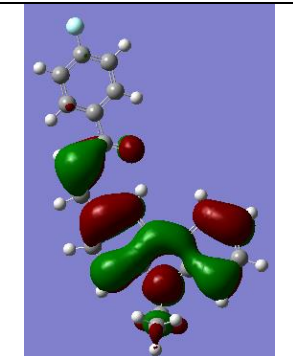
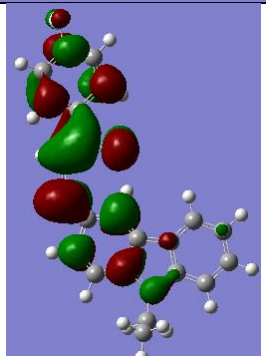
## Result and discussion

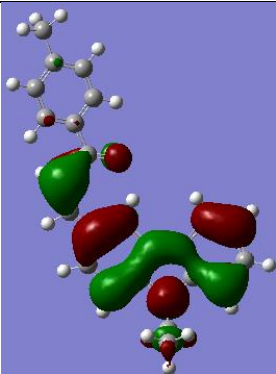
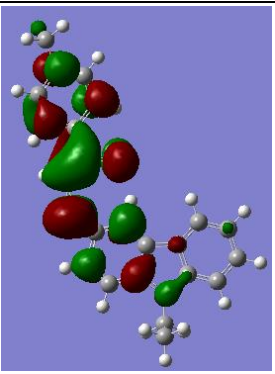
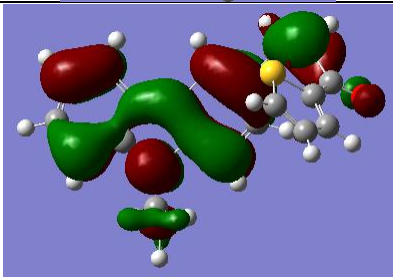
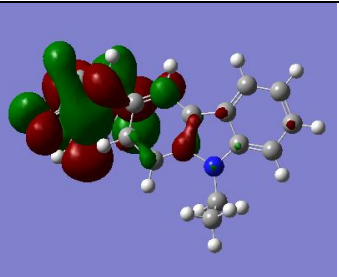
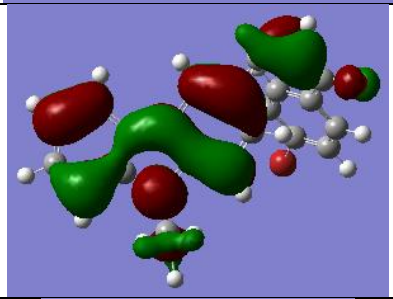
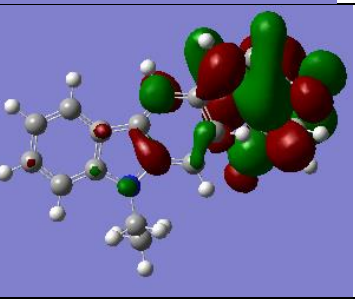
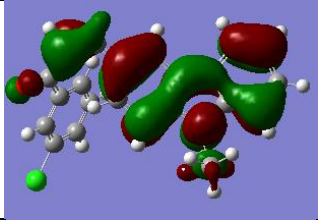
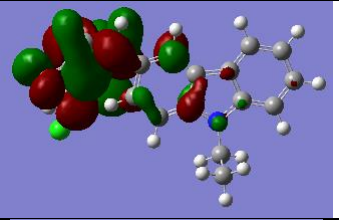
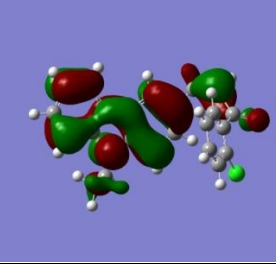
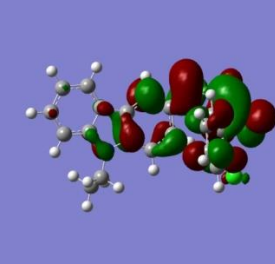
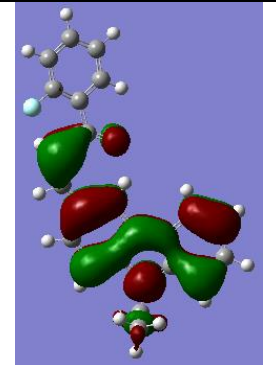
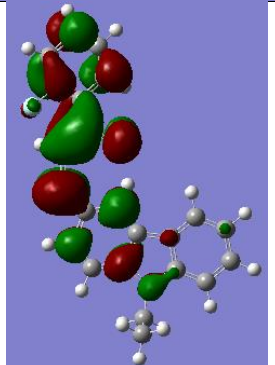
a) The detection of these observed frequencies of the bands has been made in the gas state.[2]

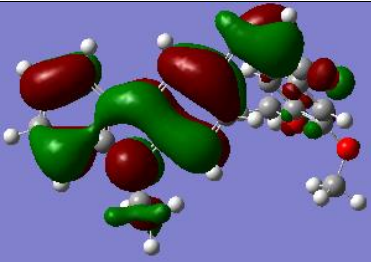
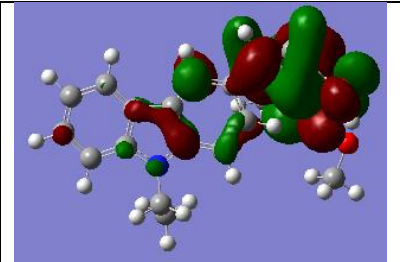
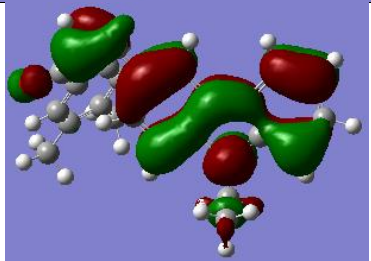
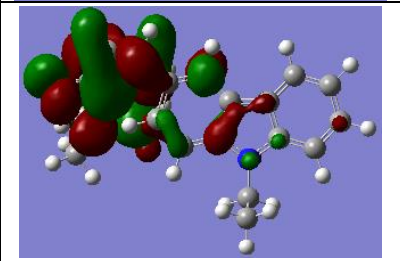
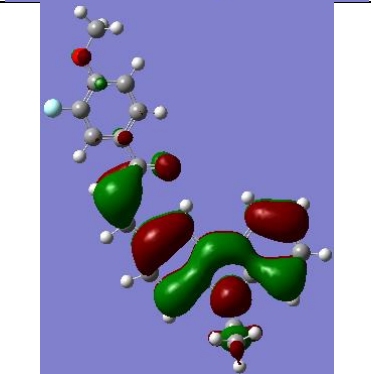
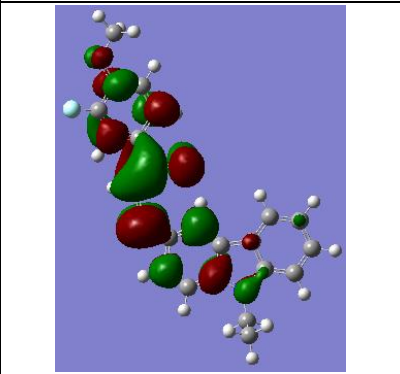
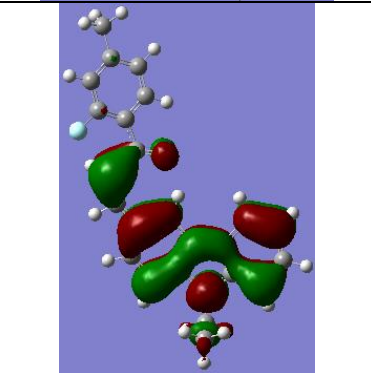
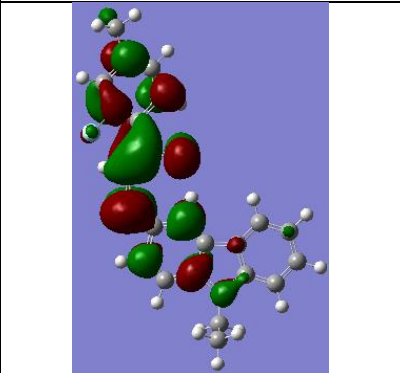
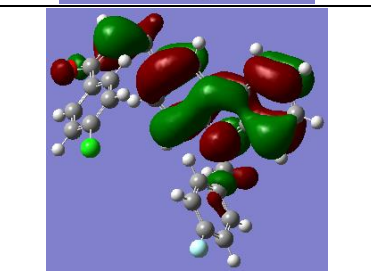
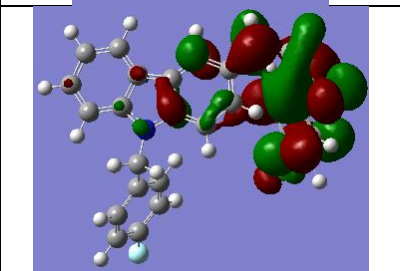
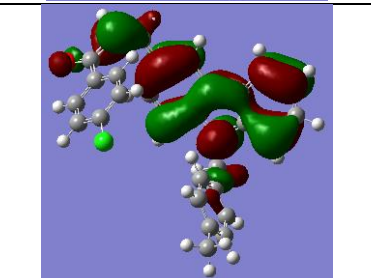
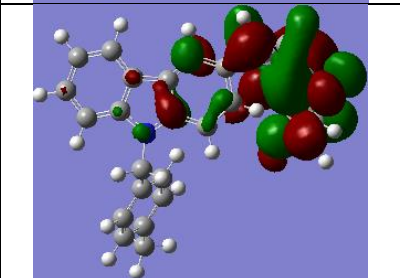
Since carbazole is the scaffold for Topo II inhibition, we studied its reactivity. A powerful practical model for describing chemical reactivity is the frontier molecular orbital theory, which is useful to explain drug–receptor interactions. [32] These are related to the overlap between the highest occupied molecular orbital (HOMO) and the lowest unoccupied molecular orbital (LUMO) of the two molecular entities, which provides information on their electron-donating and electron-withdrawing character, [33] respectively. These molecular orbitals (MOs) are displayed in Table 6. This figure shows that the HOMO and LUMO correspond to  $\pi$  bonding and anti-bonding MOs, respectively, spreading over the whole carbazole molecule.

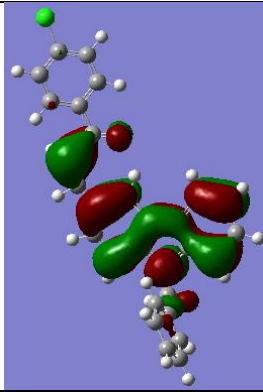
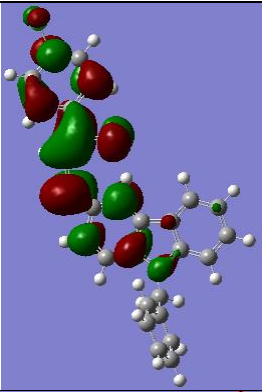
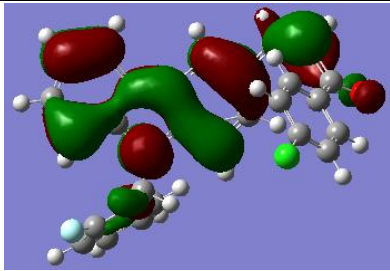
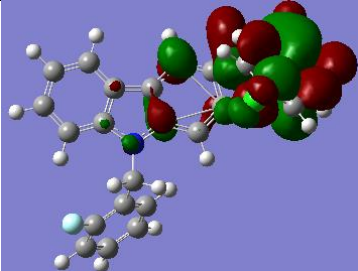
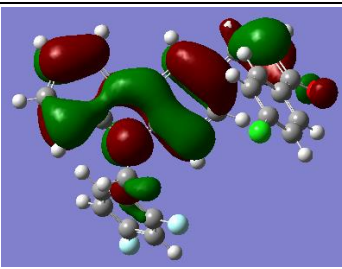
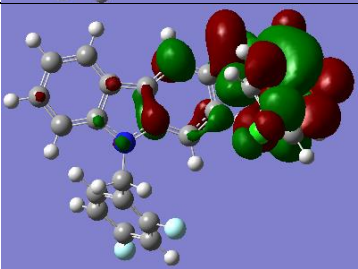
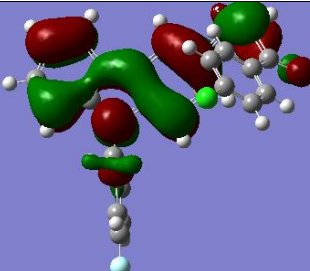
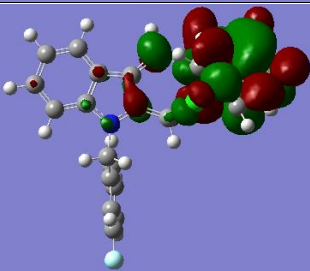
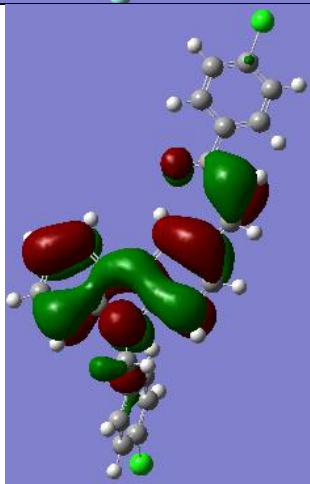
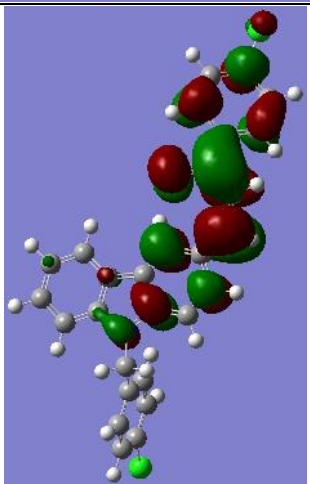
**Table 6:** Outermost molecular orbitals of carbazole and of its derivatives of interest in the present study.  $\Delta E$  (in eV) corresponds to the energy HOMO – LUMO gap.

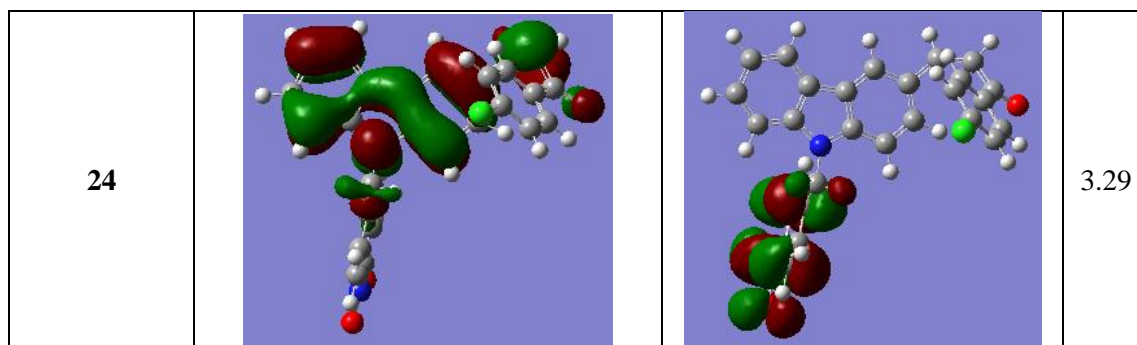
Compound	HOMO	LUMO	$\Delta E$
Carbazole			4.73
Chalcone			4.13
1			3.47

2				3.53
3				3.63
4				3.31
5				3.84
6				3.45

7			3.50
8			3.70
9			3.65
10			3.65
11			3.76
12			3.41

13			3.94
14			3.86
15			3.48
16			3.43
17			3.71
18			3.67

19			3.42
20			3.67
21			3.75
22			3.75
23			3.46



In addition, we analyzed the Fukui function of carbazole. This function describes how the electron density responds to the change in the total number of electrons and allows us to recognize the favored sites for electrophilic and nucleophilic attacks. [17,34,35] The reactivity of an atom A in a molecule can be described by the following condensed Fukui functions [17]:

$$f_+(A) = [q_{N+1}(A) - q_N(A)]$$

$$f_-(A) = [q_N(A) - q_{N-1}(A)]$$

$$f_0(A) = [q_{N+1}(A) - q_{N-1}(A)] / 2$$

where  $q_N(A)$ ,  $q_{N+1}(A)$  and  $q_{N-1}(A)$  are the electronic populations of atom A in a neutral molecule and in the corresponding anionic and cationic species, respectively. Atoms with large values of  $f_+(A)$ ,  $f_-(A)$  and  $f_0(A)$  in a given molecule will be more easily attacked by nucleophiles, electrophiles and radicals, respectively.

We also computed the dual function,  $\Delta f(r)$ , [37] which is calculated as the difference between the nucleophilic and electrophilic condensed Fukui functions:

$$\Delta f(A) = [f_+(A) - f_-(A)]$$

Thus,  $\Delta f$  is positive for atoms that are more easily attacked by nucleophiles and negative for those that are more easily attacked by electrophiles. [37] Results are given in Table 7.

**Table 7:** Values of the Fukui functions of carbazole. See text for the definition of the different terms.

Atoms	$q(N)$	$q(N+1)$	$q(N-1)$	$f_+$	$f_-$	$f_0$	$\Delta f$
C1	0.2050	0.1950	0.1990	-0.0100	0.0060	-0.0020	-0.0160

## Result and discussion

C2	-0.0660	0.0060	-0.1350	0.0720	0.0690	0.0705	0.0030
C3	-0.0960	-0.0750	-0.1590	0.0210	0.0630	0.0420	-0.0420
C4	-0.1110	-0.0580	-0.1120	0.0530	0.0010	0.0270	0.0520
C5	-0.0390	0.0070	-0.1290	0.0460	0.0900	0.0680	-0.0440
C6	-0.0920	-0.0710	-0.0940	0.0210	0.0020	0.0115	0.0190
C7	-0.0920	-0.0710	-0.0940	0.0210	0.0020	0.0115	0.0190
C8	-0.0390	0.0071	-0.1290	0.0461	0.0900	0.0681	-0.0439
C9	-0.1110	-0.0580	-0.1120	0.0530	0.0010	0.0270	0.0520
C10	-0.0960	-0.0750	-0.1590	0.0210	0.0630	0.0420	-0.0420
C11	-0.0660	0.0060	-0.1350	0.0720	0.0690	0.0705	0.0030
C12	0.2050	0.1950	0.1990	-0.0100	0.0060	-0.0020	-0.0160
N13	-0.5250	-0.4350	-0.5310	0.0900	0.0060	0.0480	0.0840
H14	0.0850	0.1430	0.0230	0.0580	0.0620	0.0600	-0.0040
H15	0.0910	0.1470	0.0240	0.0560	0.0670	0.0615	-0.0110
H16	0.0890	0.1520	0.0270	0.0630	0.0620	0.0625	0.0010
H17	0.0820	0.1330	0.0270	0.0510	0.0550	0.0530	-0.0040
H18	0.0820	0.1330	0.0270	0.0510	0.0550	0.0530	-0.0040
H19	0.0890	0.1520	0.0270	0.0630	0.0620	0.0625	0.0010
H20	0.0910	0.1470	0.0240	0.0560	0.0670	0.0615	-0.0110
H21	0.0850	0.1430	0.0230	0.0580	0.0620	0.0600	-0.0040
H22	0.2250	0.2770	0.1860	0.0520	0.0390	0.0455	0.0130

Apart from the hydrogens atoms, (Table 7, Figure 36) shows that negative  $\Delta f$  values are determined for the C<sub>1</sub>, C<sub>3</sub>, C<sub>5</sub>, C<sub>8</sub>, C<sub>10</sub> and C<sub>12</sub> atoms. This reveals that the ortho positions of the aromatic cycles in carbazole are highly reactive with respect to electrophilic attacks. In contrast, the other carbon atoms, except C<sub>2</sub> and C<sub>11</sub>, of carbazole and especially the nitrogen

## Result and discussion

atom present positive  $\Delta f$  values. Therefore, these atomic centers are mostly subject to nucleophilic attacks. We expect that the C<sub>2</sub> and C<sub>11</sub> atoms, i.e. those associated with the largest  $f_0$  values (Table 7), will be the most probable sites for radical attacks.

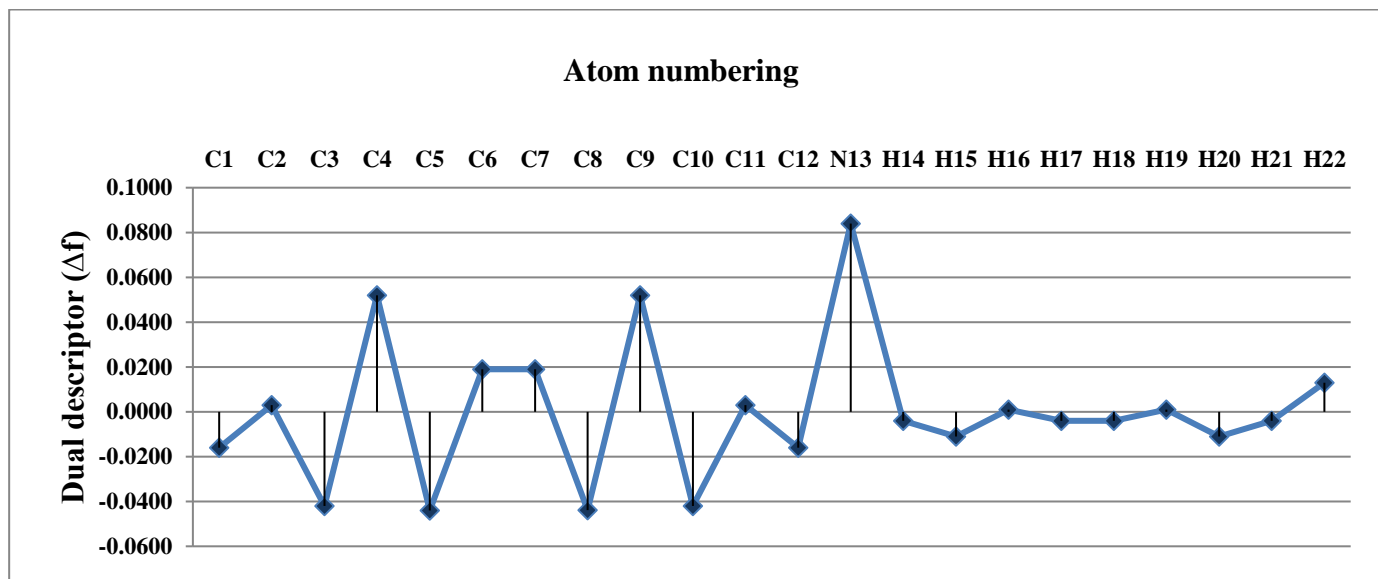


Figure.36. Dual descriptor ( $\Delta f$ ) Vs Atoms.

### III .3 Carbazole derivatives structures

At first, we preoptimized the CDCAs to get minimal energy structures using the Molecular Mechanics Force Field (MM+) followed by the semi-empirical AM1 method, with a convergence threshold of 0.01 kcal/Å in the gradient norm, as implemented in the HyperChem (version 8.08) package. [38] This allowed us to identify the most stable forms that were further optimized using the DFT B3LYP/6-311++G(d,p) method. The resulting structures, in Cartesian coordinates, are displayed in Table S1 (in Appendix). Close examination of this table reveals that the carbazole subunit exhibits slight changes compared to the isolated carbazole, whereas the chalcone part of the CDCAs either resembles the isolated chalcone or presents strong changes. This justifies a posteriori the choice of chalcone for the above-mentioned benchmark computations.

## Result and discussion

According to the structure of the chalcone moiety, we can easily classify the CDCAs into two conformational types: i) Type 1 compounds, showing slight changes in the chalcone subunit, and ii) Type 2 compounds, with a non-planar arrangement of the enone/chalcone moiety.

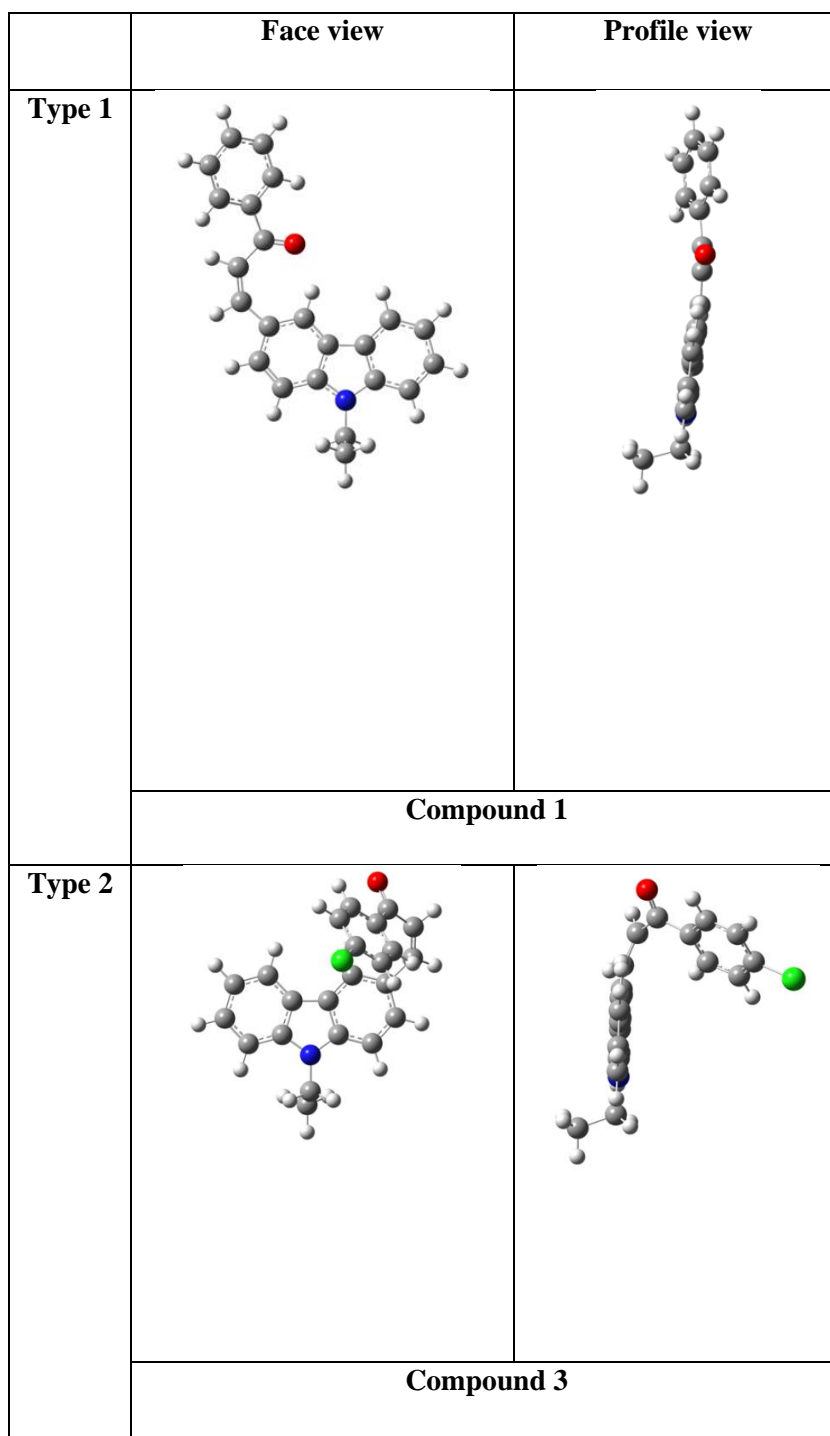


Figure .37. Face and profile views of Compounds 1 and 3.

The central part of Type 1 compounds, the one formed by the chalcone and carbazole moieties, is almost planar. Type 1 molecules have similar shapes as Compound 1, displayed in the upper part of Figure 37, and correspond to Compounds 1, 2, 4, 5, 6, 7, 12, 15, 16, 19 and 23. These molecules are stabilized by extended electron conjugation over the aromatic rings of carbazole and chalcone through the connecting enone. Type 2 molecules have similar shapes as Compound 3, displayed in the lower part of Figure 37, and correspond to Compounds 3, 8, 9, 10, 11, 13, 14, 17, 18, 20, 21, 22 and 24. The stabilization here is due to  $\pi$ -stacking interactions between the phenyl of chalcone and the aromatic rings of carbazole. Indeed, the mesomerism and the  $\pi$ -stacking interactions are in competition to lead to Type 1 or Type 2 compounds. Nevertheless, we cannot observe any clear relation between the structure of these CDCAs and their measured biological activity (Table 3). For instance, Compounds 15 and 7 have  $pIC_{50}$  values of  $\sim 3.5$  and 6.7 despite both of them being of Type 1. Table 3 shows also that Compound 20 has a  $pIC_{50}$  of 6.174 close to that of Compound 7, despite being of Type 2. Consequently, different shapes are obtained for these CDCAs even if all of them possess similar biological and cytotoxic effects. Therefore, the interaction of these CDCAs with Topo II should be more complex than the commonly admitted key-lock mechanism, which is based on shape complementarity between the substrate and enzymatic active site. We conclude that an induced-fit mechanism is more plausible, where conformational fluctuations in the enzyme-substrate complex should influence the dynamics of the inhibition process, thus affecting the biological activity of the studied compounds.

### III.4 CDCAs derivatives physicochemical properties, descriptors and drug-likeness scoring

The molecular orbital theory is extremely useful for physicists and chemists. In particular, the HOMO and LUMO of a chemical species are important for discussing the molecular reactivity and can help to interpret the intermolecular protein-ligand interactions. The DFT B3LYP/6-311G(d,p) method as implemented in Gaussian 09

## Result and discussion

was employed to derive the outermost molecular orbitals (HOMO, LUMO and related energies) of carbazole derivatives. These orbitals are displayed in Table 6. These compounds have a HOMO/LUMO mostly localized on the carbazole and chalcone moiety, respectively. Interestingly the HOMO-LUMO gap for all CDCAs is almost the same (of  $\sim 3.5$  eV).

In order to obtain validated QSAR models, several molecular descriptors, encoding various information about size, hydrophilicity, electronic and topological properties, were calculated using the Molecular Operating Environment (MOE) [39] software and the QSAR Properties (version 8.0.6) module integrated in the HyperChem package. The deduced properties correspond to molar weight (MW), surface area grid (SAG), volume (V), molecular refractivity (MR), polarizability (Pol), octanol-water partition coefficient ( $\log_{10}P$ ), hydration energy (HE), hydrogen bond donors (HBDs, counting the sum of all NH and OH groups), hydrogen bond acceptors (HBA, counting all N and O atoms), number of rotatable bonds ( $N_{\text{brot}}$ ) and topological polar surface area (TPSA). We also deduced the number of atoms ( $N_{\text{atom}}$ ) and the number of heavy atoms ( $N_{\text{H}}$ ). These data are listed in Tables 8 and 9. These tables show that large values of MR and Pol correspond to large values of V and MW, in agreement with the Lorentz-Lorenz equation. [40] For example, Compound 24, the one with the p-chlorophenyl and nitrophenyl groups, has rather large values of Pol ( $68.74 \text{ \AA}^3$ ) and MR ( $149.41 \text{ \AA}^3$ ), which are associated with large values of V ( $1409.29 \text{ \AA}^3$ ) and MW (466.92 amu). Whereas, Compound 1 has the smallest values of MR ( $115.47 \text{ \AA}^3$ ) and Pol ( $55.05 \text{ \AA}^3$ ). HE is an important parameter connected to the stabilization of molecules bearing polar groups and a great predictive index for molecule accessibility in biologic media. [41,42] Compound 14 has the smallest |HE| value (1.1 kcal/mol), while the largest |HE| values are observed for Compounds 24 and 25 (VP-16) (9.05 and 22.75 kcal/mol, respectively), which bear hydrophilic groups (e.g.  $\text{NO}_2$ , CO, CN, and OH).

**Table 8:** Physicochemical properties of CDCAs derivatives. For each compound, we give the energies of the HOMO ( $E_{\text{HOMO}}$  in a.u.) and of the LUMO ( $E_{\text{LUMO}}$  in a.u.), the polarizability (Pol in  $\text{ \AA}^3$ ), the volume (V in  $\text{ \AA}^3$ ), the surface area grid (SAG in  $\text{ \AA}^3$ ) and the hydration energy (HE in kcal/mol). \* denotes the selected compounds for external validation (test set).

Compound	E <sub>HOMO</sub>	E <sub>LUMO</sub>	Pol	V	SAG	HE
<b>1*</b>	-0.2052	-0.07763	55.05	953.84	559.04	-2.86
<b>2</b>	-0.19969	-0.06997	68.66	1177.74	678.02	-3.56
<b>3</b>	-0.20881	-0.0735	56.56	955.41	543.72	-2.47
<b>4*</b>	-0.21087	-0.08925	57.82	1033.16	601.92	-2.29
<b>5</b>	-0.20883	-0.06771	58.42	1020.74	604.76	-7.10
<b>6</b>	-0.20716	-0.08021	54.94	962.56	566.94	-2.57
<b>7</b>	-0.20385	-0.07526	58.14	1007.58	584.98	-4.46
<b>8</b>	-0.20599	-0.06983	53.10	906.05	535.90	-3.12
<b>9</b>	-0.21001	-0.07562	57.43	983.06	557.22	-2.76
<b>10</b>	-0.21069	-0.07664	56.56	976.37	573.38	-2.70
<b>11</b>	-0.21046	-0.07214	56.56	992.69	584.95	-2.89
<b>12*</b>	-0.20561	-0.08033	54.94	960.25	562.34	-2.68
<b>13</b>	-0.20507	-0.06008	62.84	1065.32	596.47	-5.22
<b>14</b>	-0.20475	-0.06289	61.24	1092.35	596.88	-1.10
<b>15</b>	-0.20476	-0.07672	58.84	1039.58	609.74	-3.87
<b>16</b>	-0.20417	-0.07786	58.03	1014.3	588.16	-1.55
<b>17</b>	-0.21414	-0.07771	66.59	1089.36	597.18	-3.76
<b>18</b>	-0.21053	-0.07575	69.79	1133.75	618.72	-2.92
<b>19</b>	-0.21022	-0.08467	66.70	1144.15	665.11	-4.04
<b>20</b>	-0.21105	-0.07607	66.59	1123.72	634.55	-3.92
<b>21</b>	-0.21356	-0.0757	66.48	1127.34	637.58	-3.72
<b>22</b>	-0.21514	-0.07723	66.59	1132.60	644.85	-4.02
<b>23</b>	-0.21404	-0.08698	68.21	1189.24	693.69	-3.74
<b>24*</b>	-0.22107	-0.10003	68.74	1183.65	676.29	-9.05
<b>25 (VP-16)</b>	-0.21034	-0.02485	82.80	1409.29	785.78	-22.75

Ideally, from a pharmacological point of view, a drug should be orally bioavailable. The oral route is particularly praised especially for those drugs that have to be self-administered by the patients on a continuous basis. [43]The quickest strategy for assessing the drug-likeness of a given compound is to apply "rules" as a standard guideline. Orally ingested drugs should, in general, obey Lipinski's rule of five,

## Result and discussion

[44] which is summarized as:  $MW < 500$ ;  $HBD < 5$ ;  $\log_{10}P < 5$ ; and  $HBA_s < 10$ . Additionally, Veber and Ghose's rules complement the Lipinski's one. For instance, Veber et al. [45]

showed that compounds with  $N_{\text{brot}} < 10$  and  $TPSA < 140 \text{ \AA}^2$  present a good oral bioavailability in rats. Also, Ghose et al. [46] suggested a qualifying range that could be used in the development of drug-like chemical libraries, recommending the following constraints:  $160 \leq MW \leq 480$ ;  $-0.4 \leq \log_{10} P \leq 5.6$ ;  $40 \leq MR \leq 130$  and  $20 \leq N_{\text{atom}} \leq 70$ . In the following, we will discuss the oral bioavailability of the CDCAs of interest in light of the parameters presented in Tables 8 and 9:

- MW is closely connected to the molecular size. As the size of a compound gets larger, a bigger cavity must be shaped in water to accommodate it, thus decreasing the corresponding solubility. Growing MW reduces the compound fixation at the surface of the intestinal epithelium, hence reducing its absorption. In addition, a large molecular size obstructs passive diffusion through the firmly pressed aliphatic side chains of the cellular bilayer membrane. [47] Table 9 shows that all the considered compounds, except Compound 25, verify both Ghose and Lipinski's rules, because their MW are in the 325 – 470 range. Most likely, all these compounds will easily pass through cell membranes.
- The relative hydrophilic/hydrophobic properties of a drug are crucial in influencing its solubility, ADME (Absorption, Distribution, Metabolism, and Excretion) properties, as well as pharmacological activity. Absorption in the gastrointestinal tract is most effective when the drug has the right balance of solubility in water and fat, which is the case for moderate values of  $\log_{10}P$  (i.e.  $0 < \log_{10}P < 3$ ). If the drug is polar with low  $\log_{10}P$  (hydrophilic), it will fail to penetrate across the intestinal epithelial cell layer. Whereas if the molecule is nonpolar, with high  $\log_{10}P$  (hydrophobic), it will dissolve in fat globules, leading to poor contact with the intestinal walls and resulting in malabsorption. [14] As can be seen in Table 9, all compounds present a  $\log_{10}P$  in this range, except Compounds 24 and 25, which have out-of-range values of -2.22 and -4.27, respectively.

## Result and discussion

- TPSA of a molecule corresponds to the surface sum over every single polar atom (e.g., oxygen, nitrogen), where we include also attached hydrogens. Generally, a molecule with  $TPSA > 140 \text{ \AA}^2$  will have low oral absorption. For the central nervous system, the upper limit of TPSA for the drug to cross the blood-brain barrier is even reduced to  $80 \text{ \AA}^2$ . [48] Table 9 shows that the TPSA values are in the range 22-40 for Compounds 1-23 and that Compound 24 is still within the acceptable range ( $< 140 \text{ \AA}^2$ ), whereas Compound 25 is out-of-range. The percentage of absorption (%ABS, Table 9) is related to TPSA via  $\%ABS = 109 \pm 0.345 \times TPSA$ . [49] Except Compound 25, %ABS values are close to 100%. Again, these compounds should have good cellular plasmatic membrane permeability.
- $N_{\text{brot}}$  counts any single bond bound to a nonterminal heavy atom and not being part of a ring. [50,51] Table 9 shows that  $N_{\text{brot}}$  is smaller than 8 for all compounds. This is a signature of relatively good molecular flexibility, which helps the drug to traverse the membrane and better interact with the enzyme.
- Ligand efficiency ( $LE = 1.4 \times pIC_{50}/N_H$ ) measures the potency per heavy atom of a given compound, where, for drugs of comparable activity, the smaller ones have greater LE than the larger ones. As can be seen in Table 9, Compounds 7, 3 and 11 have a rather small number of  $N_H$ , and thus possess relatively high LE values (of 0.358, 0.299, 0.277, 0.273), whereas Compounds 15, 23, 25 have higher values of  $N_H$  leading to small values of LE (0.179, 0.209, 0.224). Hence, the latter ones may exhibit bad physicochemical and ADME properties.
- Lipophilic ligand efficiency ( $LLE = pIC_{50} - \log_{10}P$ ) gives insight into the interaction of a molecule with its own receptor, where low lipophilicity should be maintained [52] for good interaction. Concerning the studied series, Table 9 shows that all compounds have positive LLE values, which is considered as a favorable quality to create highly efficient interactions with the biological targets.

## **Result and discussion**

In sum, the Lipinski, Veber and Ghose's rules are verified by most of our compounds, except number 25. Therefore, these compounds are ideal for oral bioavailability. They have also large chance of achieving high intestinal permeability and solubility.

Compound	log <sub>10</sub> P	MW	HBA	HBD	TPSA	N <sub>atom</sub>	MR	N <sub>brot</sub>	Lipinski Score	Ghose Score	Veber Score	N <sub>H</sub>	LE	LLE	ABS %
1*	2.01	325	1	0	22.00	44	115.47	4	4	4	2	25	0.273	2.864	101.41
2	0.72	411	3	0	34.47	57	138.17	5	4	3	2	31	0.208	3.880	97.11
3	1.78	360	2	0	22.00	44	120.19	4	4	4	2	26	0.299	3.765	101.41
4*	2.58	393	4	0	22.00	47	120.69	5	4	4	2	29	0.251	2.629	101.41
5	0.21	369	3	0	40.46	47	121.06	4	4	4	2	28	0.229	4.364	95.04
6	1.41	343	2	0	22.00	44	115.60	4	4	4	2	26	0.263	3.478	101.41
7	2.16	339	1	0	22.00	47	119.75	4	4	4	2	26	0.358	4.498	101.41
8	0.62	331	1	0	22.00	41	112.77	4	4	4	2	26	0.258	4.167	101.41
9	2.06	404	2	0	22.00	44	123.01	4	4	4	2	26	0.249	2.563	101.41
10	2.52	360	2	0	22.00	44	120.19	4	4	4	2	26	0.271	2.518	101.41
11	1.78	360	2	0	22.00	44	120.19	4	4	4	2	26	0.277	3.364	101.41
12*	0.02	343	2	0	22.00	44	115.60	4	4	4	2	26	0.280	5.175	101.41
13	2.31	385	3	0	40.46	52	128.22	6	4	4	2	29	0.254	2.955	95.04
14	2.31	353	1	0	22.00	50	124.04	4	4	4	2	27	0.235	2.215	101.41
15	0.41	373	3	0	31.23	48	121.97	5	4	4	2	28	0.179	3.163	98.23
16	1.56	357	2	0	22.00	47	119.88	4	4	4	2	27	0.281	3.853	101.41
17	1.85	440	3	0	22.00	51	144.32	5	4	4	2	32	0.263	4.163	101.41
18	2.61	436	2	0	22.00	54	148.47	5	4	3	2	32	0.248	3.056	101.41
19	2.46	422	2	0	22.00	51	144.19	5	4	3	2	31	0.244	2.951	101.41
20	1.85	440	3	0	22.00	51	144.32	5	4	3	2	32	0.270	4.324	101.41
21	1.25	458	4	0	22.00	51	144.45	5	4	3	2	33	0.233	4.235	101.41
22	1.85	440	3	0	22.00	51	144.32	5	4	3	2	32	0.234	3.493	101.41
23	2.23	456	3	0	22.00	51	148.91	5	4	3	2	32	0.209	2.558	101.41
24*	-2.22	467	4	0	67.82	53	149.41	6	4	2	2	34	0.243	8.123	85.60
25 (VP-16)	-4.27	589	12	3	160.83	74	145.81	5	2	0	1	42	0.224	10.991	53.51

**Table 9:** Drug-likeness parameters and lipophilicity indices for the CDCAs under study. See text for the definition of these parameters and their description.

### III.5 QSAR modelling studies

QSAR studies have proved their applicability in modern drug discovery protocols. The goal of QSAR models is to establish quantitative relations connecting the physicochemical properties of classes of drugs to their biological activity. Typically, this involves the synthesis of a series of differently substituted analogue compounds, and the study of how their biological activities depend on the physicochemical properties of the substituents. [14] Several linear and nonlinear statistical model-building methods have been applied to QSAR, [53] where the needed physicochemical descriptors are treated as independent variables. We used both multiple linear regressions (MLR) and artificial neural network (ANN), as implemented in the software JMP 8.0.2 and XLSTAT, [54,55] to correlate these parameters with the biological activities of CDCAs. For internal, external validation and Y-randomization [56,57] of the QSAR model, we used different statistical parameters such as:

- (i) The leave-one-out cross-validation coefficient ( $R^2_{CV(LOO)}$ ), used to predict the internal validation of a model. The threshold for acceptability is  $R^2_{CV(LOO)} > 0.5$ . [58]
- (ii) The significance level (P-value). It should be  $< 0.05$ .
- (iii) The square correlation coefficient for external validation ( $R^2_{ext}$ ). It is taken as a good indicator when its value is greater than 0.6. [58-60]
- (iv) The PRESS/SSY ratio, where PRESS is the predicted residual sum of squares and SSY is the sum of squares deviation. It should be smaller than 0.4. [61]
- (v) The  $r_m^2$  metric introduced by Roy et al. [62] It should be ensured that  $\bar{r}_m^2 > 0.5$  and  $\Delta r_m^2 < 0.2$  to prevent bias in model predictability. This applies to both the training (internal validation) and the test (external validation) sets.

#### III.5.1.1 Internal validation

The internal validation of a QSAR model is carried out using a cross-validation method, using the molecules from the training set. In this paper, we used the cross-

## Result and discussion

validation leave-one-out (LOO) approach, where a large value of the cross-validated squared correlation coefficient  $R^2_{cv}$  is considered as a proof of high predictive capacity of the model. [58]

An acceptable  $Q^2_{cv}$  does not guarantee that the predicted activity values are close to the observed ones, but simply attests that a good overall correlation exist between them. So, to avoid this error and better highlight the predictability of the model, we considered also the  $r_m^2$  metrics, including average  $r_{m^2(LOO)}$  (the average value of  $r_m^2$  and  $r'^2_m$ ) and  $\Delta r^2_{m(LOO)}$  (the absolute difference between  $r_m^2$  and  $r'^2_m$ ) (Table 10), introduced by Roy and colleagues. [62] For a good prediction of the QSAR model  $\Delta r^2_{m(LOO)}$  should be less than 0.2, provided that the average value of  $r_m^2$  is greater than 0.5.

### III.5.1.2 External validation

External validation guarantees the predictability of the developed QSAR model and its applicability to potential new drugs. The correlation between observed and predicted data is measured by the  $R^2_{ext}$  metric (Table 10). According to Golbraikh and Tropsha [58-60], the following criteria for the external validation, based on the validation set, were adopted:

- (i)  $R^2_{ext} > 0.6$
- (ii)  $(r^2 - r_0^2 / r^2) < 0.1$  and  $0.85 \leq k \leq 1.15$  or  $(r^2 - r'^2_0 / r^2) < 0.1$  and  $0.85 \leq k' \leq 1.15$
- (iii)  $|r_m^2 - r'^2_m| < 0.3$

### III.5.1.3 Y-randomization

Y-randomization [56] is a widely accepted validation technique used to check the robustness of the models. In this validation approach, the values of the target variable are randomly redistributed over the entire learning set and a new model is derived. The whole operation is repeated several times. For robustness, the squared mean correlation coefficient ( $R^2_r$ ) of randomized models should be less than the squared correlation coefficient ( $R^2$ ) of non-randomized ones. Based on the results of the

## Result and discussion

randomization tests, the  $R^2_p (= R^2\sqrt{(R^2 + R_r^2)})$  [53] value should be greater than 0.5 to ensure that the good predictive capacity of the so-developed models is not reached by mere chance.

### III.6 Multiple linear regression (MLR)

Despite being the oldest, MLR still remains one of the most popular approaches to build QSAR models. This is due to its simple practical use, ease of interpretation and transparency. Indeed, the key algorithm is available and accurate predictions can be provided. [63] The values of the calculated descriptors are those listed in Tables 8 and 9. Data were randomly divided into two groups: a training set (internal validation) and a testing set (external validation). The significant correlation analysis between Topo II inhibition activity and descriptors is represented by the following equation:

$$pIC_{50} = 6,759 - 0,135 \times TPSA + 0,314 \times N_{atom} - 0,015 \times V - 0,485 \times HE + 0,314 \times \log_{10} P \dots \dots \quad (\text{Eq.1})$$

**Table 10:** Numerical parameters used to confirm the QSAR model validity. See text for more details.

Model	Training set						Test set					
	$R^2_{inter}$	$R^2_{cv}$	$\bar{r}_m^2(LOO)$	$\Delta r_m^2(LOO)$	RMSE	PRESS/SST	$R^2_{ext}$	$\bar{r}_m^2(test)$	$\Delta r_m^2(test)$	RMSE	PRESS/SST	
MLR	0.768	0.686	0.601	0.162	1.224	0.341	0.800	0.596	0.197	0.545	0.092	
ANN	0.999	0.991	0.988	0.000	0.005	0.000	0.650	0.598	0.108	0.372	0.135	

The statistical parameters of this model are listed in Table 10. The high values of the correlation coefficient ( $R^2$ ) for the training set ( $R^2_{inter}= 0.768$ ) and test set ( $R^2_{ext}=0.800$ ) indicate the significant correlation between different independent variables with Topo II inhibition activity. In addition, Table 10 shows that RMSE and PRESS/SSY ratio are low for both internal validation ( $= 0.341 < 0.4$ ) and external validation ( $= 0.092 < 0.4$ ). This confirms the reliability of our model.

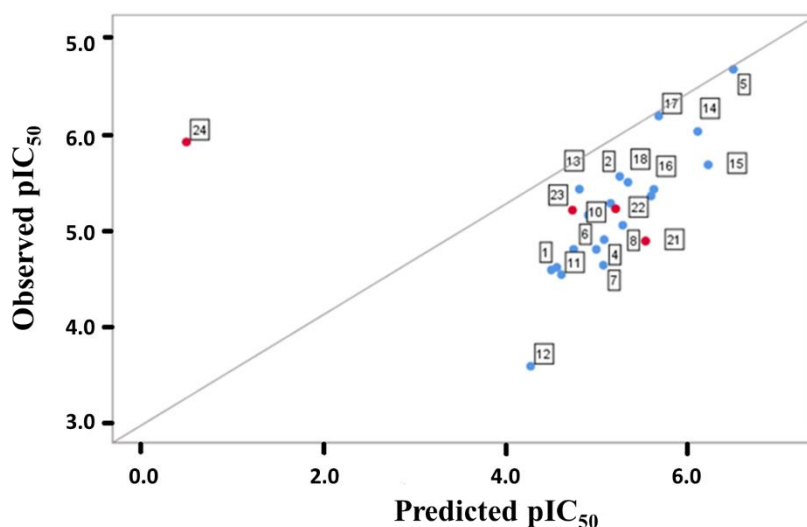


**Figure.38.** Generic leverage plot of observed [11] (Observed  $pIC_{50}$ ) versus predicted (Predicted  $pIC_{50}$ ) activity according to the MLR model. The oblique line is the diagonal.

The model was checked by applying the Y-randomisation test. Several Y vector random shuffles were performed and small average values of 0.1445 for  $R^2$  and -0.327 for  $Q^2$  (Table 11) were obtained after 1000 random tests, thus proving that the good results of our original model are not due to chance correlation or structural dependence of the training set.

**Table 11:** Random MLR model parameters.

Average R	0.3646
Average $R^2$	0.1445
Average $Q^2$	-0.327
${}^cR_p^2$	0.768

## Result and discussion

For further testing the reliability and stability of our model (Eq.1), we used the "Leave-One-Out" (LOO) technique. Again, the high value of cross-validation correlation coefficient ( $R^2_{cv} = 0.686 > 0.5$ ) for this model allows us to qualify it as valid. [58] Other criteria such as parameters metric ( $\bar{r}_m^2$  and  $\Delta r_m^2$ , Table 10) confirm that this QSAR model is acceptable. The plot of the predicted values of biological activity  $pIC_{50}$  vs. the experimental values is shown in Figure 38, which certifies once more the validity of the predicted model.

Let us now analyze the coefficients in Eq.1. The positive values of  $\log_{10}P$  and  $N_{atom}$  indicate a promoter effect on Topo II inhibition activity. Indeed, any increase in the octanol-water partition coefficient and number of atoms of the molecules causes an increase in the biological activity. This is related to the stabilization of the polar groups in the CDCAs and represents a good criterion for molecule accessibility in the biologic medium. Also, since the octanol-water partition coefficient provides an indication of the lipophilic character of the drug and its aptitude to cross the cell membrane, it represents a key parameter to measure the drug inhibitory activity.

No contribution from the HOMO-LUMO gap appears in Eq.1. Thus, the model is independent of this parameter. This may be related to the almost constant value of this gap computed for all the CDCAs of interest, as noted earlier. Eq.1 does not include any dependence on HBD since this parameter is zero for all compounds, except Compound 25 (Table 9). Similarly, MR and HBA parameters seem to have no influence on the biological activity, since they do not appear in our model.

### III.7 Artificial Neural Networks (ANN)

ANN [64,65] is a popular nonlinear model, which is used to predict the biological activity (i.e.  $IC_{50}$ ) of the datasets of therapeutic molecules. It presents several benefits like better prediction, adaptation and generalization capacity beyond the studied sample, and better stability of the coefficients. It is employed in complex drug design, drug engineering and medicinal chemistry domains. [66]

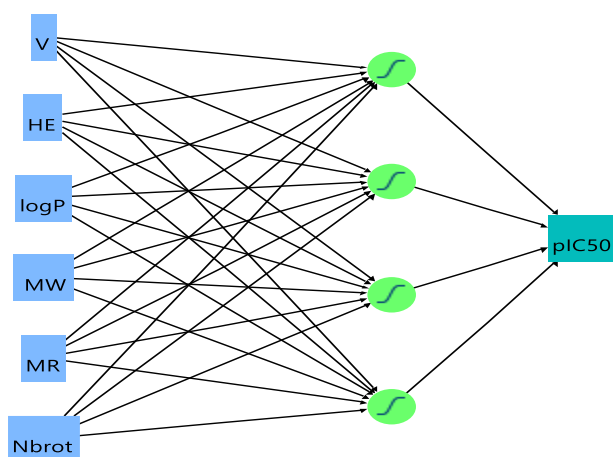


**Figure .39.**The architecture (6-4-1) of the adopted ANN model.

In this work, the neural network is a system of fully interconnected neurons arranged in three layers. The input layer is made of six neurons, where each of them receive one of the six descriptors selected from the correlation matrix of the model. The intermediate (hidden) layer is composed of four neurons that form the deep internal pattern that discovers the most significant correlations between predicted and experimental data. One neuron constitutes the output layer, which returns the value of  $IC_{50}$  (Figure 39). [67]

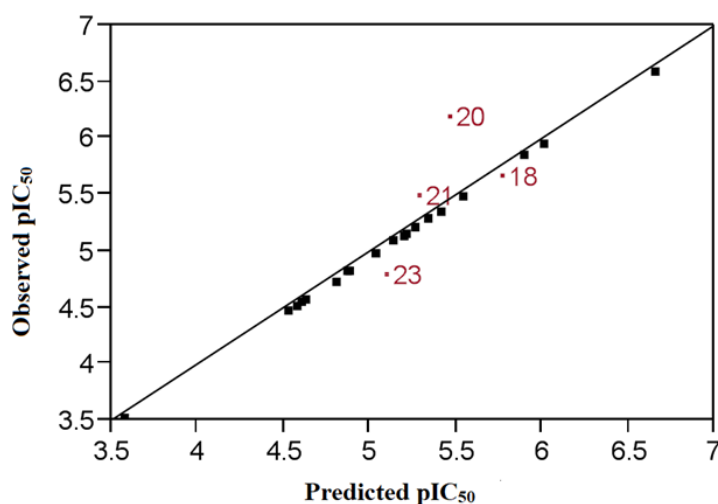


**Figure .40.**Correlation plot of observed (Observed  $pIC_{50}$ ) [11] versus predicted activity (Predicted  $pIC_{50}$ ) calculated using ANN.

## Result and discussion

As can be seen in Figure 40, a good agreement between experimental data and predicted  $pIC_{50}$  issued from the ANN model is observed. Indeed, the statistical parameters for this model, as given in Table 10, reveal a correlation coefficient close to 1 ( $R^2_{inter}=0.999$ ), associated with lower values of RMSE and PRESS/SSY for both external and internal validations. Note that these parameters are better than those found for the MLR model, indicating that the ANN one is more reliable. Furthermore, the robustness of the model was further confirmed by the significant  $R^2_{ext}$  value of the test data set ( $R^2_{ext}= 0.650$ ). To further evaluate our model, we applied the Leave-One-Out cross-validation method. The resulting  $\bar{r}_m^2(LOO)$ ,  $\Delta r_m^2(LOO)$ ,  $\bar{r}_m^2(test)$ ,  $\Delta r_m^2(test)$  statistical criteria (Table 10) support the validity of our model, since they fall within the ranges specified by Roy et al. [62]

# **General Conclusion**

## General conclusion

Using first principle methodologies, we studied the molecular structure and the vibrational/electronic spectroscopic properties of the set of CDCAs recently synthesized by Li et al. as potential Topo II inhibitors. We also characterized the carbazole subunit of these CDCAs. Afterwards, we derived a set of physicochemical parameters for these compounds, which are incorporated later into MPO, MLR and ANN methods for screening the lipophilicity indices, structure-activity relationship and to construct a QSAR model. The results indicate that these compounds have a 98% chance of being orally active. As can be seen in Table 10, the ANN network has substantially better predictive capabilities compared to MLR, leading to pIC<sub>50</sub> values closer to the experimental determinations. Nevertheless, both models remain satisfactory and exhibit a high predictive power, thus validating their use to explore and propose new molecules as active inhibitors of Topo II.

**Table .10.** Measured [11] and predicted pIC<sub>50</sub> using MLR and ANN methods. \* denotes the compounds selected for external validation (test set).

Compound	MLR predicted pIC <sub>50</sub>	ANN predicted pIC <sub>50</sub>	Observed pIC <sub>50</sub>
1*	5.496	4.873	4.874
2	4.600	4.599	4.600
3	5.574	5.536	5.545
4*	5.166	5.209	5.209
5	4.456	4.573	4.574
6	5.039	4.886	4.888
7	6.466	6.656	6.658
8	4.953	4.804	4.787
9	5.031	4.623	4.623
10	5.245	5.039	5.038
11	4.864	5.138	5.144
12*	4.690	5.195	5.195
13	5.111	5.265	5.265
14	4.568	4.527	4.525
15	4.228	3.574	3.573
16	4.766	5.413	5.413
17	6.073	6.013	6.013

## General conclusion

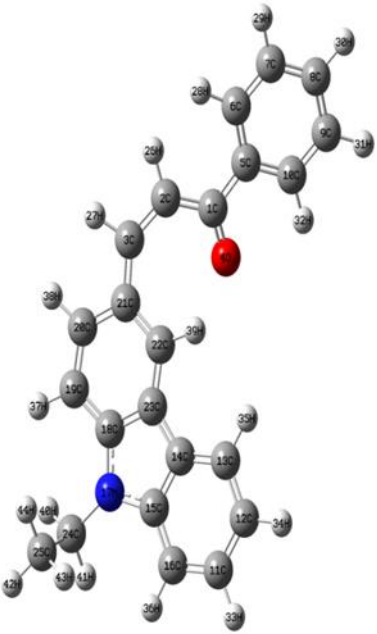
18	6.188	5.768	5.666
19	5.588	5.411	5.411
20	5.642	5.466	6.174
21	5.303	5.284	5.485
22	5.558	5.342	5.343
23	4.703	5.098	4.788
24*	0.427	5.898	5.903

The investigation of CDCAs at the microscopic level allows a screening of the physicochemical properties related to their activity in biological media. In contrast to the statement by Li et al., we did not notice any obvious relation between the incorporation of a halogen on the chemical composition of these CDCAs and their biological activity. Our work shows, however, that among the physicochemical parameters considered here, only  $\log_{10}P$  and  $N_{\text{atom}}$  play a role. These two parameters are connected with the flexibility of these compounds, which seems increasing the Topo II inhibitory activity and more generally improves the anticancer potency of these compounds. For instance, the coefficient in front of  $\log_{10}P$  in our model (Eq.1) is positive and relatively large. This means that the flexibility of the CDCAs, by facilitating cell membrane crossing, will enhance the Topo II inhibition. This may be related to the mechanism of action of Topo II itself, which consists in a balanced flexibility-rigidity associated with structural changes of the quaternary structure [68] of this enzyme during the CDCA-Topo II-DNA interaction. These findings were already suggested by Guedes et al. [69] This work discloses the phenomenological relations existing between potential biological activities and molecular descriptors of a relatively large panel of compounds to be used as Topo II inhibitors, and pave the way for specific investigations of their complex mechanisms of action at a molecular dynamics level.

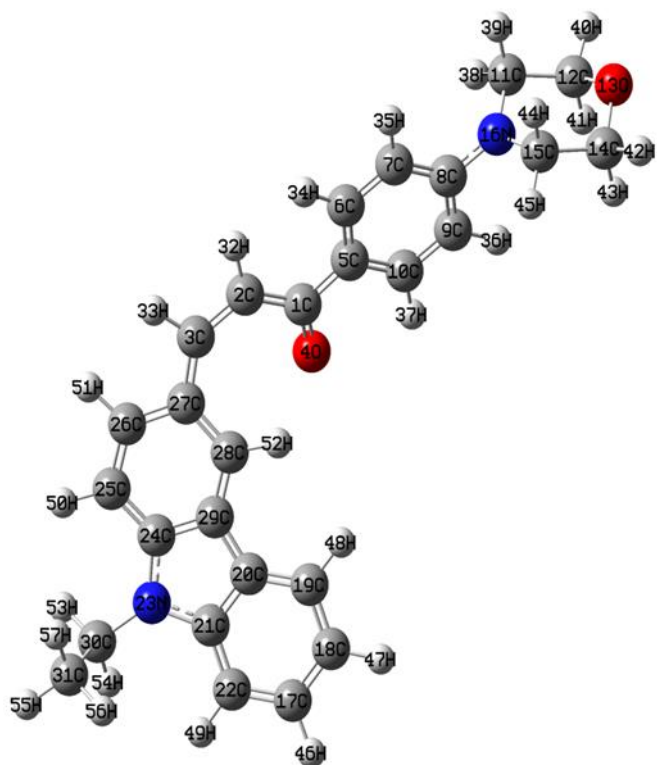
# APPENDIX

## Appendix

**Table S1:** Chemical structure of the investigated CDCAs (Table 1) as configured at the theory level of B3LYP/6-311G(d,p). In Angstrom, we give the Cartesian coordinates (X,Y,Z). The number of the atom in the structure and its atomic number, respectively, correspond to CN(Center Number) and AN (Atomic Number).

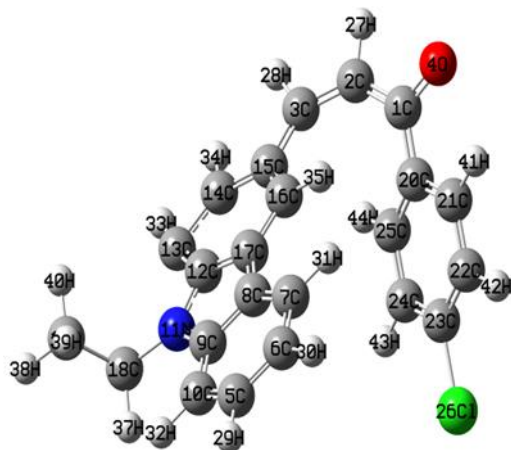
N	Molecular Structure	Cartesian coordinates				
		CN	AN	X	Y	Z
1		1	6	-0.000003050	0.000046017	0.000000586
		2	6	0.000009707	-0.000001908	0.000016748
		3	6	-0.000003806	0.000002246	-0.000009254
		4	8	0.000007744	-0.000022231	-0.000002513
		5	6	-0.000006171	-0.000031415	-0.000006993
		6	6	-0.000001642	0.000006633	0.000006829
		7	6	0.000001428	0.000002239	0.000003030
		8	6	0.000002843	0.000001175	0.000003104
		9	6	0.000006202	-0.000001955	-0.000001558
		10	6	-0.000002367	-0.000004444	0.000004983
		11	6	-0.000001696	-0.000004343	-0.000002963
		12	6	0.000001241	0.000000475	-0.000003286
		13	6	0.000002966	-0.000001139	0.000002132
		14	6	-0.000003638	0.000008892	-0.000005424
		15	6	0.000000664	-0.000004022	-0.000009217
		16	6	-0.000004033	-0.000002056	0.000002141
		17	7	-0.000003881	-0.000003033	0.000019400
		18	6	-0.000010756	0.000003415	-0.000005437
		19	6	-0.000001163	-0.000007095	-0.000000147
		20	6	-0.000002334	0.000005217	0.000003301
		21	6	0.000010187	-0.000002566	0.000013611
		22	6	-0.000002590	0.000015244	-0.000001697
		23	6	0.000004705	-0.000007651	-0.000004148
		24	6	0.000001421	0.000004393	-0.000010450
		25	6	-0.000002366	-0.000001141	0.000000919
		26	1	-0.000001982	-0.000000900	-0.000001167
		27	1	0.000002322	0.000000383	-0.000000748
		28	1	0.000003833	-0.000001051	0.000000212
		29	1	0.000003203	-0.000002667	0.000002383
		30	1	0.000002952	-0.000002687	0.000001044
		31	1	0.000000745	-0.000001871	0.000001063
		32	1	0.000001546	0.000000716	-0.000001274
		33	1	-0.000002432	0.000000461	-0.000003325
		34	1	-0.000002370	-0.000000561	-0.000002722
		35	1	-0.000001085	-0.000001607	-0.000003734
		36	1	-0.000002025	0.000001164	-0.000004006
		37	1	-0.000000086	0.000003956	0.000003030
		38	1	0.000000588	0.000000411	0.000001401
		39	1	0.000000561	-0.000001691	-0.000003108
		40	1	-0.000001273	0.000001401	0.000000682
		41	1	-0.000002250	0.000001394	-0.000000986
		42	1	-0.000000617	0.000001449	-0.000000526
		43	1	-0.000001582	0.000000758	-0.000001424
		44	1	0.000000339	-0.000000002	-0.000000492

2



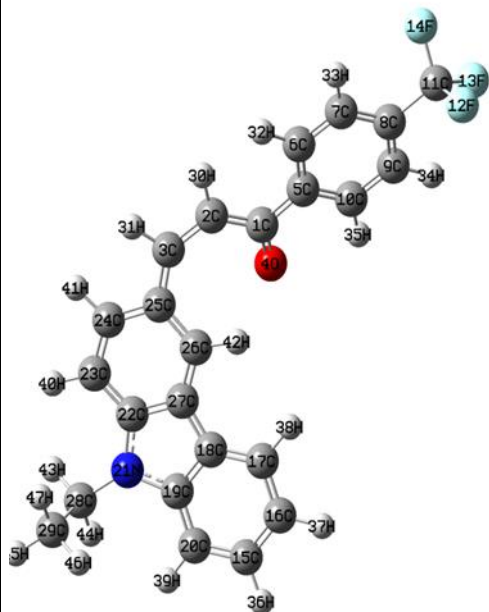
1	6	0.000005387	-0.000004291	0.000005055
2	6	-0.000010761	-0.000000836	-0.000009164
3	6	0.000002187	-0.000000116	0.000009235
4	8	-0.000002039	-0.000001701	-0.000001332
5	6	0.000000563	0.000006155	0.000002983
6	6	-0.000002893	-0.000005957	-0.000001186
7	6	0.000010163	0.000000633	-0.000001397
8	6	-0.000013025	0.000000884	-0.000001906
9	6	0.000001471	-0.000002870	-0.000001129
10	6	0.000000979	0.000000460	-0.000001512
11	6	-0.000002885	0.000000903	-0.000001141
12	6	0.000001241	-0.000003722	-0.000002768
13	8	-0.000006310	0.000002407	0.000007805
14	6	0.000011419	0.000001828	-0.000007113
15	6	-0.000003881	-0.000001208	-0.000006346
16	7	0.000005697	0.000000083	0.000009302
17	6	-0.000000034	-0.000000185	-0.000000674
18	6	-0.000000526	0.000000430	-0.000001540
19	6	0.000000763	-0.000001891	0.000001662
20	6	-0.000001633	0.000004432	-0.000001487
21	6	-0.000000230	-0.000001176	-0.000000515
22	6	0.000000764	0.000001237	0.000000291
23	7	-0.000000637	-0.000009731	-0.000006108
24	6	0.000000173	0.000006351	0.000003561
25	6	-0.000000570	-0.000000985	0.000002625
26	6	-0.000000715	-0.000000172	0.000000424
27	6	0.000000294	0.000001569	-0.000002272
28	6	0.000001029	0.000003560	-0.000000204
29	6	0.000001304	-0.000005790	0.000000135
30	6	0.000001908	0.000004972	0.000003962
31	6	-0.000000009	0.000000505	0.000001836
32	1	0.000001095	0.000002038	0.000000116
33	1	-0.000000477	0.000000801	0.000002154
34	1	-0.000000579	0.000000581	0.000000512
35	1	-0.000000173	0.000000058	0.000000884
36	1	0.000000600	0.000001193	-0.000001678
37	1	0.000000266	-0.000000267	-0.000000440
38	1	-0.000001697	-0.000000939	-0.000002156
39	1	-0.000000049	0.000001418	-0.000001530
40	1	-0.000000988	0.000000958	-0.000001660
41	1	-0.000000035	0.000000265	-0.000001426
42	1	-0.000000035	0.000000240	-0.000000748
43	1	-0.000000894	-0.000001478	0.000000059
44	1	-0.000001051	-0.000000026	-0.000000076
45	1	0.000001538	0.000000578	0.000000977
46	1	0.000000254	0.000000002	-0.000000707
47	1	0.000000140	0.000000202	-0.000000846
48	1	-0.000000028	-0.000000064	-0.000002091
49	1	0.000000118	-0.000000411	-0.000001126
50	1	0.000000108	-0.000000189	0.000000669
51	1	0.000000021	0.000000105	0.000001935
52	1	0.000000547	0.000000935	0.000001451
53	1	-0.000001101	-0.000001152	-0.000001084
54	1	0.000001128	0.000000387	0.000002688
55	1	0.000000585	0.000000101	0.000000562
56	1	0.000000699	-0.000000653	0.000001224
57	1	0.000000816	-0.000000462	0.000001256

3



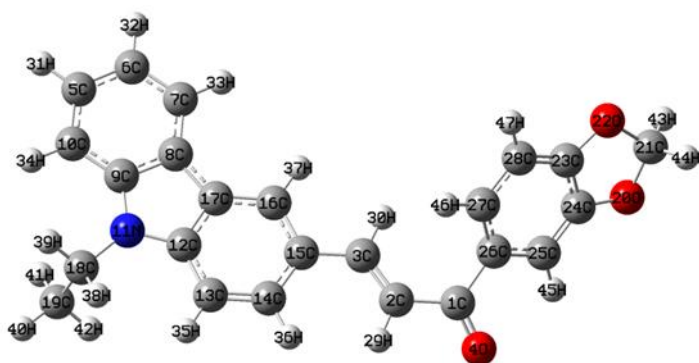
1	6	-0.000002374	0.000007476	0.000004949
2	6	0.000002054	-0.000002553	-0.000004138
3	6	0.000001781	0.000003233	0.000001714
4	8	0.000001748	-0.000002198	-0.000001319
5	6	-0.000001364	0.000001494	0.000000223
6	6	-0.000001931	-0.000000292	-0.000000019
7	6	0.000000625	0.000003596	-0.000000494
8	6	0.000001917	-0.000004596	-0.000005448
9	6	0.000000256	0.000000398	0.000004834
10	6	-0.000001224	0.000000733	-0.000003669
11	7	-0.000005575	-0.000002626	-0.000007410
12	6	0.000008422	0.000011938	0.000000365
13	6	-0.000005594	-0.000008105	-0.000005551
14	6	0.000006020	0.000013871	0.000010474
15	6	0.000004224	-0.000008850	-0.000012944
16	6	-0.000007568	0.000002809	0.000006967
17	6	-0.000001471	-0.000001042	0.000005360
18	6	0.000000487	0.000001726	0.000000965
19	6	0.000001729	0.000000780	-0.000001226
20	6	0.000001918	-0.000009630	0.000003597
21	6	-0.000000113	0.000001721	0.000000444
22	6	-0.000000471	-0.000002961	0.000002398
23	6	-0.000000716	-0.000001259	-0.000000655
24	6	0.000000269	-0.000004837	0.000003692
25	6	-0.000001674	0.000005013	0.000000404
26	17	-0.000001129	-0.000002381	0.000001497
27	1	0.000000696	0.000000668	0.000002053
28	1	0.000001785	0.000000085	0.000001143
29	1	-0.000001276	0.000000258	-0.000001698
30	1	-0.000000889	0.000000322	-0.000000922
31	1	-0.000000302	-0.000000242	0.000000055
32	1	-0.000001018	0.000000843	-0.000001107
33	1	-0.000001468	-0.000004245	-0.000001668
34	1	0.000002528	0.000000933	0.000000111
35	1	0.000001925	-0.000001633	0.000000505
36	1	0.000000203	-0.000000605	-0.000000926
37	1	-0.000001016	0.000000861	-0.000001798
38	1	0.000000253	0.000001703	-0.000001758
39	1	0.000000037	0.000001681	-0.000001378
40	1	0.000000496	0.000001548	-0.000001383
41	1	-0.000000406	-0.000001817	0.000001532
42	1	-0.000001454	-0.000001223	0.000001198
43	1	-0.000000665	-0.000000942	0.000000464
44	1	0.000000324	-0.000001653	0.000000568

4



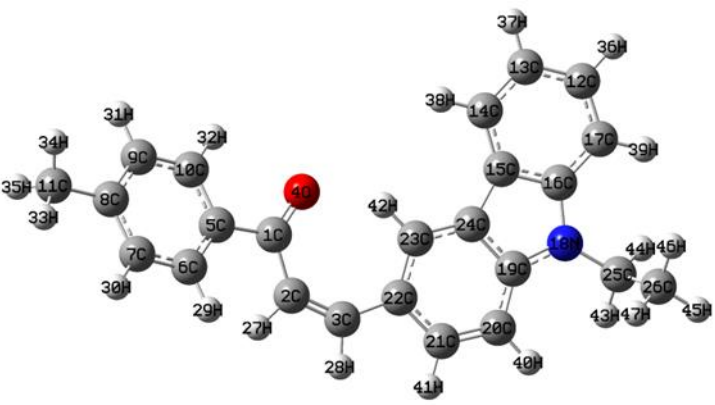
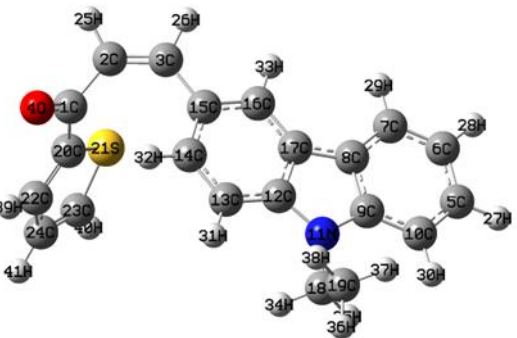
1	6	-0.000000245	-0.000015843	0.000000210
2	6	-0.000002401	0.000001093	-0.000000207
3	6	-0.000000417	-0.000000467	0.000002526
4	8	-0.000003639	0.000006264	-0.000002060
5	6	0.000004245	0.000011963	0.000006543
6	6	-0.000001543	-0.000006354	-0.000002494
7	6	0.000004917	0.000001076	-0.000001337
8	6	-0.000003356	0.000003583	0.000005249
9	6	0.000000444	-0.000004398	-0.000000491
10	6	0.000001564	0.000000637	0.000000578
11	6	-0.000001944	0.000000809	0.000000800
12	9	0.000000538	-0.000000856	-0.000001947
13	9	0.000004028	-0.000000908	-0.000003148
14	9	0.000000921	-0.000001692	0.000005133
15	6	-0.000000333	0.000000610	-0.000002877
16	6	-0.000000538	-0.000000757	-0.000002757
17	6	-0.000001373	0.000000950	-0.000002915
18	6	0.000000322	-0.000001589	-0.000000629
19	6	-0.000000542	0.000000900	0.000000181
20	6	-0.000000380	0.000000327	-0.000003794
21	7	-0.000001036	-0.000002034	-0.000006681
22	6	0.000001327	0.000003093	0.000002785
23	6	-0.000000348	-0.000001088	0.000000036
24	6	0.000002724	0.000001074	0.000000806
25	6	-0.000001596	0.000000421	0.000003740
26	6	-0.000000742	0.000003271	-0.000003837
27	6	-0.000001544	-0.000000787	0.000002471
28	6	0.000000293	0.000001225	0.000002763
29	6	0.000000194	0.000000014	-0.000000486
30	1	0.000000418	0.000000071	0.000000134
31	1	-0.000000136	0.000000731	0.000002777
32	1	0.000001043	0.000000103	0.000002882
33	1	0.000000843	-0.000000491	0.000002367
34	1	0.000000315	-0.000000167	-0.000000046
35	1	-0.000000129	0.000000378	-0.000000595
36	1	-0.000000705	-0.000000345	-0.000003662
37	1	-0.000000373	-0.000000143	-0.000003847
38	1	-0.000000251	-0.000000050	-0.000001829
39	1	-0.000000360	-0.000000102	-0.000001482
40	1	-0.000000213	0.000000547	0.000002141
41	1	-0.000000489	0.000000486	0.000002563
42	1	0.000000398	-0.000000820	0.000000798
43	1	-0.000000833	0.000000359	-0.000000347
44	1	-0.000000636	0.000000477	-0.000000320
45	1	0.000000190	-0.000000257	0.000000363
46	1	0.000000767	-0.000000768	-0.000000694
47	1	0.000000608	-0.000000542	0.000000635

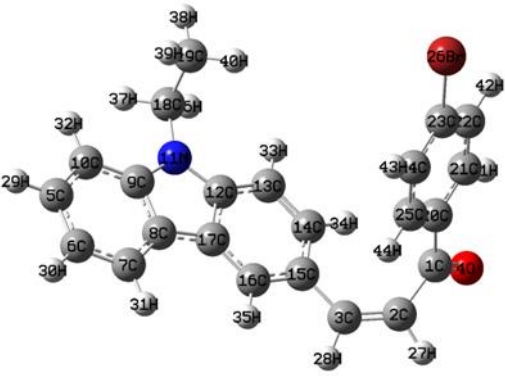
5

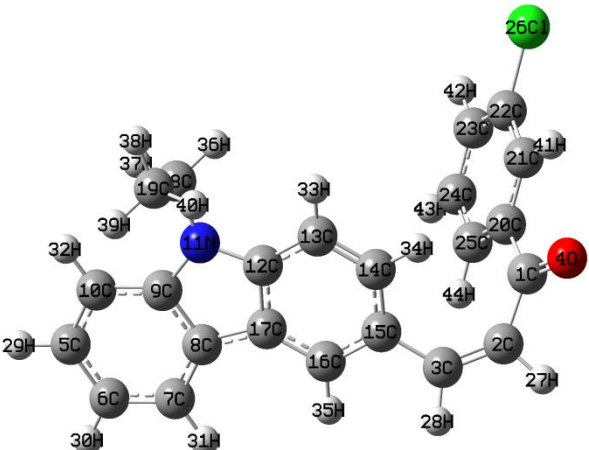
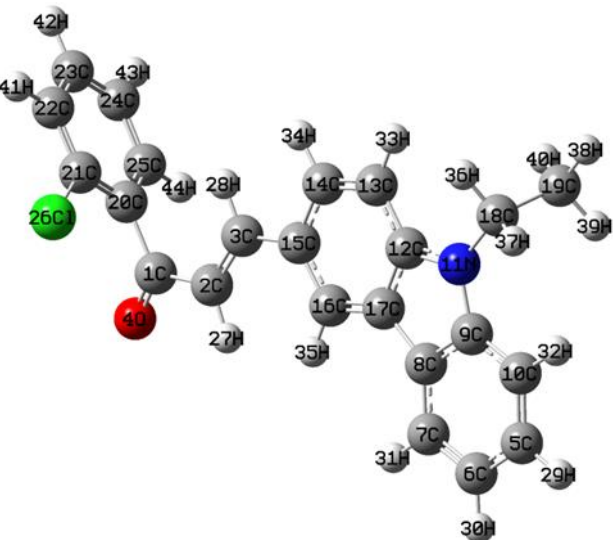


1	6	-0.000000917	0.000002148	0.000008893
2	6	0.000003255	0.000001271	0.000001916
3	6	0.000008782	0.000000812	-0.000000308
4	8	0.000000697	0.000002432	-0.000002872
5	6	-0.000000730	-0.000000215	0.000001289
6	6	-0.000000506	-0.000000282	0.000000693
7	6	0.000000158	-0.000001116	-0.000000112
8	6	-0.000002040	0.000000293	0.000004727
9	6	-0.000000977	-0.000001941	-0.000002262
10	6	-0.000000425	-0.000001220	0.000000695
11	7	0.000000789	0.000000843	0.000001810
12	6	0.000000051	-0.000002468	-0.000002802
13	6	-0.000001908	-0.000000064	0.000001955
14	6	0.000002927	0.000000667	0.000002162
15	6	-0.000009636	-0.000001427	-0.000003537
16	6	-0.000000238	-0.000002222	0.000000321
17	6	0.000004068	0.000003565	-0.000002278
18	6	-0.000000612	-0.000001321	0.000001087
19	6	-0.000000944	0.000000400	-0.000000221
20	8	0.000005673	0.000001600	0.000015939

		21	6	0.000009296	0.000008942	-0.000016977
		22	8	-0.000007658	-0.000005574	-0.000001730
		23	6	-0.000007464	-0.000008029	0.000019520
		24	6	-0.000004329	0.000003487	-0.000027465
		25	6	0.000014262	0.000006844	0.000009267
		26	6	-0.000016985	-0.000010820	-0.000006638
		27	6	0.000001716	0.000002631	-0.000011352
		28	6	0.000007421	0.000004481	0.000005813
		29	1	-0.000000072	-0.000001195	-0.000000209
		30	1	-0.000000822	-0.000000312	-0.000000078
		31	1	0.000000820	-0.000000992	0.000000472
		32	1	0.000000284	-0.000001148	0.000000001
		33	1	-0.000000408	0.000000005	-0.000000476
		34	1	0.000000703	-0.000000088	0.000000325
		35	1	0.000000539	0.000000726	-0.000000125
		36	1	-0.000000563	-0.000000157	-0.000000086
		37	1	-0.000000207	0.000000133	-0.000000517
		38	1	-0.000000121	0.000000738	0.000000510
		39	1	0.000000824	-0.000000528	0.000000913
		40	1	0.000000207	-0.000000116	0.000001350
		41	1	-0.000000347	-0.000000903	-0.000000185
		42	1	-0.000000684	-0.000000563	0.000000885
		43	1	-0.000000536	-0.000000500	-0.000000515
		44	1	-0.000001539	0.000000708	0.000001319
		45	1	-0.000001925	-0.000000769	-0.000001035
		46	1	0.000000248	0.000001440	0.000001504
		47	1	-0.000000128	-0.000000193	-0.000001585
6		1	6	-0.000012637	0.000029245	0.000006654
		2	6	0.000015818	-0.000001369	0.000013279
		3	6	-0.000006526	-0.000009624	-0.000006276
		4	8	0.000011426	-0.000011925	-0.000000264
		5	6	-0.000001131	-0.000020433	-0.000015415
		6	6	0.000001827	0.000005072	0.000011336
		7	6	0.000000334	-0.000001511	0.000003382
		8	6	0.000013312	0.000007952	0.000001249
		9	6	0.000005907	0.000000908	-0.000001180
		10	6	-0.000008047	-0.000004047	0.000003204
		11	9	-0.000002459	-0.000010057	0.000000683
		12	6	-0.000001780	-0.000003358	-0.000004536
		13	6	-0.000000180	0.000000580	-0.000004932
		14	6	0.000002483	-0.000001438	0.000000547
		15	6	-0.000006187	0.000008278	-0.000004855
		16	6	0.000001178	-0.000003977	-0.000006192
		17	6	-0.000004291	-0.000001583	-0.000000266
		18	7	-0.000004314	-0.000002658	0.000008506
		19	6	-0.000010476	0.000002919	-0.000000531
		20	6	-0.000001292	-0.000003972	-0.000000796
		21	6	-0.000004025	0.000002312	0.000004528
		22	6	0.000005593	0.000010956	0.000000025
		23	6	0.000000185	0.000004550	0.000003692
		24	6	0.000006558	-0.000005177	-0.000000610
		25	6	0.000000771	0.000004515	-0.000006641
		26	6	-0.000001125	-0.000001359	0.000003236
		27	1	-0.000001938	-0.000003190	0.000004858
		28	1	0.000002180	0.000001582	0.000002257
		29	1	0.000005617	0.000001497	0.000000683
		30	1	0.000002284	-0.000003294	0.000002894
		31	1	0.000000250	-0.000002619	-0.000000684
		32	1	0.000002397	0.000000005	-0.000002329
		33	1	-0.000002967	0.000000624	-0.000004794
		34	1	-0.000003036	-0.000000532	-0.000004554
		35	1	-0.000001874	-0.000001143	-0.000004468
		36	1	-0.000002413	0.000001548	-0.000004187
		37	1	0.000000529	0.000003549	0.000004318
		38	1	0.000001078	0.000001421	0.000001953
		39	1	-0.000000741	-0.000000054	-0.000002451
		40	1	-0.000000141	0.000002356	0.000001477

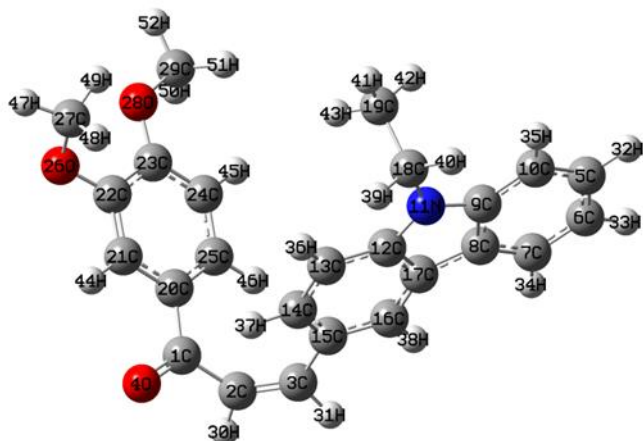
		41	1	-0.000001888	0.000001773	-0.000001689
		42	1	0.000000327	0.000001622	-0.000000745
		43	1	-0.000001295	0.000000352	-0.000000904
		44	1	0.000000707	-0.000000300	0.000000538
7		1	6	0.000000263	-0.000002846	-0.000000061
		2	6	0.000000057	0.000001263	0.000001454
		3	6	-0.000000105	-0.000000014	0.000002205
		4	8	-0.000000484	0.000000472	0.000000514
		5	6	0.000001578	0.000001591	0.000001030
		6	6	0.000001485	-0.000000891	0.000001965
		7	6	0.000001870	-0.000000647	0.000002021
		8	6	0.000002336	-0.000001011	0.000000785
		9	6	0.000001142	-0.000000428	-0.000000367
		10	6	-0.000000286	-0.000001253	-0.000000290
		11	6	0.000000685	-0.000001721	-0.000000341
		12	6	-0.000001610	-0.000000111	-0.0000003890
		13	6	-0.000001307	-0.0000000614	-0.0000003975
		14	6	-0.000001360	0.000000326	-0.0000002911
		15	6	-0.000000649	-0.000000220	-0.0000002023
		16	6	-0.000001581	0.000000551	-0.0000003260
		17	6	-0.000001707	0.000000138	-0.0000002433
		18	7	-0.000000783	0.000000627	0.0000005274
		19	6	-0.000000821	0.000001316	-0.0000001670
		20	6	-0.000000569	0.000000538	0.0000002240
		21	6	0.000000527	0.000001360	0.0000002032
		22	6	-0.000000304	0.000000776	0.0000002185
		23	6	-0.000000501	0.000001625	-0.000000504
		24	6	-0.000001029	0.000000305	-0.0000000936
		25	6	-0.000001127	0.000000873	-0.0000002612
		26	6	-0.000000304	0.000000079	-0.0000000031
		27	1	0.000000663	0.000000006	0.0000002617
		28	1	0.000000455	0.000000969	0.0000003472
		29	1	0.000002328	-0.000000682	0.0000002890
		30	1	0.000002483	-0.000001231	0.0000002457
		31	1	0.000000670	-0.000000929	-0.0000001067
		32	1	0.000000104	-0.000000245	-0.0000001055
		33	1	0.0000003080	-0.000001789	0.0000001548
		34	1	0.000002672	-0.000002170	0.0000000060
		35	1	0.000001829	-0.000000699	0.0000001424
		36	1	-0.000002052	-0.000000141	-0.0000004895
		37	1	-0.000001655	-0.000000446	-0.0000004942
		38	1	-0.000001002	-0.000000318	-0.0000002879
		39	1	-0.000001683	0.000000432	-0.0000002716
		40	1	-0.000000356	0.000001332	0.0000002329
		41	1	0.0000000044	0.000001067	0.0000003292
		42	1	-0.000000156	-0.000000079	0.0000000042
		43	1	-0.000001343	0.000001538	0.000001100
		44	1	-0.000001852	0.000001279	-0.000000681
		45	1	-0.000000187	0.000000447	0.0000000553
		46	1	0.000000020	-0.000000275	-0.0000000773
		47	1	0.000000524	-0.000000153	0.0000000823
8		1	6	0.000020849	-0.000000797	-0.0000018457
		2	6	-0.000013177	0.0000010498	0.0000001562
		3	6	0.000008409	0.000009858	0.000000403
		4	8	-0.000006825	-0.000001494	0.0000007098
		5	6	-0.000000087	0.000003333	0.000000326
		6	6	-0.000001451	-0.000002032	-0.0000000019
		7	6	0.000001281	0.000000188	-0.0000000194
		8	6	0.000005854	0.000002389	-0.0000002187
		9	6	-0.000000450	-0.000001958	-0.0000001315
		10	6	0.000001476	-0.000000552	-0.0000000727
		11	7	-0.000002881	-0.000001632	0.0000003013
		12	6	0.000003321	0.000004800	-0.0000003469
		13	6	-0.000002343	-0.000005571	0.0000001667
		14	6	0.000002765	0.000010946	0.0000004173
		15	6	-0.000008291	-0.000016475	0.0000001661
		16	6	0.000005036	0.0000003166	-0.0000000526

		17	6	-0.000009241	-0.000003528	0.000000067
		18	6	-0.000000006	0.000000117	-0.000002094
		19	6	0.000000529	-0.000000282	0.000000519
		20	6	-0.000003769	-0.000012050	0.000006869
		21	16	-0.000004732	-0.000003182	0.000007910
		22	6	-0.000000542	0.000012726	-0.000014923
		23	6	0.000002310	0.000006492	-0.000004905
		24	6	-0.000002343	-0.000007565	0.000016548
		25	1	0.000002128	-0.000001572	-0.000000264
		26	1	0.000000178	-0.000000560	0.000000706
		27	1	0.000000067	-0.000000301	-0.000000466
		28	1	-0.000000215	0.000000214	-0.000000915
		29	1	-0.000000072	0.000000014	-0.000000655
		30	1	-0.000000341	0.000000506	-0.000000771
		31	1	0.000000175	0.000000970	-0.000000577
		32	1	0.000001353	-0.000001930	0.000000604
		33	1	-0.000000656	-0.000000430	-0.000000250
		34	1	-0.000000113	-0.000000067	0.000000271
		35	1	0.000000146	-0.000000086	0.000000180
		36	1	0.000000020	0.000000436	-0.000000404
		37	1	0.000000178	0.000000015	-0.000000329
		38	1	0.000000332	0.000000136	-0.000000057
		39	1	0.000001573	-0.000003697	0.000003122
		40	1	-0.000001937	-0.000001353	-0.000001099
		41	1	0.000001495	0.000000312	-0.000002097
9		1	6	0.000000458	-0.000016797	-0.000027164
		2	6	-0.000009286	-0.000002275	0.000002749
		3	6	0.000005989	0.000009311	0.000001144
		4	8	0.000006042	-0.000001585	0.000007678
		5	6	-0.000002159	0.000001702	-0.000000638
		6	6	-0.000001610	0.000003897	-0.000000471
		7	6	0.000002802	0.000003328	-0.000000746
		8	6	-0.000006912	-0.000001436	-0.000005925
		9	6	0.000003596	0.000000007	-0.000005410
		10	6	-0.000002223	-0.000001883	-0.000001025
		11	7	0.000001852	0.000000950	0.000004247
		12	6	-0.000004530	-0.000000681	0.000005340
		13	6	0.000001499	-0.000000026	-0.000001123
		14	6	0.000002579	-0.000004577	0.000002726
		15	6	-0.000002319	-0.000002621	-0.000000099
		16	6	0.000000566	-0.000000037	-0.000003285
		17	6	0.000007772	0.000004099	0.000005506
		18	6	-0.000003750	0.000000428	-0.000001825
		19	6	-0.000002603	0.000000771	-0.000002038
		20	6	0.000001708	0.000016431	0.000023921
		21	6	0.000002209	-0.000008924	-0.000001393
		22	6	0.000001735	-0.000003179	0.000005431
		23	6	-0.000001149	-0.000001686	-0.000001726
		24	6	-0.000001737	0.000001079	-0.000000795
		25	6	-0.000001839	0.000000812	-0.000006705
		26	35	-0.000000400	-0.000001887	0.000000565
		27	1	0.000004824	-0.000002851	-0.000001466
		28	1	0.000001236	-0.000001810	-0.000000805
		29	1	0.000000531	0.000002851	-0.000000679
		30	1	0.000001493	0.000001464	-0.000000884
		31	1	0.000000484	0.000000999	0.000001315
		32	1	-0.000001085	0.000003142	0.000001069
		33	1	-0.000000560	0.000000549	-0.000000172
		34	1	-0.000000646	-0.000000502	-0.000001058
		35	1	0.000001395	0.000000429	0.000001689
		36	1	0.000000205	0.000002039	-0.000003675
		37	1	-0.000001675	0.000001995	0.000002473
		38	1	-0.000002579	0.000002262	0.000000136
		39	1	-0.000000318	0.000000092	0.000000127
		40	1	-0.000001424	-0.000000189	-0.000000229
		41	1	-0.000000893	-0.000000997	0.000000795
		42	1	-0.000001206	-0.000001482	-0.000000845

		43	1	0.000001390	-0.000001632	0.000000704
		44	1	0.000000537	-0.000001581	0.000002563
10		1	6	-0.000013947	-0.000008364	0.000024202
		2	6	-0.00002657	-0.000016791	-0.000010074
		3	6	0.000005463	0.000011580	-0.000000548
		4	8	0.000008547	0.000001360	-0.000010796
		5	6	0.000000312	0.000001391	0.000002380
		6	6	0.000001011	0.000000983	0.000000675
		7	6	0.000000549	0.000000295	0.000001152
		8	6	-0.000009502	-0.000001562	0.000001210
		9	6	-0.000001728	0.000006856	-0.000006834
		10	6	0.000000787	-0.000001214	0.000004555
		11	7	0.000007110	-0.000007136	0.000018747
		12	6	-0.000003074	-0.000002686	-0.000007821
		13	6	-0.000001202	0.000000956	0.000004789
		14	6	0.000001559	-0.000004744	-0.000001981
		15	6	-0.000002210	-0.000000815	0.000002755
		16	6	-0.000003984	-0.000004762	-0.000004497
		17	6	0.000011295	0.000008160	0.000000988
		18	6	-0.000004862	0.000003269	-0.000004812
		19	6	-0.000003277	-0.000000467	0.000001415
		20	6	0.000003873	0.000015963	-0.000022679
		21	6	-0.000001179	-0.000002536	-0.000001030
		22	6	0.000003545	-0.000004562	-0.000001827
		23	6	-0.000000808	0.000002739	-0.000000452
		24	6	0.000001462	0.000002690	-0.000003253
		25	6	-0.000001479	-0.000003420	0.000007828
		26	17	-0.000002148	0.000001844	-0.000000519
		27	1	0.000004287	-0.000000324	-0.000000347
		28	1	0.000000027	-0.000001567	-0.000001589
		29	1	-0.000000262	0.000002044	0.000002498
		30	1	0.000000720	0.000001617	0.000001935
		31	1	0.000000890	0.000001494	0.000000181
		32	1	-0.000000314	0.000001018	0.000001914
		33	1	-0.000000198	-0.000000804	-0.000000392
		34	1	0.000001232	-0.000001220	-0.000000504
		35	1	0.000001874	0.000000653	0.000000617
		36	1	-0.000000777	0.000000647	0.000000415
		37	1	0.000000177	-0.000000377	0.000003050
		38	1	-0.000001847	-0.000000823	0.000002025
		39	1	-0.000001521	-0.000000099	0.000001956
		40	1	-0.000001039	-0.000001125	0.000001001
		41	1	-0.000000298	-0.000000795	-0.000001963
		42	1	0.000000788	-0.000000293	-0.000001022
		43	1	0.000001460	0.000000244	-0.000000266
		44	1	0.000001344	0.000000685	-0.000003085
11		1	6	-0.000002954	0.000016443	-0.000012367
		2	6	-0.000012066	0.000003650	0.000003206
		3	6	0.000005797	-0.000001726	-0.000002509
		4	8	0.000002263	-0.000004701	0.000001724
		5	6	0.000000564	0.000000324	-0.000000401
		6	6	-0.000000805	-0.000000784	0.000000829
		7	6	0.000001161	-0.000001369	0.000000412
		8	6	-0.000006983	0.000000333	0.000001223
		9	6	0.000000479	0.000006460	0.000002178
		10	6	0.000000869	-0.000000368	-0.000001694
		11	7	0.000002216	-0.000011663	-0.000012554
		12	6	-0.000002319	0.000005243	0.000004459
		13	6	-0.000000061	-0.000000061	-0.000001563
		14	6	0.000000647	0.000004526	-0.000000725
		15	6	-0.000005754	-0.000002979	0.000005192
		16	6	0.000001303	-0.000003627	-0.000002154
		17	6	0.000005379	-0.000002074	0.000003654
		18	6	0.000000017	0.000004542	0.000005120
		19	6	-0.000000292	0.000000103	0.000000162
		20	6	0.000011094	-0.000018236	0.000004400
		21	6	-0.000007823	0.000010071	-0.000000258

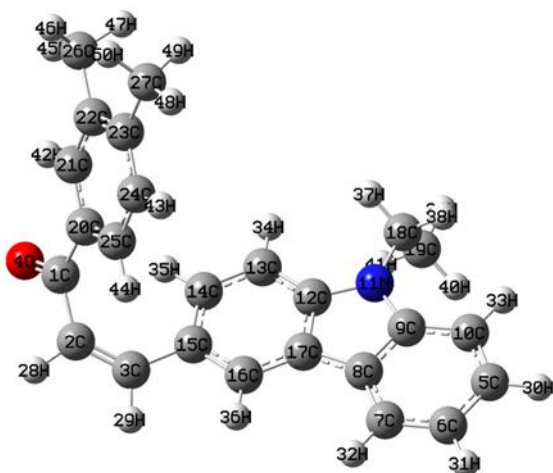
		22	6	0.000004382	-0.000004301	-0.000001352
		23	6	-0.000000811	0.000003326	0.000003693
		24	6	-0.000001354	0.000000355	-0.000002733
		25	6	0.000001659	0.000002724	0.000003179
		26	17	0.000003331	-0.000002980	0.000001686
		27	1	0.000001254	0.000000859	0.000001783
		28	1	-0.000000119	-0.000002792	-0.000002899
		29	1	-0.000000141	-0.000000016	0.000000001
		30	1	-0.000000021	0.000000000	-0.000000100
		31	1	-0.000000003	-0.000000015	0.000000071
		32	1	-0.000000188	-0.000000163	0.000000188
		33	1	-0.000000111	-0.000000393	0.000000288
		34	1	-0.000000398	-0.000000489	0.000000246
		35	1	-0.000000610	-0.000000281	-0.000000892
		36	1	0.000000707	0.000000594	-0.000000138
		37	1	0.000000156	0.000001018	-0.000000484
		38	1	-0.000000129	-0.000000689	-0.000000343
		39	1	-0.000000005	-0.000000343	-0.000000221
		40	1	-0.000000097	-0.000000035	-0.000000051
		41	1	0.000000096	0.000000452	-0.000000043
		42	1	0.000000177	-0.000000265	-0.000000303
		43	1	-0.000000174	-0.000000090	0.000000216
		44	1	-0.000000332	-0.000000585	-0.000000126
12		1	6	-0.000003771	-0.000005174	0.000000741
		2	6	0.000002717	0.000000045	-0.000000009
		3	6	-0.000000715	-0.000001061	0.000002023
		4	8	0.000000340	0.000000502	-0.000000522
		5	6	0.000004466	0.000004597	-0.000000075
		6	6	0.000000877	-0.000002481	0.000000319
		7	6	0.000003539	-0.000000152	0.000000239
		8	6	0.000000489	-0.000000044	0.000000488
		9	6	0.000000993	-0.000002123	-0.000001605
		10	6	0.000000230	-0.000000806	-0.000000459
		11	9	0.000002069	-0.000000219	0.000001491
		12	6	-0.000001090	-0.000000252	-0.000002206
		13	6	-0.000001123	-0.000000486	-0.000002432
		14	6	-0.000000846	-0.000000292	-0.000001429
		15	6	-0.000001042	0.000000715	-0.000001349
		16	6	-0.000000559	0.000000241	-0.000001061
		17	6	-0.000001652	0.000000334	-0.000001320
		18	7	-0.000001238	-0.000000436	-0.000000567
		19	6	-0.000001033	0.000001148	0.000001462
		20	6	-0.000000016	-0.000000442	0.000000956
		21	6	0.000000404	0.000001063	0.000001240
		22	6	0.000000625	0.000001572	0.000001399
		23	6	-0.000000394	0.000001182	-0.000000090
		24	6	0.000000165	-0.000000492	0.000000370
		25	6	-0.000000580	0.000001689	0.000000955
		26	6	-0.000000584	0.000000529	0.000000750
		27	1	0.000000949	0.000000159	0.000001088
		28	1	0.000000625	0.000000793	0.000002482
		29	1	0.000002329	-0.000000863	0.000000841
		30	1	0.000001936	-0.000001352	-0.000000691
		31	1	0.000000657	-0.000000850	-0.000001340
		32	1	0.000000228	-0.000000473	-0.000001286
		33	1	-0.000001630	-0.000000362	-0.000002739
		34	1	-0.000001206	-0.000000693	-0.000003049
		35	1	-0.000000598	-0.000000642	-0.000002048
		36	1	-0.000001534	0.000000208	-0.000001220
		37	1	-0.000000539	0.000001308	0.000002190
		38	1	0.000000027	0.000001017	0.000002576
		39	1	-0.000000031	-0.000000542	-0.000000163
		40	1	-0.000001454	0.000000937	0.000000951
		41	1	-0.000001693	0.000000861	0.000000599
		42	1	-0.000000511	0.000000784	0.000001140
		43	1	-0.000000070	0.000000154	0.000000139
		44	1	0.000000244	0.000000396	0.000001221

13



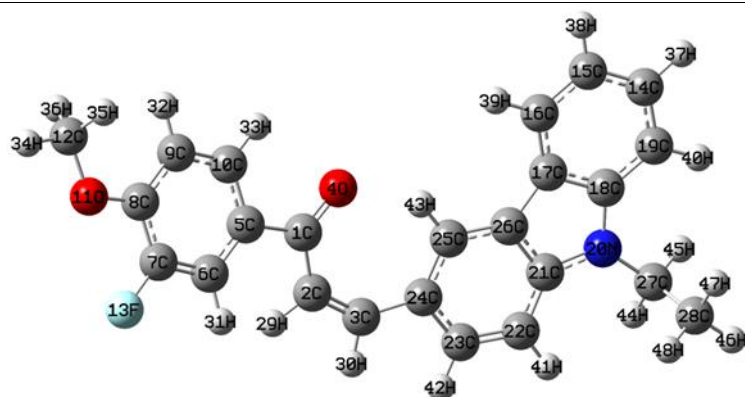
1	6	-0.000003788	0.000011923	0.000010914
2	6	0.000003004	-0.000005077	-0.000006946
3	6	0.000007071	0.000007869	-0.000000638
4	8	-0.000001271	0.000001846	-0.000002419
5	6	-0.000002528	-0.000002486	-0.000000200
6	6	-0.000001007	0.000001144	-0.000003076
7	6	-0.000000395	0.000001349	-0.000001136
8	6	-0.000000026	-0.000002381	-0.000004144
9	6	-0.000000401	-0.000000929	0.000001853
10	6	-0.000001800	-0.000003096	-0.000000512
11	7	0.000006189	0.000001025	-0.000006550
12	6	-0.000008793	-0.000001310	0.000001469
13	6	0.000007489	-0.000000395	0.000000662
14	6	0.000000548	-0.000002107	0.000001511
15	6	-0.000008884	-0.000003971	-0.000002006
16	6	0.000004861	0.000002081	-0.000002977
17	6	-0.000001242	-0.000000082	0.000003998
18	6	-0.000002359	-0.000000841	0.000004138
19	6	0.000000836	-0.000000824	0.000000647
20	6	0.000000778	-0.000006786	-0.000002920
21	6	0.000000467	0.000002953	0.000003182
22	6	-0.000003658	0.000003912	-0.000004733
23	6	0.000007476	-0.000007477	0.000002844
24	6	-0.000005745	0.000007880	-0.000000252
25	6	-0.000003004	-0.000001938	-0.000004169
26	8	0.000004409	-0.000002394	-0.000000391
27	6	0.000000649	0.000000977	0.000002668
28	8	-0.000001923	0.000000585	0.000004058
29	6	0.000001147	-0.000001352	-0.000000907
30	1	-0.000000851	0.000000290	0.000001410
31	1	-0.000001097	-0.000001002	-0.000001544
32	1	0.000001003	-0.000000984	-0.000000566
33	1	0.000000281	-0.000001979	-0.000000517
34	1	-0.000000679	-0.000001580	-0.000000701
35	1	0.000000166	0.000000169	-0.000000481
36	1	-0.000000901	0.000001506	-0.000000222
37	1	0.000000130	0.000000500	-0.000001069
38	1	-0.000000619	-0.000000482	-0.000000009
39	1	-0.000000551	0.000000915	-0.000001571
40	1	0.000000995	0.000000103	-0.000000171
41	1	0.000000481	0.000000652	0.000000294
42	1	0.000000815	0.000000364	0.000001855
43	1	-0.000000803	-0.000000178	0.000000941
44	1	-0.000001026	0.000001669	-0.000000438
45	1	0.000002173	-0.000001487	0.000000337
46	1	0.000000561	-0.000000474	0.000000502
47	1	-0.000000586	0.000000555	0.000001635
48	1	0.000000715	0.000000005	0.000000814
49	1	0.000000439	0.000000954	0.000001968
50	1	-0.000000144	-0.000001111	0.000001981
51	1	0.000001188	-0.000001232	-0.000000232
52	1	0.000000210	0.000000110	0.000001817

14

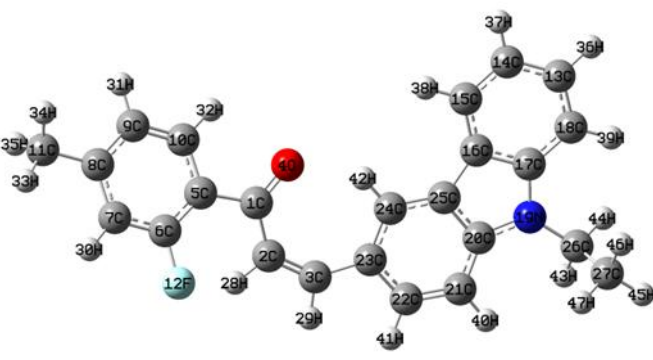


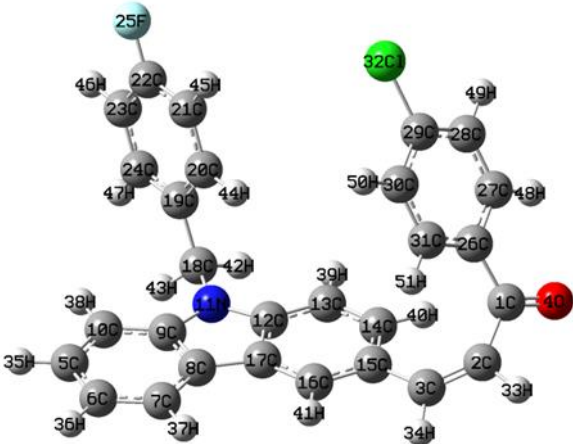
1	6	0.000001667	-0.000015735	0.000012842
2	6	-0.000007798	-0.000002308	-0.000001298
3	6	0.000011391	0.000014491	0.000000457
4	8	0.000002293	0.000003062	-0.000006049
5	6	-0.000000899	-0.000000059	-0.000000207
6	6	-0.000000454	0.000002121	0.000000805
7	6	0.000001467	0.000001562	-0.000001736
8	6	-0.000008593	-0.000003864	0.000005984
9	6	0.000000466	0.000001895	-0.000004312
10	6	-0.000000726	-0.000001267	0.000002682
11	7	0.000009840	-0.000003859	0.000013148
12	6	-0.000010675	0.000001492	-0.000006164
13	6	0.000006301	-0.000000347	0.000002472
14	6	0.000001204	-0.000003627	-0.000003115
15	6	-0.000009749	-0.000008825	0.000001964
16	6	0.000001508	-0.000000759	-0.000002404
17	6	0.000008649	0.000006294	-0.000004788
18	6	-0.000004041	-0.000001189	-0.000004674
19	6	0.000000069	0.000000153	0.000000130
20	6	-0.000001978	0.000017268	-0.000013129
21	6	0.000002091	-0.000006538	-0.000000570
22	6	0.000000459	0.000000468	-0.000000674
23	6	0.000001090	-0.000002482	0.000001741
24	6	-0.000002651	0.000006949	-0.000002453
25	6	-0.000001473	-0.000005510	0.000007267
26	6	0.000001017	-0.000000809	-0.000001111
27	6	-0.000001080	0.000002311	-0.000000061
28	1	0.000002372	-0.000001205	-0.000002703
29	1	-0.000000073	-0.000002247	-0.000000261
30	1	0.000000688	0.000000820	0.000000917
31	1	0.000000487	0.000000531	-0.000000152
32	1	0.000000323	0.000000486	-0.000000749
33	1	-0.000000601	0.000000898	0.000000639
34	1	-0.000001107	-0.000000242	-0.000000078
35	1	-0.000000205	-0.000000636	0.000000583
36	1	0.000001030	0.000000269	-0.000000672
37	1	-0.000001190	0.000000547	0.000001403
38	1	-0.000000386	-0.000000072	0.000000487
39	1	-0.000000316	0.000000420	0.000001827
40	1	0.000000016	-0.000000810	0.000001320
41	1	-0.000000274	-0.000000998	0.000000379
42	1	-0.000000891	0.000000616	0.000000349
43	1	0.000000866	-0.000000060	0.000000307
44	1	0.000000186	0.000000904	-0.000002400
45	1	-0.000000391	-0.000000514	0.000000517
46	1	-0.000000946	-0.000000589	0.000000081
47	1	0.000000305	-0.000000097	0.000000578
48	1	0.000000518	0.000000641	0.000000295
49	1	0.000000327	0.000000465	0.000000577
50	1	-0.000000135	-0.000000015	0.000000006

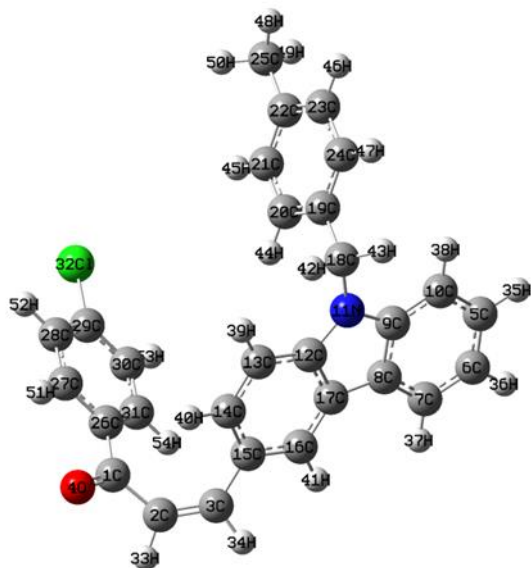
15



1	6	0.000008162	-0.000017837	-0.000002323
2	6	-0.000008618	0.000001749	0.000001814
3	6	0.000003462	0.000005606	0.000004070
4	8	-0.000004583	0.000009666	0.000001028
5	6	0.000006219	0.000005729	0.000002135
6	6	0.000002048	-0.000000293	0.000000557
7	6	-0.000002021	-0.000000045	0.000003135
8	6	0.000002605	-0.000006838	0.000001376
9	6	0.000002066	0.000004350	-0.000000104
10	6	-0.000005643	-0.000002849	-0.000000297
11	8	0.000001601	0.000002401	-0.000003174
12	6	0.000002192	-0.000000875	0.000001785
13	9	0.000002910	-0.000002507	0.000002695
14	6	-0.000001375	0.000000353	-0.000004087
15	6	-0.000001188	-0.000000569	-0.000004317
16	6	-0.000001740	0.000000432	-0.000002903
17	6	-0.000001571	0.000000894	-0.000003899

		18	6	-0.000002307	0.000001679	-0.000001464
		19	6	-0.000000140	0.000000232	-0.000003883
		20	7	-0.000000135	-0.000004066	-0.000003559
		21	6	-0.000000423	0.000006480	0.000002552
		22	6	0.000000271	-0.000003034	0.000001121
		23	6	0.000003904	0.000004264	0.000001864
		24	6	-0.000003438	-0.000006545	0.000001449
		25	6	-0.000002275	0.000004294	-0.000002787
		26	6	-0.000001227	-0.000003745	0.000005198
		27	6	0.000000651	0.000001757	0.000001376
		28	6	0.000000245	-0.000000047	0.000000577
		29	1	0.000000965	0.000000677	0.000002717
		30	1	0.000000122	0.000000274	0.000004322
		31	1	0.000001184	-0.000000202	0.000003825
		32	1	-0.000001626	-0.000001355	-0.000001570
		33	1	0.000000218	0.000000593	-0.000001462
		34	1	0.000001864	-0.000001840	-0.000000326
		35	1	0.000001475	-0.000001254	-0.000002355
		36	1	0.000000720	0.000000729	-0.000000928
		37	1	-0.000001524	0.000000188	-0.000005473
		38	1	-0.000001372	-0.000000096	-0.000005786
		39	1	-0.000000915	-0.000000222	-0.000002956
		40	1	-0.000000860	0.000000458	-0.000002302
		41	1	-0.000000025	0.000001265	0.000003651
		42	1	-0.000000272	0.000000111	0.000004224
		43	1	0.000000197	-0.000000523	0.000000982
		44	1	-0.000000851	0.000001039	0.000001221
		45	1	-0.000001245	0.000001267	-0.000000089
		46	1	0.000000528	-0.000000144	0.000001435
		47	1	0.000000741	-0.000000660	-0.000000477
		48	1	0.000001028	-0.000000941	0.000001414
16		1	6	-0.000045981	0.000010417	0.000007197
		2	6	0.000029447	0.000003099	-0.000009129
		3	6	-0.000008299	-0.000016162	0.000010334
		4	8	0.000018975	-0.000019707	-0.000004895
		5	6	0.000011783	0.000016129	0.000000304
		6	6	-0.000000773	-0.000001902	0.000010274
		7	6	0.000001981	-0.000001122	0.000002517
		8	6	-0.000004319	0.000003024	-0.000015453
		9	6	0.000004196	0.000000391	0.000002266
		10	6	-0.000004146	-0.000006013	0.000007164
		11	6	0.000003411	-0.000000340	-0.000009531
		12	9	0.000005892	-0.000001944	-0.000002636
		13	6	-0.000000889	-0.000001060	-0.000001452
		14	6	-0.000001215	0.000001388	-0.000001726
		15	6	0.000001142	-0.000001150	0.000000353
		16	6	-0.000004675	0.000001637	-0.000005046
		17	6	0.000003352	-0.000006137	0.000000534
		18	6	-0.000002512	0.000002081	-0.000004588
		19	7	-0.000000425	0.000014976	-0.000014645
		20	6	-0.000005627	-0.000012027	0.000005089
		21	6	-0.000002767	0.000008520	-0.000002475
		22	6	-0.000006083	-0.000006268	-0.000001475
		23	6	0.000003053	0.000018874	0.000002072
		24	6	0.000000019	-0.000007346	-0.000005711
		25	6	0.000008771	0.000003940	0.000006565
		26	6	-0.000009365	-0.000005478	0.000009425
		27	6	0.000002067	0.000002490	-0.000001256
		28	1	0.000000430	0.000000979	-0.000002610
		29	1	0.000000919	0.000001964	0.000004487
		30	1	-0.000000437	0.000000294	0.000000736
		31	1	0.000000144	0.000000863	-0.000002054
		32	1	0.000000686	0.000001030	-0.000001544
		33	1	0.000002085	-0.000002011	0.000007931
		34	1	0.000002524	-0.000002064	0.000004487
		35	1	0.000000953	-0.000004709	0.000007382
		36	1	-0.000001747	-0.000000281	-0.000002936

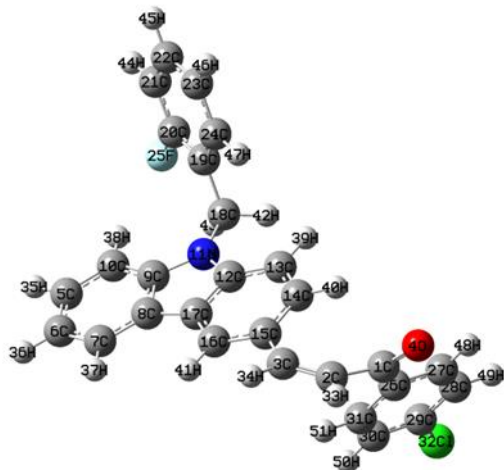
		37	1	-0.000001218	-0.000000613	-0.000002993
		38	1	-0.000000974	-0.000000266	-0.000001759
		39	1	-0.000000772	0.000000092	-0.000000958
		40	1	0.000000115	0.000000404	0.000002602
		41	1	0.000000154	0.000001431	0.000002856
		42	1	-0.000000857	-0.000002615	0.000003101
		43	1	0.000001337	0.000002117	-0.000002098
		44	1	0.000001665	0.000002611	-0.000001544
		45	1	-0.000000695	0.000001120	0.000000217
		46	1	-0.000001115	-0.000000464	-0.000000335
		47	1	-0.000000211	-0.000000193	0.000000956
17		1	6	-0.000002426	0.000000512	-0.000001029
		2	6	0.000003871	-0.000004230	-0.000000769
		3	6	-0.000000668	0.000000069	-0.000002333
		4	8	-0.000000233	-0.000003485	0.000000333
		5	6	0.000000567	0.000002480	-0.000001305
		6	6	0.000000531	0.000001132	-0.000001280
		7	6	0.000003705	0.000000467	-0.000004465
		8	6	-0.000002795	0.000001789	0.000002567
		9	6	-0.000002085	0.000003444	0.000000695
		10	6	0.000001718	0.000002170	-0.000001161
		11	7	0.000000662	0.000000794	-0.000000576
		12	6	0.000000487	0.000002691	-0.000000466
		13	6	-0.000000091	0.000001317	-0.000001033
		14	6	0.000000548	-0.000000255	-0.000001757
		15	6	0.000004925	0.000002046	0.000002105
		16	6	-0.000001523	-0.000000331	-0.000001446
		17	6	0.000003480	0.000001363	-0.000003112
		18	6	-0.000000596	0.000000198	0.000000788
		19	6	-0.000001982	0.000000606	0.000003147
		20	6	0.000000434	-0.000001832	0.000000410
		21	6	-0.000001943	0.000001494	0.000003204
		22	6	-0.000003708	-0.000002963	0.000003655
		23	6	-0.000001625	0.000000004	0.000000989
		24	6	-0.000001826	0.000001897	0.000003303
		25	9	-0.000002380	-0.000001266	0.000003616
		26	6	0.000003365	0.000002225	-0.000000815
		27	6	0.000000973	-0.000003409	-0.000001584
		28	6	-0.000000179	-0.000002279	0.000002800
		29	6	0.000000337	-0.000005042	-0.000001220
		30	6	-0.000000010	-0.000000810	0.000001404
		31	6	-0.000000122	-0.000004029	-0.000002394
		32	17	-0.000000987	-0.000004137	0.000001964
		33	1	0.000002336	0.000000653	-0.000005151
		34	1	0.000002139	0.000000776	-0.000004704
		35	1	0.000000279	0.000002317	-0.000000832
		36	1	0.000002003	0.000001930	-0.000003008
		37	1	0.000001388	0.000001655	-0.000001827
		38	1	-0.000001096	0.000002199	0.000001197
		39	1	-0.000001194	0.000000827	0.000000684
		40	1	-0.000000695	0.000000659	0.000000188
		41	1	0.000001942	0.000001206	-0.000001594
		42	1	-0.000001364	0.000002538	0.000002037
		43	1	-0.000001129	0.000002620	0.000000936
		44	1	-0.000001162	-0.000000169	0.000000734
		45	1	-0.000000768	-0.000002357	0.000001957
		46	1	-0.000003034	0.000000365	0.000003996
		47	1	-0.000002802	0.000002364	0.000002271
		48	1	-0.000000100	-0.000001435	0.000000836
		49	1	-0.000000489	-0.000003451	0.000000961
		50	1	0.000001061	-0.000003572	-0.000001129
		51	1	0.000002260	-0.000001755	-0.000001785



1	6	-0.000002392	0.000013555	0.000007636
2	6	0.000007207	-0.000011040	-0.000003831
3	6	0.000005100	0.000006459	-0.000000324
4	8	-0.000000023	-0.000003003	-0.000000846
5	6	0.000001101	0.000002482	-0.000000903
6	6	0.000000857	0.000002000	-0.000001404
7	6	0.000004466	0.000001370	-0.000005038
8	6	-0.000008605	-0.000000599	0.000003877
9	6	-0.000000266	0.000006024	0.000002010
10	6	0.000001474	0.000001839	-0.000002278
11	7	0.000002565	0.000002603	-0.000000058
12	6	-0.000002266	0.000000728	-0.000004393
13	6	0.000001447	0.000000822	0.000001005
14	6	0.000000937	0.000001856	-0.000000863
15	6	-0.000002582	-0.000005279	-0.000002614
16	6	-0.000000011	0.000000760	0.000000741
17	6	0.000008415	0.000001377	-0.000004346
18	6	-0.000000286	-0.000000332	0.000001338
19	6	-0.000001681	0.000001335	0.000002701
20	6	-0.000000472	-0.000000986	-0.000000367
21	6	-0.000000248	0.000001780	0.000002938
22	6	-0.000004579	-0.000003042	0.000003553
23	6	-0.000000741	0.000000895	-0.000000185
24	6	-0.000001781	0.000002119	0.000003266
25	6	-0.000002067	-0.000000979	0.000002812
26	6	0.000001003	-0.000006924	-0.000009285
27	6	0.000000238	-0.000001164	0.000000563
28	6	-0.000000567	-0.000003584	-0.000001264
29	6	0.000000948	-0.000001392	0.000004590
30	6	-0.000000057	-0.000001550	-0.000000406
31	6	0.000000031	-0.000003433	-0.000000621
32	17	-0.000000468	-0.000005289	-0.000001661
33	1	0.000002172	-0.000000333	-0.000002414
34	1	0.000002080	0.000000056	-0.000003464
35	1	0.000000599	0.000002408	-0.000000620
36	1	0.000001919	0.000002006	-0.000002436
37	1	0.000001621	0.000001516	-0.000001220
38	1	-0.000001084	0.000002406	0.000001041
39	1	-0.000000799	0.000001238	0.000000172
40	1	-0.000000162	0.000000199	-0.000000899
41	1	0.000002204	0.000000856	-0.000002218
42	1	-0.000001567	0.000000837	0.000001512
43	1	-0.000000652	0.000002493	0.000000200
44	1	-0.000000758	-0.000000713	0.000000657
45	1	-0.000001618	-0.000001535	0.000001284
46	1	-0.000002876	0.000000725	0.000003264
47	1	-0.000002248	0.000002004	0.000001714
48	1	-0.000002918	-0.000001006	0.000003222
49	1	-0.000002158	-0.000001695	0.000002364
50	1	-0.000002516	-0.000001960	0.000002741
51	1	-0.000000081	-0.000001626	0.000000329
52	1	-0.000000495	-0.000002941	0.000000510
53	1	0.000001165	-0.000003279	-0.000000879
54	1	0.000001479	-0.000001063	-0.000001206

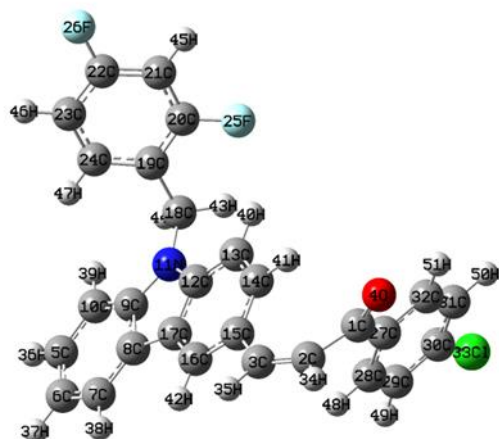


20

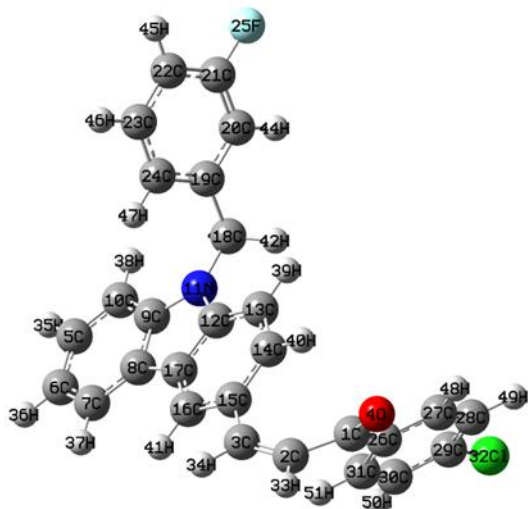


1	6	-0.000010461	0.000016231	-0.000007361
2	6	0.000014637	-0.000014618	0.000002000
3	6	-0.000001170	0.000001789	-0.000004260
4	8	0.000004174	-0.000002502	-0.000004488
5	6	-0.000003105	0.000004766	-0.000002149
6	6	-0.000000244	0.000003075	-0.000003505
7	6	-0.000001977	0.000005114	-0.000005393
8	6	0.000005202	0.000002079	-0.000001922
9	6	-0.000008326	0.000001064	0.000002255
10	6	0.000002420	0.000000820	-0.000004633
11	7	0.000005047	-0.000001778	-0.000007620
12	6	0.000008770	-0.000002520	0.000000806
13	6	0.000003684	0.000009600	0.000010511
14	6	-0.000000566	-0.000034796	-0.000020747
15	6	-0.000008057	0.000006183	0.000009135
16	6	0.000003806	0.000008259	-0.000006007
17	6	-0.000004801	0.000001445	-0.000002044
18	6	0.000000381	0.000008051	0.000009563
19	6	-0.000004571	-0.000005322	0.000000431
20	6	-0.000002040	-0.000003125	0.000002895
21	6	-0.000000224	-0.000003251	0.000005826
22	6	0.000002396	-0.000001407	0.000000499
23	6	0.000000995	-0.000005283	0.000000146
24	6	0.000002285	-0.000002019	0.000003931
25	9	-0.000001084	0.000003314	0.000002667
26	6	-0.000001317	-0.000008152	0.000009308
27	6	0.000003131	-0.000002004	0.000002046
28	6	-0.000001786	0.000001412	0.000003853
29	6	-0.000001447	0.000001724	0.000002154
30	6	-0.000002850	0.000002923	0.000003445
31	6	-0.000002149	-0.000001029	-0.000004592
32	17	-0.000003693	0.000003376	0.000004173
33	1	0.000002388	-0.000001740	-0.000006711
34	1	0.000002909	-0.000001146	-0.000003909
35	1	-0.000000905	0.000004286	-0.000002435
36	1	-0.000000140	0.000005163	-0.000005977
37	1	0.000000920	0.000002635	-0.000004259
38	1	-0.000000726	0.000002174	0.000001239
39	1	-0.000000888	-0.000001498	-0.000000928
40	1	0.000002063	0.000004896	0.000005480
41	1	0.000000251	0.000000292	-0.000003965
42	1	-0.000000943	-0.000000805	0.000001318
43	1	-0.000001755	0.000001419	0.000003617
44	1	-0.000000462	-0.000001721	0.000002644
45	1	0.000001411	-0.000005642	0.000003022
46	1	0.000001860	-0.000005571	0.000001758
47	1	0.000000979	-0.000002707	0.000001756
48	1	-0.000000911	-0.000000971	0.000002624
49	1	-0.000001968	0.000000351	0.000004686
50	1	-0.000002156	0.000003155	-0.000000437
51	1	0.000001016	0.000004013	-0.000000444

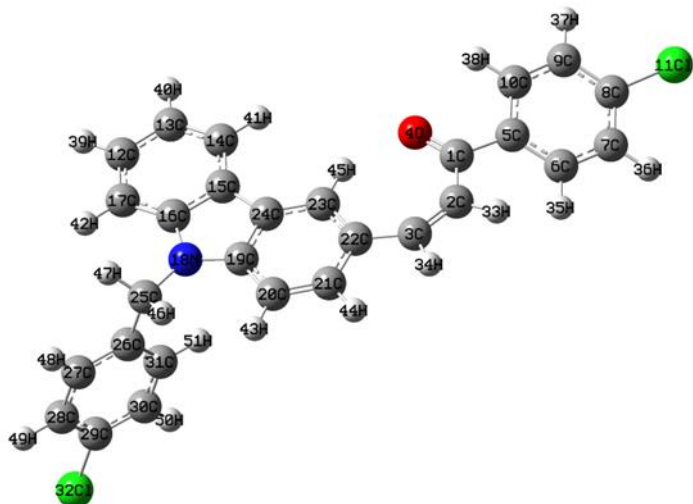
21



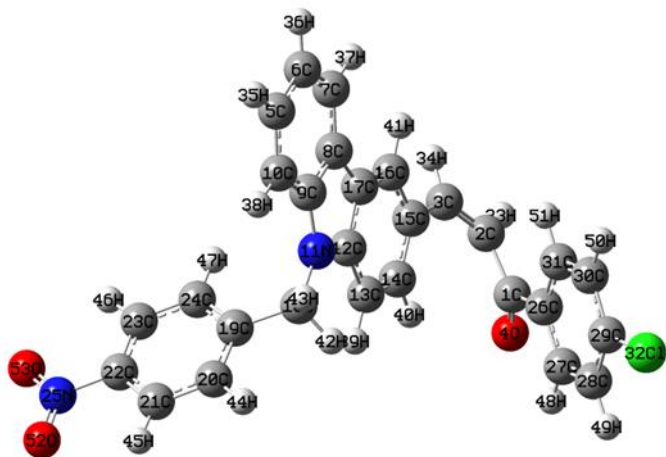
1	6	-0.000000405	-0.000011249	0.000010399
2	6	-0.000005744	0.000003737	-0.000000983
3	6	0.000001887	0.000003888	0.000001620
4	8	0.000001215	0.000003370	-0.000005319
5	6	0.000001876	-0.000002588	0.000003209
6	6	0.000001575	-0.000003583	0.000004601
7	6	0.000002283	-0.000003540	0.000004833
8	6	-0.000001918	0.000001454	0.000000253
9	6	-0.000001162	-0.000002529	0.000001995
10	6	0.000001662	-0.000001043	0.000002696
11	7	0.000004155	0.000007453	-0.000002328
12	6	-0.000008551	-0.000003731	0.000005764
13	6	0.000005589	0.000000168	-0.000003261
14	6	-0.000001644	0.000001580	-0.000000142
15	6	-0.000005750	0.000000378	0.000004031
16	6	0.000002586	0.000001213	-0.000002558
17	6	0.000003305	-0.000002720	0.000006859
18	6	0.000000516	-0.000005367	-0.000001657
19	6	-0.000003558	0.000002285	0.000000103
20	6	-0.000002693	0.000003968	-0.000007759
21	6	-0.000000582	0.000002994	0.000001266
22	6	-0.000006290	0.000004968	0.000001528
23	6	0.000000116	0.000001675	-0.000002742
24	6	0.000000373	0.000000202	0.000002992
25	9	0.000000869	0.000000017	-0.000001982
26	9	-0.000003653	0.000004462	-0.000001514
27	6	0.000000971	0.000009514	-0.000009965
28	6	0.000000299	-0.000002821	-0.000000478
29	6	0.000001977	-0.000000967	-0.000003021
30	6	0.000002832	-0.000002909	-0.000003253
31	6	0.000000505	0.000000014	-0.000005088
32	6	0.000002070	-0.000001294	-0.000002516
33	17	0.000003356	-0.000002846	-0.000005397
34	1	-0.000000064	0.000000936	0.000000904
35	1	-0.000001145	0.000000283	0.000002588
36	1	0.000001567	-0.000003436	0.000004302
37	1	0.000001550	-0.000003288	0.000005767
38	1	0.000000636	-0.000002273	0.000005052
39	1	0.000000902	-0.000002465	0.000001197
40	1	-0.000001628	-0.000001199	-0.000002709
41	1	-0.000000512	0.000001952	-0.000000676
42	1	-0.000000203	-0.000001408	0.000004710
43	1	0.000000482	0.000000500	-0.000001689
44	1	0.000000832	-0.000000545	0.000000102
45	1	-0.000002795	0.000004072	-0.000003065
46	1	-0.000003064	0.000002912	0.000001775
47	1	-0.000001293	0.000000766	0.000001575
48	1	0.000001654	-0.000001063	0.000000142
49	1	0.000002634	-0.000002986	-0.000001525
50	1	0.000002432	-0.000000282	-0.000005911
51	1	-0.000000053	0.000001371	-0.000004725



1	6	-0.000012863	-0.000009099	0.000027887
2	6	0.000002756	-0.000013252	-0.000003203
3	6	0.000007935	0.000014903	-0.000001548
4	8	0.000007442	0.000000303	-0.000003480
5	6	-0.000000807	0.000003577	-0.000003963
6	6	0.000000494	0.000002764	-0.000004499
7	6	-0.000001224	0.000001288	-0.000006273
8	6	-0.000010334	-0.000006657	-0.000000018
9	6	-0.000003356	0.000005126	-0.000002353
10	6	0.000004393	0.000003434	-0.000006987
11	7	0.000002643	0.000004218	-0.000010627
12	6	-0.000002608	0.000006868	0.000004254
13	6	-0.000000980	0.000001033	0.000000281
14	6	-0.000000102	0.000000855	-0.000000186
15	6	-0.000004241	-0.000013322	-0.000002755
16	6	-0.000001410	-0.000002972	-0.000005079
17	6	0.000010015	0.000009661	0.000002429
18	6	0.000001716	-0.000002141	0.000002675
19	6	-0.000002959	0.000010913	-0.000001203
20	6	0.000001914	-0.000004708	-0.000000931
21	6	0.000003135	0.000000154	0.000009575
22	6	0.000000830	0.000002315	-0.000000097
23	6	0.000003441	-0.000009097	-0.000003395
24	6	0.000004726	-0.000007927	0.000006783
25	9	0.000002389	-0.000006123	0.000002352
26	6	0.000001470	0.000018347	-0.0000020384
27	6	-0.000000416	-0.000009636	0.000009487
28	6	-0.000002641	0.000005337	-0.000000427
29	6	-0.000003411	-0.000000788	0.000007468
30	6	-0.000003030	0.000005126	-0.000002542
31	6	0.000000017	-0.000001166	0.000008547
32	17	-0.000004434	0.000004334	0.000002365
33	1	0.000002226	0.000000519	0.000001664
34	1	0.000000641	-0.000001830	-0.000003683
35	1	-0.000001821	0.000002048	-0.000004665
36	1	-0.000002080	0.000002812	-0.000006959
37	1	0.000000948	0.000002178	-0.000004680
38	1	-0.000001963	0.000000535	0.000000887
39	1	0.000000534	-0.000001540	0.000001031
40	1	0.000000663	-0.000001317	0.000001079
41	1	0.000001248	0.000001326	-0.000002015
42	1	-0.000000501	-0.000000886	-0.000000667
43	1	-0.000000604	-0.000000515	0.000002275
44	1	0.000000347	-0.000002561	0.000001877
45	1	0.000004086	-0.000003659	0.000000897
46	1	0.000003754	-0.000001739	-0.000001139
47	1	0.000000944	0.000000699	-0.000001955
48	1	-0.000000385	0.000000219	0.000003630
49	1	-0.000002314	-0.000000412	0.000006539
50	1	-0.000003036	0.000002987	0.000002723
51	1	-0.000003186	0.000001204	-0.000000994



1	6	-0.00009834	-0.00006857	-0.00002839
2	6	0.00009038	0.00002586	0.00006305
3	6	-0.00007015	-0.00008730	-0.000014712
4	8	-0.00002497	-0.00001697	0.000003871
5	6	0.00005858	0.00008849	0.00000992
6	6	-0.00005227	-0.00004626	-0.00002866
7	6	-0.00000235	0.00003960	-0.00000914
8	6	-0.00003874	0.00003258	0.00003137
9	6	-0.00000604	0.00004765	0.00004444
10	6	-0.00009140	-0.00002254	0.00005158
11	17	-0.00004900	0.00001979	0.00002770
12	6	0.00003985	0.00000685	0.00004794
13	6	0.00003367	0.00000174	0.00005937
14	6	0.00002403	0.00000029	0.00006204
15	6	-0.00000643	0.00004978	-0.00003351
16	6	0.00000136	0.00000275	-0.00001835
17	6	0.00004772	0.00002228	0.00006240
18	7	0.00006410	-0.00015523	0.00003148
19	6	-0.00003067	0.00010156	0.00002565
20	6	0.00002128	-0.00008059	-0.00006362
21	6	0.00005773	0.00001489	-0.00003642
22	6	0.00002633	0.00002080	0.00009641
23	6	-0.00003804	0.00010742	-0.00008802
24	6	0.00006848	-0.00009023	0.00003010
25	6	0.00003318	0.00002070	-0.00002433
26	6	-0.00007825	-0.00005220	-0.00007610
27	6	0.00009262	0.00005482	-0.00009404
28	6	0.00003666	0.00000666	0.00009467
29	6	-0.00011309	-0.00011697	-0.00002113
30	6	0.00002240	0.00008997	-0.000010154
31	6	0.00000704	-0.00002752	0.000011497
32	17	-0.00002381	0.00003130	-0.00005556
33	1	-0.00003645	0.00000387	-0.00004389
34	1	-0.00001063	0.00000085	-0.00005363
35	1	-0.00004819	0.00002229	-0.00000762
36	1	-0.00006708	0.00001531	0.00000130
37	1	-0.00000401	0.00001331	0.00004623
38	1	0.00003114	0.00001870	0.00003166
39	1	0.00004537	-0.00000218	0.00006468
40	1	0.00004613	0.00001516	0.00007294
41	1	0.00003217	0.00001078	0.00004315
42	1	0.00003302	-0.00001381	0.00000579
43	1	-0.00000376	-0.00000471	-0.00003277
44	1	-0.00002097	-0.00002162	-0.00005870
45	1	0.00003609	-0.00001457	0.00002528
46	1	0.00002740	-0.00003374	-0.00004710
47	1	0.00002837	-0.00004225	-0.00001629
48	1	-0.00000282	-0.00002133	-0.00002521
49	1	-0.00001337	-0.00001357	-0.00005015
50	1	-0.00004530	0.00001659	-0.00000064
51	1	-0.00002898	0.00002952	-0.00002089



1	6	-0.000001169	0.000002971	0.000001256
2	6	0.000000558	-0.000004440	-0.000008397
3	6	-0.000002299	0.000000481	0.000003322
4	8	0.000001275	0.000000700	0.000000477
5	6	-0.000001527	0.000000783	-0.000000479
6	6	-0.000000376	-0.000000834	-0.000000506
7	6	-0.000000376	0.000000338	-0.000001924
8	6	-0.000004703	-0.000002660	0.000001113
9	6	-0.000000840	0.000002756	0.000004446
10	6	0.000000616	-0.000001492	-0.000002517
11	7	-0.000000406	0.000003398	-0.000012724
12	6	0.000000975	-0.000003151	0.000003892
13	6	-0.000000978	0.000002216	0.000000398
14	6	0.000000927	-0.000005225	0.000000358
15	6	0.000002523	0.000006454	-0.000001820
16	6	-0.000003515	-0.000003802	-0.000004454
17	6	0.000005935	0.000004693	0.000000337
18	6	0.000001670	-0.000002552	0.000006920
19	6	-0.000000244	-0.000002865	-0.000001343
20	6	0.000000565	-0.000001022	0.000000137
21	6	0.000001896	-0.000002214	0.000002095
22	6	-0.000000483	-0.000000155	0.000000800
23	6	0.000000464	-0.000000287	-0.000000414
24	6	-0.000000478	-0.000000517	0.000001884
25	7	0.000006080	0.000002554	0.000006280
26	6	-0.000001235	0.000004290	-0.000005017
27	6	0.000000361	-0.000001772	0.000002183
28	6	-0.000002208	0.000001766	0.000000872
29	6	0.000002022	-0.000001648	0.000000684
30	6	-0.000001728	0.000005765	-0.000003113
31	6	-0.000000135	0.000000073	0.000006958
32	17	-0.000000944	0.000002438	0.000000502
33	1	-0.000000135	0.000000721	0.000001196
34	1	-0.000001174	-0.000000346	0.000002053
35	1	-0.000000160	-0.000000075	-0.000000567
36	1	-0.000000639	-0.000000153	-0.000001849
37	1	-0.000000375	-0.000000269	-0.000001062
38	1	0.000000664	-0.000000370	-0.000000122
39	1	0.000001233	-0.000000182	0.000000387
40	1	-0.000001129	-0.000000465	-0.000000004
41	1	0.000000103	0.000000367	-0.000000547
42	1	-0.000000444	0.000001147	-0.000000737
43	1	0.000000159	0.000000695	0.000001967
44	1	0.000001343	0.000000133	0.000001515
45	1	0.000000957	-0.000000256	0.000000932
46	1	0.000000578	-0.000002518	-0.000000270
47	1	0.000000844	-0.000000932	-0.000000266
48	1	-0.000000685	0.000001367	0.000000259
49	1	0.000000021	0.000001608	0.000001118
50	1	-0.000000664	0.000000928	0.000000322
51	1	-0.000001268	0.000000336	-0.000001383
52	8	-0.000001061	-0.000005883	-0.000002149
53	8	-0.000000389	-0.000002891	-0.000002999

- [1] J.R. Stepherson, C.E. Ayala, T.H. Tugwell, J.L. Henry, F.R. Fronczek, R. Kartika, Carbazole Annulation via Cascade Nucleophilic Addition–Cyclization Involving 2-(Silyloxy) pentadienyl Cation, *J Org. Lett* 18(12) (2016) 3002-3005.
- [2] G.-M. Tang, R.-H. Chi, W.-Z. Wan, Z.-Q. Chen, T.-X. Yan, Y.-P. Dong, Y.-T. Wang, Y.-Z. Cui, Tunable photoluminescent materials based on two phenylcarbazole-based dimers through the substituent groups, *J. Lumin* 185 (2017) 1-9.
- [3] A. Głuszyńska, Biological potential of carbazole derivatives, *Eur. J. Med. Chem* 94 (2015) 405-426.
- [4] L. S. Tsutsumi, D. Gündisch, D. Sun, Carbazole scaffold in medicinal chemistry and natural products: a review from 2010-2015, *J Curr. Top. Med. Chem* 16(11) (2016) 1290-1313.
- [5] E. Asma, D. Banibrata, Y. Deepthi, X. Liping, A. Tamara, E.A.R. Maarten, K.D. Alope Design, Synthesis, and Pharmacological Characterization of Carbazole Based Dopamine Agonists as Potential Symptomatic and Neuroprotective Therapeutic Agents for Parkinson's Disease, *J ACS Chem. Neurosci* 10 (2019) 396–411.
- [6] L.-X. Liu, X.-Q. Wang, B. Zhou, L.-J. Yang, Y. Li, H.-B. Zhang, X.-D. Yang, Synthesis and antitumor activity of novel N-substituted carbazole imidazolium salt derivatives, *Sci. Rep* 5 (2015) 13101.
- [7] M.S. Sinicropi, D. Iacopetta, C. Rosano, R. Randino, A. Caruso, C. Saturnino, N. Muià, J. Ceramella, F. Puoci, M. Rodriquez, N-thioalkylcarbazoles derivatives as new anti-proliferative agents: synthesis, characterisation and molecular mechanism evaluation, *J Enzyme Inhib Med Chem* 33(1) (2018) 434-444.
- [8] W. Wang, X. Sun, D. Sun, S. Li, Y. Yu, T. Yang, J. Yao, Z. Chen, L. Duan, Carbazole aminoalcohols induce antiproliferation and apoptosis of human tumor cells by inhibiting topoisomerase I, *J ChemMedChem* 11(24) (2016) 2675-2681.
- [9] A. Głuszyńska, B. Juskowiak, M. Kuta-Siejkowska, M. Hoffmann, S. Haider, Carbazole ligands as c-myc G-quadruplex binders, *Int. J. Biol. Macromol* 114 (2018) 479-490.
- [10] M.H. Kaulage, B. Maji, S. Pasadi, A. Ali, S. Bhattacharya, K. Muniyappa, Targeting G-quadruplex DNA structures in the telomere and oncogene promoter regions by benzimidazole–carbazole ligands, *Eur. J. Med. Chem* 148 (2018) 178-194.
- [11] P.-H. Li, H. Jiang, W.-J. Zhang, Y.-L. Li, M.-C. Zhao, W. Zhou, L.-Y. Zhang, Y.-D. Tang, C.-Z. Dong, Z.-S. Huang, Synthesis of carbazole derivatives containing chalcone analogs as non-intercalative topoisomerase II catalytic inhibitors and apoptosis inducers, *Eur. J. Med. Chem* 145 (2018) 498-510.

## References

- [12] R. Fleming, A. Miller, C. Stewart, Etoposide: an update, *J Clin Pharm* 8(4) (1989) 274-293.
- [13] K. R. Hande, Etoposide: four decades of development of a topoisomerase II inhibitor. *Eur. J. Cancer* 34, 1514-1521 (1998).
- [14] G.L. Patrick, *An Introduction to Medicinal Chemistry*, OUP Oxford, United Kingdom, 2013.
- [15] P.W. Ayers, J.S. Anderson, L.J. Bartolotti, Perturbative perspectives on the chemical reaction prediction problem, *Int. J. Quantum Chem* 101(5) (2005) 520-534.
- [16] P. Geerlings, F. De Proft, W. Langenaeker, Conceptual density functional theory, *Chem. Rev* 103(5) (2003) 1793-1874.
- [17] R.G. Parr, W. Yang, *Density-Functional Theory of Atoms and Molecules*, Oxford University Press, New York, 1989.
- [18] C. Hansch, R.M. Muir, T. Fujita, P.P. Maloney, F. Geiger, M. Streich, The correlation of biological activity of plant growth regulators and chloromycetin derivatives with Hammett constants and partition coefficients, *J. Am. Chem. Soc* 85(18) (1963) 2817-2824.
- [19] M. Alloui, S. Belaidi, H. Othmani, N. E. Jaidane, M. Hochlaf, Imidazole derivatives as angiotensin II AT1 receptor blockers: Benchmarks, drug-like calculations and quantitative structure-activity relationships modeling, *Chem. Phys. Lett.* 696 (2018) 70-78.
- [20] S. Boudergua, M. Alloui, S. Belaidi, M.M. Al Mogren, U.A.E. Ibrahim, M.Hochlaf, QSAR Modeling and Drug-Likeness Screening for Antioxidant Activity of Benzofuran Derivatives, *J. Mol. Struct.* 1189 (2019) 307-314.
- [21] M. Manachou, Z. Gouid, Z. Almi, S. Belaidi, S. Boughdiri, M. Hochlaf, Pyrazolo [1, 5-a][1, 3, 5] triazin-2-thioxo-4-ones derivatives as thymidine phosphorylase inhibitors: Structure, drug-like calculations and quantitative structure-activity relationships (QSAR) modeling, *J. Mol. Struct.* 1199 (2020) 127027.
- [22] I. Almi, S. Belaidi, E. Zerroug, M. Alloui, R. B. Said, R. Linguerra, M. Hochlaf, QSAR investigations and structure-based virtual screening on a series of nitrobenzoxadiazole derivatives targeting human glutathione-S-transferases, *J. Mol. Struct.* (2020) 128015.
- [23] LuanaJanaína de Campos, E.B.d. Melo, A QSAR study of integrase strand transfer inhibitors based on a large set of pyrimidine, pyrimidone, and pyridopyrazine carboxamide derivatives, *J. Mol. Struct* 1141 (2017) 252-260.
- [24] M. Ghamali, S. Chtita, A. Ousaa, B. Elidrissi, M. Bouachrine, T. Lakhlifi, QSAR analysis of the toxicity of phenols and thiophenols using MLR and ANN, *J Taibah Univ Sci* 11(1) (2017) 1-10.

## References

- [25] P. Maldivi, L. Petit, C. Adamo, V. Vetere, Theoretical description of metal–ligand bonding within f-element complexes: A successful and necessary interplay between theory and experiment, *J C. R. Chim* 10(10-11) (2007) 888-896.
- [26] A. Toropova, A. Toropov, E. Benfenati, G. Gini, Co-evolutions of correlations for QSAR of toxicity of organometallic and inorganic substances: an unexpected good prediction based on a model that seems untrustworthy, *J Chemometr. Intell. Lab* 105(2) (2011) 215-219.
- [27] J. Thijssen, *Computational Physics*, Cambridge University Press 2007.
- [28] A.D. Becke, Density-functional thermochemistry. III. The role of exact exchange, *J. Chem. Phys* 98(7) (1993) 5648-5652.
- [29] M. Frisch, G. Trucks, H.B. Schlegel, G. Scuseria, M. Robb, J. Cheeseman, G. Scalmani, V. Barone, B. Mennucci, G. Petersson, H.C. Nakatsuji, M.; Li, X., H.P.I. Hratchian, A. F.; Bloino, J., G.S. Zheng, J. L., M.E. Hada, M.; Toyota, , R.H. K.; Fukuda, J., M.N. Ishida, T., Y.K. Honda, O.; Nakai, H.; Vreven, , J.A. T.; Montgomery, Jr.; Peralta, , F.B. J. E.; Ogliaro, M., J.J.B. Heyd, E., K.N.S. Kudin, V. N., R.N. Kobayashi, J., K.R. Raghavachari, J.C.I. A.; Burant, S. S, J.C. Tomasi, M.; Rega, N.J.K. N.; Millam, M., J.E.C. Knox, J. B.; Bakken, V., C.J. Adamo, J.; Gomperts, R., R.E.Y. Stratmann, O., A.J.C. Austin, R., C.O. Pomelli, J. W., R.L.M. Martin, K., V.G.V. Zakrzewski, G. A., P.D. Salvador, J. J., S.D. Dapprich, A. D., Ö.F. Farkas, J. B., J.V.C. Ortiz, J., D.J. Fox, Gaussian 09, Gaussian, Inc., Wallingford, CT (2009).
- [30] R.E. Gerkin, W.J. Reppart, The structure of carbazole at 168 K, *Acta Cryst* 42(4) (1986) 480-482.
- [31] A. Bree, R. Zwarich, Vibrational Assignment of Carbazole from Infrared, Raman, and Fluorescence Spectra, *J. Chem. Phys* 49(8) (1968) 3344-3355.
- [32] S. Premkumar, T. Rekha, R.M. Asath, T. Mathavan, A.M.F. Benial, Vibrational spectroscopic, molecular docking and density functional theory studies on 2-acetylamino-5-bromo-6-methylpyridine, *Eur. J. Pharm. Sci* 82 (2016) 115-125.
- [33] K. Fukui, Role of frontier orbitals in chemical reactions, *J Science* 218(4574) (1982) 747-754.
- [34] R. Parr, W. Yang, Density functional approach to the frontier-electron theory of chemical reactivity, *J. Am. Chem. Soc* 106(14) (1984) 4049-4050.
- [35] P.W. Ayers, R.G. Parr, Variational principles for describing chemical reactions: the Fukui function and chemical hardness revisited, *J. Am. Chem. Soc* 122(9) (2000) 2010-2018.
- [36] C. Morell, A. Grand, A. Toro-Labbe, New dual descriptor for chemical reactivity, *J. Phys. Chem* 109(1) (2005) 205-212.
- [37] F. Guégan, P. Mignon, V. Tognetti, L. Joubert, C. Morell, Dual descriptor and molecular electrostatic potential: complementary tools for the study of the coordination chemistry of ambiphilic ligands, *Phys. Chem. Chem. Phys* 16(29) (2014) 15558-15569.

## References

- [38] HyperChem, (Molecular modeling system) Hypercube, Inc., 1115NW, 4th Street, Gainesville, FL 32601, USA (2008).
- [39] MOE, Chemical Computing Group (CCG): Montreal, Canada
- [40] P.V. Rysselberghe, Remarks concerning the Clausius-Mossotti law, *J. Phys. Chem* 36(4) (1932) 1152-1155.
- [41] G. Pèpe, G. Guiliani, S. Loustalet, P. Halfon, Hydration free energy a fragmental model and drug design, *Eur. J. Med. Chem* 37(11) (2002) 865-872.
- [42] T. Salah, S. Belaidi, N. Melkemi, N. Tchouar, Molecular Geometry, Electronic Properties, MPO Methods and Structure Activity/Property Relationship Studies of 1, 3, 4-Thiadiazole Derivatives by Theoretical Calculations, *Rev. Theor. Sci* 3(4) (2015) 355-364.
- [43] V. Stella, R. Borchardt, M. Hageman, R. Oliyai, H. Maag, J. Tilley, *Prodrugs: Challenges and Rewards*, Springer, New York, 2007.
- [44] C.A. Lipinski, F. Lombardo, B.W. Dominy, P.J. Feeney, Experimental and computational approaches to estimate solubility and permeability in drug discovery and development settings, *Adv. Drug Deliv. Rev* 23(1-3) (1997) 3-25.
- [45] D.F. Veber, S.R. Johnson, H.-Y. Cheng, B.R. Smith, K.W. Ward, K.D. Kopple, Molecular properties that influence the oral bioavailability of drug candidates, *J. Med. Chem* 45(12) (2002) 2615-2623.
- [46] A.K. Ghose, V.N. Viswanadhan, J.J. Wendoloski, A knowledge-based approach in designing combinatorial or medicinal chemistry libraries for drug discovery. 1. A qualitative and quantitative characterization of known drug databases, *J. Comb. Chem* 1(1) (1999) 55-68.
- [47] K. Edward H, D. Li, *Drug-like Properties: Concepts, Structure Design and Methods: from ADME to Toxicity Optimization*, Elsevier Science, United kingdom, 2008.
- [48] L.J. Cseke, A. Kirakosyan, P.B. Kaufman, M.V. Westfall, *Handbook of Molecular and Cellular Methods in Biology and Medicine*, CRC Press, USA, 2011.
- [49] Y.H. Zhao, M.H. Abraham, J. Le, A. Hersey, C.N. Luscombe, G. Beck, B. Sherborne, I. Cooper, Rate-limited steps of human oral absorption and QSAR studies, *J Pharm Res* 19(10) (2002) 1446-1457.
- [50] P.A. Bath, A.R. Poirrette, P. Willett, F.H. Allen, The extent of the relationship between the graph-theoretical and the geometrical shape coefficients of chemical compounds, *J. Chem. Inf. Comput. Sci.* 35(4) (1995) 714-716.
- [51] K. Gohda, I. Mori, D. Ohta, T. Kikuchi, A CoMFA analysis with conformational propensity: an attempt to analyze the SAR of a set of molecules with different conformational flexibility using a 3D-QSAR method, *J Comput Aided Mol Des* 14(3) (2000) 265-275.

## References

- [52] R.G. Hill, *Drug Discovery and Development: Technology in Transition*, Elsevier Health Sciences, London, 2012.
- [53] F. Ghasemi, A. Mehridehnavi, A. Pérez-Garrido, H. Pérez-Sánchez, Neural network and deep-learning algorithms used in QSAR studies: merits and drawbacks, *Drug Discov. Today* 23(10) (2018) 1784-1790.
- [54] JMP.8.0.2, SAS Institute Inc, 2009.
- [55] XLSTAT, Software, XLSTATCompany, (2013). <http://www.xlstat.com>. (Accessed 17.04.2020)
- [56] H. Van Der Voet, Comparing the predictive accuracy of models using a simple randomization test, *Chemom. Intell. Lab. Syst.*, 25(2) (1994) 313-323.
- [57] C. Rücker, G. Rücker, M. Meringer, Y-randomization and its variants in QSPR/QSAR, *J. Chem. Inf. Model*, 47(6) (2007) 2345-2357.
- [58] A. Golbraikh, A. Tropsha, Beware of  $q^2$ !, *J. Mol. Graph* 20(4) (2002) 269-276.
- [59] A. Golbraikh, A. Tropsha, Predictive QSAR modeling based on diversity sampling of experimental datasets for the training and test set selection, *J. Comput. Aided Mol. Des* 16(5-6) (2002) 357-369.
- [60] A. Tropsha, P. Gramatica, V.K. Gombar, The importance of being earnest: validation is the absolute essential for successful application and interpretation of QSPR models, *QSAR Com. Sci* 22(1) (2003) 69-77.
- [61] A. Srivastava, N. Shukla, QSAR based modeling on a series of lactam fused chroman derivatives as selective 5-HT transporters, *J. Saudi Chem. Soc* 16(4) (2012) 405-412.
- [62] P.P. Roy, K. Roy, On some aspects of variable selection for partial least squares regression models, *QSAR Comb. Sci.* 27(3) (2008) 302-313.
- [63] K. Roy, S. Kar, R.N. Das, *A primer on QSAR/QSPR modeling: Fundamental concepts*, Springer, New York, 2015.
- [64] S. Erić, M. Kalinić, A. Popović, M. Zloh, I. Kuzmanovski, Prediction of aqueous solubility of drug-like molecules using a novel algorithm for automatic adjustment of relative importance of descriptors implemented in counter-propagation artificial neural networks, *Int. J. Pharm* 437(1-2) (2012) 232-241.
- [65] R. Lowe, H.Y. Mussa, J.B. Mitchell, R.C. Glen, Classifying molecules using a sparse probabilistic kernel binary classifier, *J. Chem. Inf. Model* 51(7) (2011) 1539-1544.
- [66] C. Feng, S. Vijaykumar, Applications of artificial neural network modeling in drug discovery, *Clin. Exp. Pharmacol* 2(3) (2012) 2-3.

## References

[67] B.D. Ripley, Pattern Recognition and neural networks, Cambridge University Press, NY United States, 1996.

[68] T.J. Wendorff, B.H. Schmidt, P. Heslop, C.A. Austin, J.M.J.J.o.m.b. Berger, The structure of DNA-bound human topoisomerase II alpha: conformational mechanisms for coordinating inter-subunit interactions with DNA cleavage, 424(3-4) (2012) 109-124.

[69] R.A. Guedes, N. Aniceto, M.A. Andrade, J.A. Salvador, R.C. Guedes, Chemical Patterns of Proteasome Inhibitors: Lessons Learned from Two Decades of Drug Design, Int. J. Mol. Sci 20(21) (2019) 5326.

**R**ecently, a series of carbazole derivatives containing chalcone analogues (CDCAs) were synthesized as potent anticancer agents and apoptosis inducers. These compounds target the inhibition of topoisomerase II and present cytotoxic activities. After comparison to experiment, we validated the use of B3LYP, a density functional theory-based approach, to describe the structure and molecular properties of the carbazole subunit and CDCAs compounds of interest. Then, we derived relationships between the chemical descriptors and activity of these carbazole derivatives using multi-parameter optimization and quantitative structure activity relationships (QSAR) approaches. For the QSAR studies, we used multiple linear regression and artificial neural network statistical modelling. Our predicted activities are in good agreement with the experimental ones. We found that the most important parameter influencing the activity of the considered compounds is the octanol-water partition coefficient, highlighting the importance of flexibility as a key molecular parameter to favor cell membrane crossing and enhance the action of these CDCAs against topoisomerase II. Our results provide useful guidelines for designing new oral active CDCAs medicaments for cytotoxic inhibition.

**Keywords: Carbazole derivatives; Topo II inhibition; Molecular structure; QSAR model.**

**R**écemment, une série de dérivés du carbazole contenant des analogues de la chalcone (CDCA) ont été synthétisés en tant qu'agents anticancéreux puissants et inducteurs de l'apoptose. Ces composés ciblent l'inhibition de la topoisomérase II et présentent des activités cytotoxiques. Après comparaison à l'expérience, nous avons validé l'utilisation de B3LYP, une approche basée sur la théorie fonctionnelle de la densité, pour décrire la structure et les propriétés moléculaires de la sous-unité carbazole et des composés CDCA d'intérêt. Ensuite, nous avons dérivé des relations entre les descripteurs chimiques et l'activité de ces dérivés de carbazole en utilisant des approches d'optimisation multi-paramètres et de relations quantitatives structure-activité (QSAR). Pour les études QSAR, nous avons utilisé une régression linéaire multiple et une modélisation statistique des réseaux de neurones artificiels. Nos activités prédites sont en bon accord avec celles expérimentales. Nous avons constaté que le paramètre le plus important influençant l'activité des composés considérés est le coefficient de partage octanol-eau, soulignant l'importance de la flexibilité en tant que paramètre moléculaire clé pour favoriser le franchissement de la membrane cellulaire et renforcer l'action de ces CDCA contre la topoisomérase II. Nos résultats fournissent des lignes directrices utiles pour la conception de nouveaux médicaments CDCA actifs oraux pour l'inhibition cytotoxique.

**Mots clés : Dérivés du carbazole ; Inhibition de Topo II; Structure moléculaire; Modèle QSAR.**